การพัฒนาแอมเพอโรเมทริกอิมมูโนเซนเซอร์โดยการใช้โบรอนโดปไดมอน
ร่วมกับกรดโพลีออร์โธอะมิโนเบนโซอิก

นางสาวอัญชนา ปรีชาวรพันธ์

DEVELOPMENT OF AMPEROMETRIC IMMUNOSENSOR USING BORON-DOPED DIAMOND WITH POLY(*o*-AMINOBENZOIC ACID)

Miss Anchana Preechaworapun

A Dissertation Submitted in Partial Fulfillment of the Requirements

for the Degree of Doctor of Science Program in Chemistry

Department of Chemistry

Faculty of Science

Chulalongkorn University

Academic Year 2007

Thesis Title	DEVELOPMENT OF AMPEROMETRIC IMMUNOSENSOR USING BORON-DOPED DIAMOND WITH POLY(o-AMINOBENZOIC ACID)
By	Miss Anchana Preechaworapun
Field of Study	Chemistry
Thesis Advisor	Associate Professor Orawon Chailapakul, Ph.D.
Thesis Co-advisor	Parichatr Vanalabhpatana, Ph.D.

Accepted by the Faculty of Science, Chulalongkorn University in Partial Fulfillment of the Requirements for the Doctoral Degree

.... Dean of the Faculty of Science
(Professor Supot Hannongbua, Ph.D.)

THESIS COMMITTEE

.... Chairman
(Associate Professor Sirirat Kokpol, Ph.D.)

.... Thesis Advisor
(Associate Professor Orawon Chailapakul, Ph.D.)

.... Thesis Co-advisor
(Parichatr Vanalabhpatana, Ph.D.)

.... External Member
(Winai Ouangpipat, Ph.D.)

.... Member
(Associate Professor Nattaya Ngamrojanavanich, Ph.D.)

.... Member
(Charoenkwan Kraiya, Ph.D.)

อัญชนา ปรีชาวรพันธ์ : การพัฒนาแอมเพอโรเมทริกอิมมูโนเซนเซอร์โดยการใช้โบรอน โดปไดมอนร่วมกับกรดโพลีออร์โธอะมิโนเบนโซอิก. (DEVELOPMENT OF AMPEROMETRIC IMMUNOSENSOR USING BORON-DOPED DIAMOND WITH POLY(o-AMINOBENZOIC ACID) อ.ที่ปรึกษา : รศ.ดร. อรวรรณ ชัยลภากุล, อ.ที่ปรึกษาร่วม : อาจารย์ ดร. ปาริฉัตร วนลาภพัฒนา 115 หน้า.

งานวิจัยนี้ศึกษาคุณสมบัติทางเคมีไฟฟ้าของผลิตภัณฑ์ของสารซับสเตรตของแอลคาไลน์ฟอสฟาเทส 7 ชนิด ที่ใช้ทั่วไปในอิมมูโนเซนเซอร์ทางเคมีไฟฟ้า ขั้วไฟฟ้าแบบแผ่นกลมของแกลสสิคาร์บอน แผ่นกลม ของทอง และคาร์บอนพิมพ์สกรีนถูกนำมาใช้สำหรับเทคนิคไซคลิกโวลแทมเมทรี และ แอมเพอโรเมทรี จาก ผลิตภัณฑ์เหล่านี้กรดแอล-แอสคอร์บิกแสดงสภาพไว และการตอบสนองทางแอมเพอโรเมทริกสูงสุด ซึ่ง ได้มาจากซับสเตรตของกรด 2-ฟอสโฟ-แอล-แอสคอร์บิกสำหรับการตรวจวัดทางเคมีไฟฟ้าร่วมกับฉลากของ แอลคาไลน์ฟอสฟาเทส แอมเพอโรเมทริกอิมมูโนเซนเซอร์แบบแซนวิชโดยมีแอลคาไลน์ฟอสฟาเทสเป็นตัว ขยายสัญญาณสร้างขึ้นโดยการใช้อิมมูโนโกลบูลิน-จีเป็นต้นแบบสารที่สนใจ อิมมูโนเซนเซอร์ถูกสร้างโดย กระบวนการอิเล็กโทรโพลิเมอร์ไรซ์ของกรดออร์โธ-อะมิโนเบนโซอิก (ออร์โธเอบีเอ) บนผิวหน้าของ ขั้วไฟฟ้า แอนติบอดีของอิมมูโนโกลบูลิน-จีที่ถูกอิมโมบิไลซ์ด้วยโควาเลนท์บนขั้วไฟฟ้าดัดแปรโพลีออร์โธเอ บีเอจะยึดติดกับทาเก็ทของอิมมูโนโกลบูลิน-จี ที่ยึดติดกับแอลคาไลน์ฟอสฟาเทสคอนจูเกตแอนติบอดีของอิมมู โนโกลบูลิน-จีเกิดเป็นอิมมูโนเซนเซอร์แบบแซนวิช แอลคาไลน์ฟอสฟาเทสสามารถเปลี่ยนกรด 2-ฟอสโฟ- แอล-แอสคอร์บิกเป็นกรดแอล-แอสคอร์บิกที่ว่องไวทางไฟฟ้าสามารถตรวจวัดด้วยเทคนิคแอมเพอโรเมทริก ซึ่งสัญญาณที่ได้เป็นสัดส่วนโดยตรงกับปริมาณของอิมมูโนโกลบูลิน-จี ประสิทธิภาพที่ดีที่สุดของอิมมูโน เซนเซอร์แบบแผ่นกลมของทองที่ดัดแปรด้วยโพลีออร์โธเอบีเอให้อัตราส่วนการตอบสนองความหนาแน่น ของกระแสอิมมูโนโกลบูลิน-จีสำหรับ 1000 และ 0 ng mL^{-1} เป็น 297 ต่อ 1 และอิมมูโนโกลบูลิน-จีถูกตรวจวัด ได้ต่ำถึงความเข้มข้น 1 ng mL^{-1} โดยมีช่วงเส้นตรง 3-200 ng mL^{-1}

ขั้วไฟฟ้าโบรอนโดปไดมอนวัสดุชนิดใหม่ได้รับการพัฒนาเป็นอิมมูโนเซนเซอร์อิมมูโนโกลบูลิน-จี ขั้วไฟฟ้าโบรอนโดปไดมอนที่ถูกดัดแปรด้วยโพลี-ออร์โธ-เอบีเอได้ถูกตรวจสอบคุณลักษณะด้วยสแกนนิ่ง อิเล็กตรอนไมโครสโกปี และเอ็ก-เรย์โฟโตอิเล็กตรอนสเปกโทรสโกปี ผลการทดลองของเอ็ก-เรย์โฟโต อิเล็กตรอนสเปกโทรสโกปีพบว่ามีกลุ่มของคาร์บอกซิลแสดงอยู่บนผิวของขั้วไฟฟ้า หมู่ของคาร์บอกซิลนี้ใช้ ยึดติดกับแอนติบอดีของอิมมูโนโกลบูลิน-จีด้วยโควาเลนท์ สัญญาณแอมเพอโรเมทริกของอิมมูโนโกลบูลิน-จี จากอิมมูโนเซนเซอร์ของแกลสสิคาร์บอนแบบแผ่นที่ดัดแปรด้วยโพลีออร์โธเอบีถูกเปรียบเทียบ ค่าขีดต่ำสุด ของการตรวจวัดของอิมมูโนโกลบูลิน-จีที่ขั้วไฟฟ้าโบรอนโดปไดมอนและขั้วไฟฟ้าแบบแผ่นของแกลสสิ คาร์บอนเท่ากับ 0.30 และ 3.50 ng mL^{-1} กำลังสามของช่วงเส้นตรงที่กว้าง (1-1000 ng mL^{-1}) ได้รับจาก ขั้วไฟฟ้าโบรอนโดปไดมอนในขณะที่ช่วงเส้นตรงที่แคบกว่า (10-500 ng mL^{-1}) พบได้จากขั้วไฟฟ้าแบบแผ่น ของแกลสสิคาร์บอน นอกจากนี้วิธีการที่นำเสนอยังประสบความสำเร็จในการนำมาประยุกต์ในตัวอย่างจริง ซีรัมของหนูที่มีอิมมูโนโกลบูลิน-จีอยู่

ภาควิชา.............เคมี...........ลายมือชื่อนิสิต.......................................

สาขาวิชา.............เคมี...........ลายมือชื่ออาจารย์ที่ปรึกษา.......................

ปีการศึกษา.............2550..........ลายมือชื่ออาจารย์ทีปรึกษาร่วม...............

4773849323   : MAJOR CHEMISTRY

KEY WORD: AMPEROMETRIC IMMUNOSENSOR / ALKALINE PHOSPHATASE / BDD / o-AMINOBENZOIC ACID / ASCORBIC ACID

ANCHANA PREECHAWORAPUN : DEVELOPMENT OF AMPEROMETRIC IMMUNOSENSOR USING BORON-DOPED DIAMOND WITH POLY(o-AMINOBENZOIC ACID). THESIS ADVISOR : ASSOC. PROF. ORAWON CHAILAPAKUL, Ph.D., THESIS COADVISOR : PARICHATR VANALABHPATANA, Ph.D., 115 pp.

This thesis studied the electrochemical properties of the products of seven substrates for the enzyme label, alkaline phosphatase, which is commonly used in electrochemical immunosensors. Cyclic voltammetry and amperometry of these products were carried out at glassy carbon disk, gold disk, and screen-printed carbon electrodes. Among the products, L-ascorbic acid showed the most sensitive and well-defined amperometric response, obtaining from 2-phospho-L-ascorbic acid substrate for the electrochemical detection with an alkaline phosphatase label. Using MIgG as a model analyte, the alkaline phosphatase-amplified sandwich-type amperometric immunosensor was constructed. The immunosensor was fabricated by electropolymerization of o-aminobenzoic acid (o-ABA) on the electrode surfaces. Covalently immobilized onto the poly-o-ABA modified electrodes, the anti-MIgG was bound with the target MIgG that was caught with the alkaline phosphatase conjugated anti-MIgG to form a sandwich-type immunosensor. The alkaline phosphatase is capable of changing 2-phospho-L-ascorbic acid to electroactive L-ascorbic acid, which can be determined by the amperometric detection with the signal directly proportional to the quantity of MIgG. The best performance for the poly-o-ABA modified Au disk immunosensor was 297-to-1 current density response ratio for 1000 and 0 ng mL^{-1} MIgG and detected MIgG down to the concentration of 1 ng mL^{-1} with the linear range of 3-200 ng mL^{-1}.

Boron-doped diamond, the new electrode material was developed for the MIgG immunosensor. The poly-o-ABA modified boron-doped diamond was characterized by scanning electron microscopy and X-ray photoelectron spectroscopy. X-ray photoelectron spectroscopic results revealed the presence of carboxyl groups at the modified electrode surface. These carboxyl groups were used to covalently attach to the anti-MIgG. The amperometric sensing of MIgG from poly-o-ABA modified glassy carbon plate immunosensor was compared. The LODs of 0.30 and 3.50 ng mL^{-1} for MIgG at boron-doped diamond and glassy carbon plate electrodes were obtained. Three orders of magnitude of the wide linear range (1-1000 ng mL^{-1}) was obtained from the boron-doped diamond whereas the narrower linear range (10-500 ng mL^{-1}) was found at the glassy carbon plate. In addition, the proposed method was successfully applied to a real mouse serum sample containing MIgG.

Department..........Chemistry.........Student's signature.......Anchana....Preechaworapun

Field of study........Chemistry.........Advisor's signature....................................../

Academic year.........2007..............Co-advisor's signature...........................

ACKNOWLEDGEMENTS

CONTENTS

LIST OF TABLES

LIST OF FIGURES

FIGURE   **PAGE**

ABBREVIATIONS

Au	gold
μA	microampere
μL	microliter
μM	micromolar
AA	L-ascorbic acid
AAP	2-phospho-L-ascorbic acid
AP	4-aminophenol
APP	*p*-aminophenyl phosphate
BDD	boron-doped diamond
CVD	chemical vapor deposition
^{o}C	degree celsius
E	potential
EIA	enzyme immunoassay
ELISA	enzyme-linked immunosorbent assays
E_p	peak potential
E_{pa}	anodic peak potential
E_{pc}	cathodic peak potential
g	gram
GC	glassy carbon
h	hour
HQ	hydroquinone
HQDP	hydroquinone diphosphate
i	current
IC	indigo carmine
IgG	immunoglobulin G
IP	3-indoyl phosphate
i_{pa}	anodic peak current
i_{pc}	cathodic peak current
j	current density
L	liter

LOD	limits of detection
M	molar
min	minute
mL	milliliter
nA	nanoampere
nm	nanometer
NP	4-nitrophenol
NPP	4-nitrophenol phosphate
NT	1-naphthol
NTP	1-naphthyl phosphate
o-ABA	o-aminobenzolic acid
Phe	phenol
PheP	phenyl phosphate
R^2	correlation coefficient
s	second
S/B	signal to background ratio
SEM	scanning electron microscopy
SPC	screen-printed carbon
V	volt
v/v	volume by volume
w/v	weight by volume
XPS	X-ray photoelectron spectroscopy

CHAPTER I

INTRODUCTION

1.1 Introduction

Nowadays, nanotechnology is playing an increasingly important role in the development of electrochemical sensors, biosensors, and immunosensors. Nanomaterials, or matrices with at least one of their dimensions ranging in scale from 1 to 100 nm, display unique physical and chemical features such as the quantum size effect, mini size effect, surface effect and macro-quantum tunnel effect. Classified by shape and structure, nanomaterials are quantum dots, nanotubes, nanofibers, nanobiomaterials of antibodies, and bacteria molecules. Immunosensors provide a simple and powerful tool for nanobiomaterials analysis of antibody or antigen molecules which can be applied to screening or even to quantitative method in relevant areas such as clinical, toxicological, and environmental monitoring.

In recent years, immunoassay has become an important analytical technique. Enzyme immunoassay is an analytical technique that relies on a specific immuno-interaction to quantitatively determine antibody or antigen present in an analyte by measuring the activity of an enzyme label conjugated to either the antibody or the antigen [1].

One of nanobiomaterials, Immunoglobulin G (IgG) is an antibody with a 150 kD monomer that constitutes approximately 75% of the total circulating immunoglobulin. Immunologically, IgG plays a major role in elimination of microbes by facilitating: (i) opsonization by phagocytes; (ii) antibody-dependent cell mediated cytotoxicity by natural killer cells; (iii) complement activation; and (iv) neutralization of viruses and toxins. Therefore, IgG is very well known as a model of immunosensor for use in comparison with other methods. Immunosensors have become an important feature of analytical technique. The choice of an enzyme immunosensor is based on the determination of the enzyme as a label [1]. The main advantage of using enzyme label is the remarkable signal amplification that can be

gained from the high turnover of enzyme product molecules. One of the excellent labeling enzymes currently in wide use for immunoassay is alkaline phosphatase (orthophosphoric monoester phosphohydrolase, ALP) [2]. Investigated for more than 70 years, ALP easily conjugates to haptens, antibodies, and other proteins, and has a high turnover number and broad substrate specificity.

Different substrates for ALP have been investigated in different detection systems such as spectrophotometry, fluorescence, chemiluminescence, bioluminescence, and electrochemistry. In electrochemical immunosensors, an ALP enzyme is used to generate organic electroactive products most of which can be detected and quantified. The electrochemical detector is generally sensitive and rapid for the redox reaction of the product of the enzyme hydrolysis of an ALP substrate. Several substrates for electroanalysis have been studied in immunoassays involving these enzymes such as catechol monophosphate, 3-indoyl phosphate (IP), hydroquinone diphosphate (HQDP), 4-nitrophenol phosphate (NPP), p-aminophenyl phosphate (APP), 1-naphthyl phosphate (NTP), phenyl phosphate (PheP), and 2-phospho-L-ascorbic acid (AAP). During the enzymatic process, these substrates are converted to electrochemical active species such as catechol, indigo carmine (IC), hydroquinone (HQ), 4-nitrophenol (NP), 4-aminophenol (AP), 1-naphthol (NT), phenol (Phe), and L-ascorbic acid (AA).

Electrochemical immunosensors, which combine specific immunoreactions with electrochemical transduction, have grown attention in recent years. Different electrode materials have been used for electrochemical immunosensors, including glassy carbon (GC) [3, 4], graphite [5], platinum [6, 7], screen-printed carbon (SPC) [7-13], iridium oxide [14], and gold (Au) [3, 7, 13]. The surface modified electrodes allow highly dense immobilization of biomolecules, long-term stability of attached biomolecules, low non-specific binding, and proper biomolecular orientation that permit simple and rapid specific interactions.

Au base is very good for using with self-assembled monolayers (SAM) as the base of the covalent bonding immunosensor with because of strong bonding between the Au surface and SAM and the ease of changing the Au surface to a COOH group. Therefore, SAMs of thiol are widely used as a scaffold to immobilize the primary antibody on Au surface. In this research, we also used a mixed SAM monolayer

modified on a Au electrode to convert the functional group on Au surface to carboxyl groups, which are used for forming the covalent bond with antibodies. Not only mixed SAM monolayer, but also the conduction of polymer were used as bases of sandwich immunoassay. Alternately, conducting polymers based on electrodes have gained increasing applications for the development of immunosensors. These polymers are poly(pyrrole), poly(aniline), poly(5, 2′:5′2″-terthiophene-3′-carboxylic acid), and poly(anionic perfluorosulfonated Nafion). Five main factors involved in the design of sensitive immunoassay are the orientation of the immobilized primary antibody, the format of the assay, the type of label used, the method of detection, and the minimization of non-specific binding.

Poly-*o*-aminobenzoic acid (poly-*o*-ABA), the derivative of polyaniline, was selected to be the base of covalent bonding for the immobilized primary antibody and was prepared by electropolymerization at the electrode surface. In previous studies, the electropolymerized *o*-ABA synthesis at Au, platinum, and GC were reported. These studies found that, the FTIR results showed carboxyl groups on the electrode surface, which were necessary for covalent bonding with the primary antibody.

For the new electrode material, boron-doped diamond (BDD) has many outstanding properties when compared to other electrode materials, including its physicochemical stability, wide electrochemical potential window, low background current, semimetallic electronic behavior, and chemical sensitivity [15]. This versatility makes BDD an excellent candidate for electrochemical uses with biochemical applications [16-18]. Immunosensing, a combination of specific immunoreaction with sensitive optical or electrochemical transduction, has attracted great attention due to its high sensitivity and specificity [6, 19, 20]. However, immobilization of biomolecules or proteins at BDD requires surface activation step since the inert nature of the diamond surface does not permit BDD to have stable and covalent bonds with any molecules [9, 21, 22]. The presence of a surface linker, such as carboxyl group or amine group, is needed for covalent bonding with the proteins. Polymerization at the BDD electrode can provide freely accessible carboxyl groups, which can also be used as a base for a biosensor. Gu group [8, 13] reported the impedimetric sensing of DNA hybridization on a polyaniline/polyacrylate (PANI/PAA)-modified BDD electrode. An ultrathin film of PANI/PAA copolymer

was electropolymerized onto the diamond surface to provide carboxylic groups for conjugation with DNA sensing probes. However, there has been only one report on the development of the BDD immunosensor in which impedancemetric detection of antigens was investigated [4].

This research aims to critically compare different substrates and products of the ALP enzymatic reaction towards the development of a sensitive electrochemical immunosensor. The seven products of substrates for the ALP reaction have been investigated by cyclic voltammetry and amperometry with three electrode materials which are Au disk, GC disk, and SPC. In addition, the best substrate was applied to classical amperometric immunosensors based on covalent bonding from SAMs in comparison with that of novel poly-*o*-ABA at Au electrode material. The poly-*o*-ABA base for covalent bonding immunosensors produces a higher signal. Therefore, this polymer was developed for the other electrode materials: GC disk, GC plate, SPC, and BDD for MIgG immunosensors. Poly-*o*-ABA-modified electrode surfaces can abundantly have carboxyl groups on the polymer surfaces, leading to fast and reliable amperometric responses. This research reports the investigation of amperometric immunosensors of protein attached with carboxyl groups of the modified electrodes. Poly-*o*-ABA was electropolymerized by simple cyclic voltammetry to generate carboxyl groups for the base of immunosensor at the electrode surface. Anti-mouse IgG (GaMIgG) has been used as a model antibody to be covalently immobilized with poly-*o*-ABA modified electrodes whereas mouse IgG (MIgG) was used as an antigen target for the detection. ALP conjugated GaMIgG was used as an enzyme label to prepare a sandwich type immunoassay. ALP assay using electrochemical detection has been reported [23, 24]. In this work, the ALP substrate with the highest product signal was selected. Conversion of the ALP substrate to its product will give an electrochemical signal relative to the quantity of the antigen target. The method was shown to be reproducible and very low detection limit was achieved. Application of the method to real sample analysis is also demonstrated.

1.2 Objectives of the research

MIgG is one of the interesting nanobiomolecules among nanomaterials. This research aims were fabricating and developing the sensitive amperometric immunosensor for MIgG detection using a sandwich immunoassay system. ALP was the chosen enzyme label. Seven products of ALP substrates were investigated to obtain the most effective substrate for amperometric immunosensor. In this research, conductive polymer and SAM were characterized and optimized as immunosensor bases. In addition, the best quality MIgG immunosensor was applied for a real sample analysis.

CHAPTER II

THEORY AND LITERATURE SURVEY

2.1 Nanomaterials

Nanotechnology deals with small structures or small-sized materials. The typical dimension spans from subnanometer to several hundred nanometers. A nanometer (nm) is one billionth of a meter, or 10^{-9} m. Fig. 2.1 gives a partial list of nanostructures with their typical ranges of dimensions. One nm is approximately the length equivalent to 10 hydrogen or 5 silicon atoms aligned in a line.
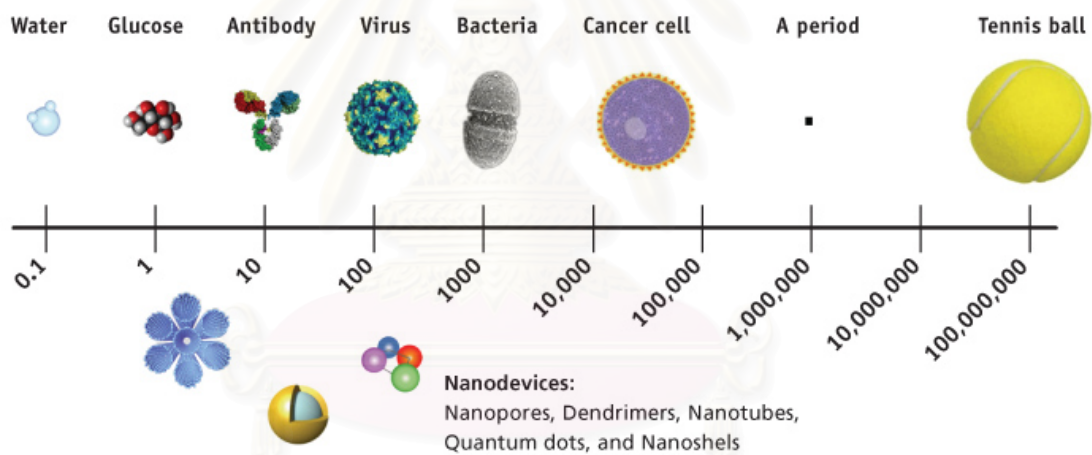
Figure 2.1 Nanotechnology scale

Nanotechnology is playing an increasingly important role in the development of electrochemical sensors and biosensors. Sensitivity and other attributes of biosensors can be improved by using nanomaterials in their construction. Nanomaterials, or matrices with at least one of their dimensions ranging in scale from 1 to 100 nm, display unique physical and chemical features because of their effects such as quantum size effect, mini-size effect, surface effect, and macro-quantum tunnel effect. Nanomaterials can be classified by shape and structure such as nanoparticles, nanotubes, nanofibers, nanorods, nanowires, and thin films. The nanobiomolecule of the antibody is also explained in this thesis.

2.2 Immunoglobulin [25, 26]

Serum contains a variety of proteins, some of which are called globulins. Their solubility properties are different from the other serum proteins. Antibodies are a subclass of serum globulins that possess selective binding properties. Antibodies are also called immunoglobulins (Ig).

All Igs have a number of structural features in common. They possess two light polypeptide chains with approximate molecular weights of 25 kDa and two heavy polypeptide chains of 50 kDa each. These four chains are bound together in a single antibody molecule by disulfide bonds and form a Y-shape with a central axis of symmetry (Fig. 2.2). The two halves of a natural Ig are identical. The N-terminal ends of the light polypeptide chains (L) occur near the top of the Y structure in the so-called F_{ab} fragments. These area are the antigen-binding fragments of the antibody and have been cleaved and used in immunoassays based on primary antigen-antibody interactions in the same manner as a whole antibody molecule is used. It is the amino acid sequence of these N-terminal ends that determine the specific antigen-binding properties of the molecule. The sequence of the heavy chains (H) called F_c fragments (crystallizable fragments) determines the antibody class: the highly abundant classes are called IgG, IgM, IgA, IgE, and IgD. Antibodies in different classes may have exactly the same antigen binding properties, but exhibit different functional properties. The abundance and functional properties of the five major classes of antibodies are listed in Fig. 2.3 and Table 2.1.
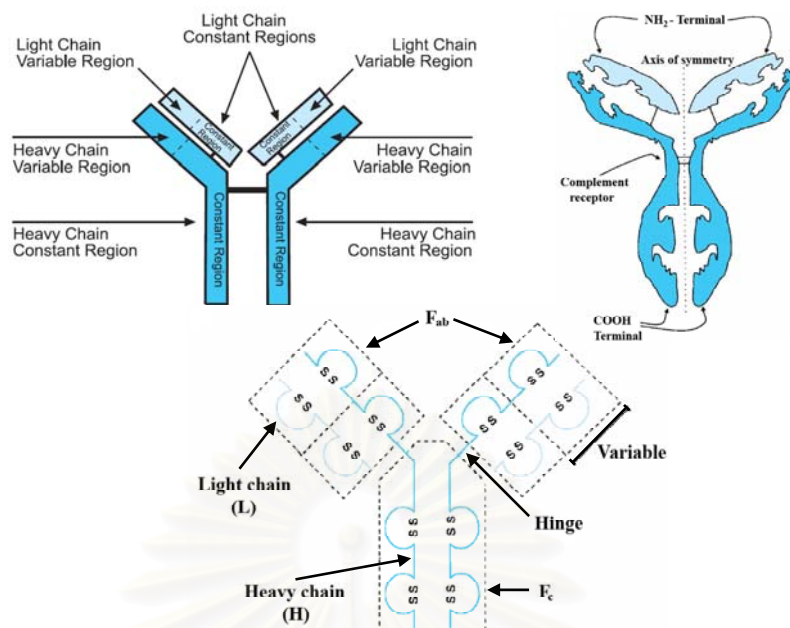
Figure 2.2 General structure of an antibody molecule (Ig). Monomeric Ig molecule consists of two identical light chains covalently linked to two identical heavy chains.
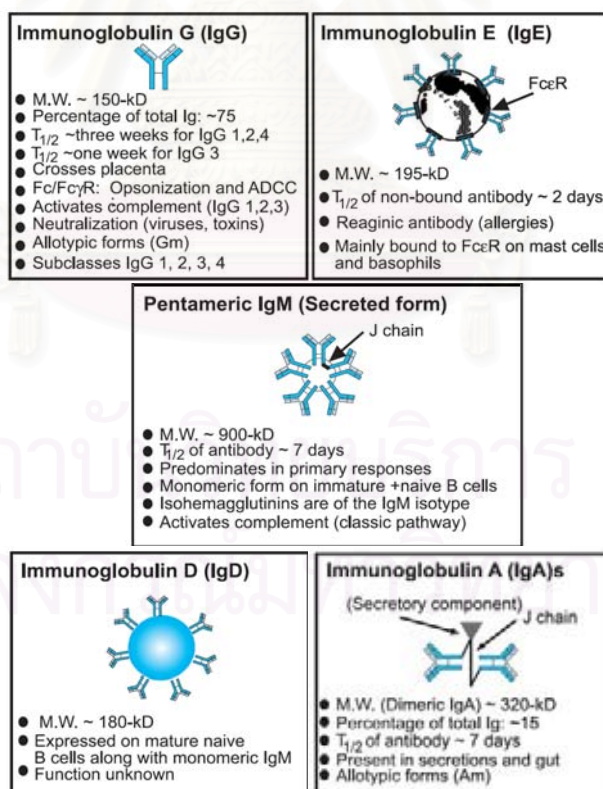
Figure 2.3 Properties of Ig isotypes

Table 2.1 Biological properties of Ig isotypes

	IgG	IgA	IgM	IgD	IgE
[Serum] (mg/dl)	~1200	~100	~150	Negligible	Negligible
Percent of Total Serum Ig	~80	~14	~7	Negligible	Negligible
Form in Serum (typical)	Monomer	Monomer, Dimer	Pentamer	Monomer	Monomer
Molecular Weight (kD)	~150	~160 (Monomer)	~900	~180	~200
% Carbohydrate	~3	~7	~10	~10	~12
Covalent Attachments	–	J chain Secretory Component	J Chain	–	–
Distribution	Vascular (intra and extra)	Vascular (intra) + Mucosa	Vascular (intra)	Membrane (naive B cells)	FcεR on Mast cells, Basophils
Subclasses	4	2	–	–	–
Allotypes	20 (Gm)	2 (Am)	–	–	–
# Fabs (Valence)	2	2 or 4	10	2	2
Milk and Colostrum	+	+++	–	–	–
Placental Transfer	++	–	–	–	–
Agglutinating Capability	+	+ (Monomer)	+++	–	–
Complement Activation (Classical Pathway)	+ (not IgG4)	–	+++	–	–
Complement Activation (Alternative Pathway)	–	Aggregated Form	–	–	–
Reaginic Antibody (Allergic Activity)	–	–	–	–	+++
Half Life	IgG 1,2,4 ~ 21 days IgG3 ~ 7 days	~ 5 days	~ 5 days	~3 days	~ 2 days (unbound)

Immunoglobulin G (IgG) is a 150 kD monomer (Fig. 2.2 and Table 2.1) that constitutes approximately 75% of the total circulating Ig. IgG circulates between blood and interstitial fluid [~12 mg/ml] with a half-life of about three weeks. IgG antibodies can be transported across the placenta and enter the fetal circulation so that the mother's immunity is transferred to the fetus. Immunologically, IgG plays a major role in elimination of microbes by facilitating:

(i) opsonization which refers to phagocytosis that is triggered following binding of the F_c region of antibodies, bound by the pathogen, to $F_c\gamma R$ on phagocytes.

(ii) antibody-dependent cell mediated cytotoxicity which refers to the process by which natural killer cells interact with, and destroy, target cells coated with antigen specific IgG. Natural killer cells express a low affinity towards $F_c\gamma R$ whose interaction with target cell-bound IgG triggers the release of molecules cytotoxic to target cells.

(iii) complement activation which requires that IgG is a component of an immune complex. A complement protein binds the IgG complex and triggers the activation of the complement cascade.

(iv) neutralization of viruses or toxins which results when IgG antibody binds antigen to inhibit the antigen's ability to bind with a cell surface receptor.

In humans, IgG is further subclassified as IgG1, IgG2, IgG3, and IgG4, differing from one another in their constant regions. Because biological potential is mediated via the F_c portion of IgG, it is not surprising that minor differences in function are observed among subtypes, including differences in serum concentration, half life, and relative biological potency. IgG1 is present in the highest concentration (9 mg/ml) whereas IgG4 is in the lowest (0.5 mg/ml). IgG3 has a half life of only one week, but it is the most effective (classic pathway) activator of complement of all IgG subtypes. IgG4 does not activate complement at all, nor does it bind to $F_c\gamma R$.

2.3 Biosensor

A biosensor is a device having a biological sensing element either intimately connected to or integrated within a transducer. The aim is to produce a digital electronic signal, which is proportional to the concentration of a specific chemical or set of chemicals. Biosensor instruments are specific, rapid, and simple to operate and can easily be fabricated with minimal sample pretreatment. One definition of a biosensor is a sensing device that incorporates a biological entity (enzyme, antibody, bacteria tissue, etc.) as a fundamental part of the sensing process.
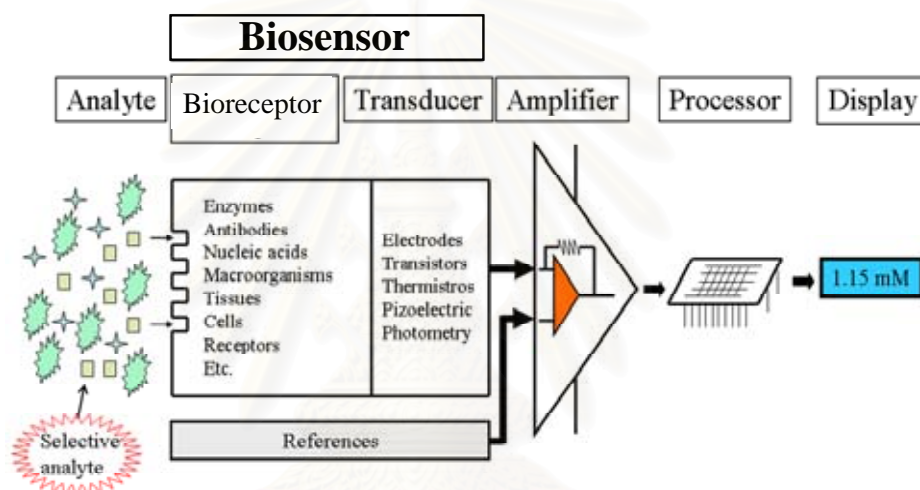
Figure 2.4 The conceptual diagram of biosensor combined with amplifier, signal processing, and readout devices

Nowadays, the electrochemical biosensors have been widely used and rapidly developed in many laboratories. Three main types of electrochemical biosensors are classified as (i) potentiometric, (ii) amperometric and (iii) conductometric sensors. For potentiometric sensors, when a local equilibrium is established at the sensor interface, where either the electrode or membrane potential is measured. Information about the composition of a sample is obtained from the potential difference between two electrodes. Amperometric sensors exploit the use of a potential applied between a reference and a working electrode, to cause the oxidation or reduction of an electroactive species; the resultant current is measured. While the conductometric sensors involve with the measurement of conductivity of

the solution between two electrodes. The adapted conceptual diagram of a general sensor is illustrated in Fig. 2.4, consisting of recognition and signal elaboration parts.

Electrochemical sensors are becoming increasingly important in three main areas: (i) health care, (ii) industrial control process, and (iii) environmental monitoring. In health care, samples might be blood, urine, gases, ions, oxidizable and reducible substances, and metabolites. Selected sensors are applied for indicating a patient's metabolite state. Many substances such as sodium, potassium, calcium, insulin, and glucose have been considered in routinely diagnostic work within patients.

2.3.1 Enzyme reaction

Enzymes are amphoteric molecules containing a large number of acidic and basic functional groups, mainly situated on their surfaces. The alternation of surface charges depends on their dissociation constants, ionic strength, and pH. This will affect the reactivity of the catalytically active groups, which are especially important in the neighbourhood of the active sites. The changes in charges with pH affect the activity, structural stability, and solubility of the enzyme.

The roughly 3,000 enzymes currently known are grouped into six main classes according to the type of catalyzed reaction. At present, only a limited number are used for analytical purposes.

2.3.1.1   *Oxidoreductases* catalyze redox reactions in which hydrogen atoms, oxygen atoms, or electrons are transferred between molecules. Their analytical importances are:

- *dehydrogenases* catalyze hydrogen transfer from the substrate; S to an acceptor, A (which is not oxygen molecule):

$$SH_2 + A \longrightarrow S + AH_2 \qquad\qquad (2.1)$$

- *oxidases* catalyze hydrogen transfer from the substrate to molecular oxygen:

$$SH_2 + 1/2O_2 \longrightarrow S + H_2O \qquad \text{or} \qquad (2.2)$$

$$SH_2 + O_2 \longrightarrow S + H_2O_2 \qquad (2.3)$$
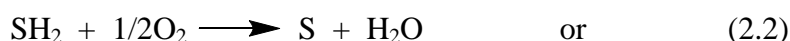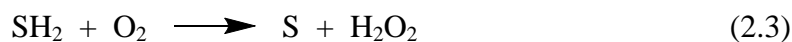
- ***oxygenases*** catalyze the oxidation of substrate by molecular oxygen with a hydrogen donor which may be the substrate itself:

$$SH + DH_2 + O_2 \longrightarrow S\text{-}OH + D + H_2O \qquad (2.4)$$

- ***peroxidases*** catalyze the oxidation of a substrate by hydrogen peroxide:

$$2SH + H_2O_2 \longrightarrow 2S + 2H_2O \quad \text{or} \qquad (2.5)$$

$$2S + 2H^+ + H_2O_2 \longrightarrow 2S^+ + 2H_2O \qquad (2.6)$$

2.3.1.2 Transferases catalyze the transfer of an atom or a group of atoms (e.g., acyl-, alkyl-, and glycosyl-) between two molecules, but some transfers (e.g., oxidoreductases and hydrolases) are classified in the other groups.

$$AX + B \longrightarrow A + BX \qquad (2.7)$$

2.3.1.3 Hydrolases catalyze the hydrolytic reactions and their reversal. This is presently the most commonly encountered class of enzymes within the field of enzyme technology. They include esterases, glycosidases, lipases, and proteases. For example; alkaline phosphatase (EC 3.1.1.1.3) undergoes the following reaction:

$$RHPO_4^- + H_2O \xrightarrow{\text{ALP}} ROH + H_2PO_4^- \qquad (2.8)$$
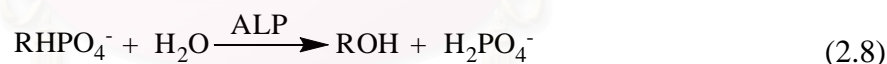
2.3.1.4 Lyases eliminate reactions in which a group of atoms is removed from the substrate. They include aldolases, decarboxylases, dehydratases, and some pectinases, but not hydrolases.

2.3.1.5 Isomerases catalyze molecular isomerizations and includes the epimerases, racemases and intramolecular transferases.

2.3.1.6 Ligases, also known as synthetases, form a relatively small group of enzymes which involve the formation of a covalent bond joining two molecules together.

2.3.2 Immunoassay [26]

The classical chemical analysis paradigm used to identify and quantitate an analyte of interest includes isolation of the analyte, separation of the analyte from other potentially interfering substances, and quantitation by instrumental or other methods. These classical methods have many shortcomings including being highly labor intensive and requiring capital expenditures for expensive equipment (i.e., gas chromatographs, liquid chromatographs, mass spectrometers, or combination of these instruments). In addition, recoveries during the separation and isolation phases of the paradigm may not be constant, and in some cases, may be associated with the level of analyte in the original sample, potentially yielding confounding systematic errors. Despite these shortcomings, however, with adequate control, classical chemical biological monitoring has the capacity to quantify the body burden of substances to the sub-ppb level. Alternatives to classical chemical analyses are immunoassays.

Immunoassays [27], especially enzyme immunoassays (EIAs) and enzyme-linked immunosorbent assays (ELISAs), are commonly used analytical techniques for clinical diagnostic measurements, drug screening, and measurements for evaluating exposure to environmental agents. The first ELISA was described in 1971. Recently, immunoassays have been shown to be useful in evaluating exposure to bioterrorism agents such as anthrax. Immunoassays are based on the formation and detection of immune complexes between antigens and antibodies. Antigens are principally macromolecules (proteins, polysaccharides, nucleic acids) that can completely act as immunogens stimulating an immune response. Other substances are too small to act as immunogens on their own (drugs, pesticides, etc.) and must be coupled with a macromolecular carrier molecule (usually a protein) to become immunogenic and elicit an immune response. These small molecules are called haptens. Many environmental agents (such as pesticides and pesticide metabolites) are haptens. The selection of the protein carrier used to form the hapten-protein conjugated immunogen is important. The number of haptens bound to the carrier, the chemistry of the conjugation reactions, as well as other factors will all impact the final affinity and avidity of the resultant antibodies. The purity of the hapten is also important since the conjugation of closely related structures with the carrier may result in the formation of non-specific antibody. Spacer molecules are often used in

conjugation with haptens to attempty increase the specificity of the antibody for the conjugated hapten. The ability of an antibody (Ab) molecule to bind an antigen (Ag) or a hapten is specifically controlled by structural and chemical interactions between the Ag and the Ab at the combining site. The Ag–Ab interaction is reversible and does not involve the formation of covalent bond. This interaction is controlled by the law of mass action:

$$Ag + Ab \longrightarrow AgAb \tag{2.9}$$

and
$$K = \frac{[AgAb]}{[Ag]\,[Ab]} \ mol^{-1} \tag{2.10}$$

where K is the affinity constant and AgAb is the Ag-Ab complex. High affinity constant, resulting from strong Ag-Ab interaction, lead to lower limits of detection (LOD) in immunoassays.

ELISAs can be performed in many different formats (direct, indirect, capture, competitive, etc.). In the following descriptions, general overviews of ELISA formats are given. Many variations of these general formats have been utilized to detect numerous analytes, the details of which would be too exhaustive to be reviewed.

- In a direct ELISA (Fig. 2.5), the most basic ELISA format, an analyte (hapten, Ab, and Ag) is attached to a solid support. An Ab, specific for the analyte and containing a reporter system (usually an enzyme), is incubated with the captured analyte. After washing, a chromogen (enzyme substrate) is added and allowed to react, forming a colored product.

- In an indirect ELISA (Fig. 2.5), an analyte (hapten, Ab, and Ag) is again attached to a solid support. A primary Ab, specific for the analyte, is incubated in the system and the excess is removed by washing. A secondary labeled Ab, specific for the primary Ab, is added to the system and incubated. After washing, chromogen is added and the color is measured by a spectrophotometer or other instrument. The amount of color produced is proportional to the amount of secondary Ab that was bound.

In Fig. 2.5 shows the process of direct and indirect immunoassay. In a direct assay (a), analyte (hapten, Ab, or Ag) is bound to a solid support (bead or

microplate). Reporter labeled Ab is introduced to the immobilized analyte, forming an Ag-Ab complex. After washing, the concentration of analyte is measured by radiometric, colorimetric, or fluorometric detection of the reporter system. In an indirect format (b and c), primary Ab specific for the analyte is introduced to the solid-support bound analyte. After washing, secondary Ab labeled with reporter, specific for the primary Ab, is added to the system. The concentration of analyte is measured by radiometric, colorimetric, fluorometric, or amperometric detection of the reporter system.

- ELISAs may also be designed in capture format (Fig. 2.6). In an Ag capture (sometimes called sandwich) ELISA, an Ag is captured by specific Ab that has been attached to the solid support. After washing, another labeled Ab, specific for another epitope on the Ag, is added. After incubation and washing, chromogen is added and the resulting color is measured by a spectrophotometer. ELISAs may also be designed as Ab capture ELISAs that are performed in a similar fashion to Ag capture ELISAs, except that the analyte of interest is an Ab. Another format of ELISA is the competitive ELISA.

- In a competitive ELISA (Fig. 2.6), the analyte (either Ab or Ag) competes with labeled analyte for binding. With higher concentrations of analyte, less of the labeled analyte is bound, yielding the reduction of signal. In the modification of this format (blocking ELISA), an unlabeled analyte is added prior to the addition of the labeled analyte.

In Fig. 2.6 shows the process of capture and competitive immunoassay. In an Ag capture (sandwich) assay, Ab, specific for the analyte, is bound to a solid support. Added analyte is bound by the first specific Ab (a). After washing, another reporter labeled Ab, specific for another epitope on the Ag, is added (b). Concentration of analyte is measured by radiometric, colorimetric, or fluorometric detection of the reporter system. In a competitive assay, analyte and a reporter labeled analyte are allowed to compete for binding sites with the immobilized Abs (c) and bind with Ab in relation to their relative concentrations (d). The concentration of analyte is measured by radiometric, colorimetric, fluorometric, or amperometric detection of the reporter system. With higher concentrations of analyte, less of the labeled analyte is bound yielding reduced signal.

In most ELISAs, Ag or Ab is coated onto microwell plates by electrostatic attraction and van der Waals force. The Ag or Ab is diluted in coating buffer to assist its immobilization on to the microplate. Commonly used coating solutions are sodium carbonate, Tris-HCl, and phosphate buffered saline. In order to minimize nonspecific binding to the microtiter plate, solution of protein is used for blocking the unbound sites. Commonly used blocking agents are bovine serum albumin, nonfat dry milk, casein, etc.
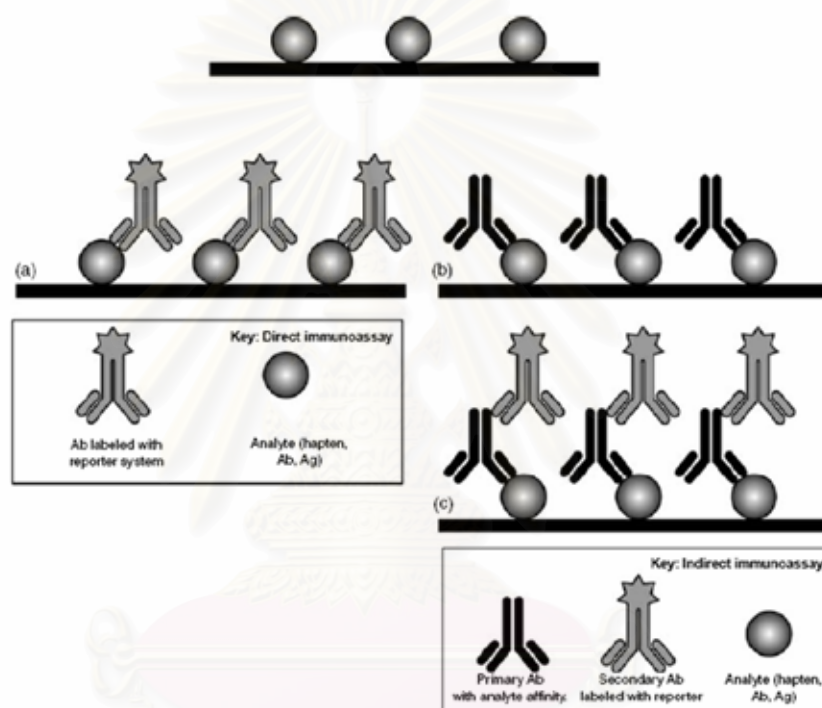
Figure 2.5 Direct and indirect immunoassay
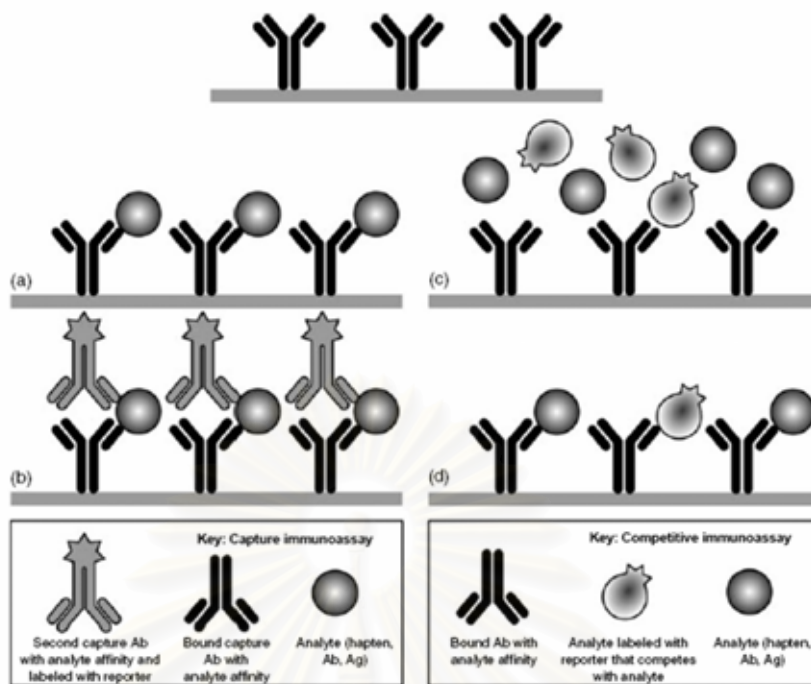
Figure 2.6 Capture and competitive immunoassay

2.3.3 Immobilization of biomolecules for biosensors

For biosensors, the preparation of biosensing surface is significantly important. The surface is made up of enzymes, antibodies, microorganisms, mammalian cells, tissues, or receptors immobilized on to a solid surface. A number of established immobilization procedures are currently used. These include:

2.3.3.1 Physical adsorption on to a solid surface

Immobilization via physical attraction or adsorption is not a reproducible and reliable method for biomolecule attachment to sensing surfaces because of the problems associated with leaching during long-term storage. Plastic, glass, and cellulose have been known to adsorb proteins via binding forces such as hydrogen bonds, van der Waals forces, salt linkages, and hydrophobic interactions. Such forces are not very stable and can be easily disrupted by changes in pH, temperature, and ionic strength. Excess protein can also form multiple layers during adsorption. The obvious advantages of adsorption as a mean of immobilization are simplicity and gentleness.
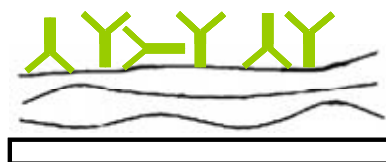
Figure 2.7 Physical adsorption on to a solid surface

2.3.3.2 Use of crosslinking reagent

Stabilization of adsorbed proteins can be achieved by using bifunctional crosslinking reagent such as glutaraldehyde. The proteins are crosslinked to each other or inert proteins such as bovine serum albumin can be mixed with the desired protein prior to crosslinking process. This method adds greater stability to the immobilized protein, although inevitably, some inactivation does occur since the crosslinking chemical may interact with the protein active site, especially the case of enzyme. With respect to immunosensors, the Ab binding site may be blocked or incorrectly oriented causing less favor able condition for Ab-Ag binding. Membranes can be cast on the electrode surface using this method.

2.3.3.3 Entrapment using a gel or polymer

Immobilization of biomolecules by physical entrapment in gel matrices such as polyacrylamide and gelatin is performed in this method.

Figure 2.8 Entrapment using a gel or polymer

2.3.3.4 Use of membrane to retain the biomolecule close to the electrode surface

Membranes with various porosities can be used to retain molecules close to transducer surfaces without the need of actual immobilization. This gentle method of retention can, however, lead to problems such as diffusional resistance. Selective membranes can also be employed in conjunction with potentiometric electrodes. Ion-selective membranes, such NH_4^+ selective membrane,

have been employed in conjunction with the enzyme urease for the measurement of urea.

2.3.3.5 Covalent attachment

Chemical coupling of biomolecules may provide stable biosensing surface that are resistant to wide ranges of pH, temperature, and interfering ions. However, covalent binding can result in some loss in bioactivity. Three types of supports have been used: inorganics, natural polymers, and synthetic polymers. The binding process must occur under conditions that do not denature the biomolecule. Often, the carrier must be activated in some way, and the introduced functional groups are then utilized for chemical coupling either directly to the biomolecule or via a crosslinking reagent such as glutaraldehyde.
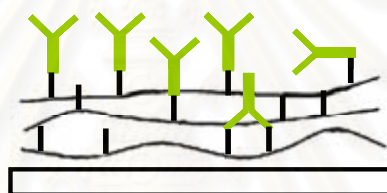
Figure 2.9 Covalent attachment

2.4 Electrochemical methods [28, 29]

The electrochemical techniques are classified by the International Union for Pure and Applied Chemistry (IUPAC) on the basis of their working principles. The different classes of electrochemical techniques are electrolytic, potentiometric, conductometric, polarographic or voltammetric, amperometric, impedimetric, and coulometric methods. In potentiometry, measurements are based on the equilibrium potential existing between a selective electrode and a reference electrode. The detection limit of this technique is in the range of micro molar. However, the detection limit of voltammetry is better than that of potentiometry, hence the latter technique can be used precisely for trace analysis. Although many electrochemical methods are available, only cyclic voltammetry, and amperometry are used thoroughly in the thesis.

2.4.1 Cyclic voltammetry

Cyclic voltammetry is a completed voltage scan (y axis) versus time (x axis) in forward and backward directions, as shown in Fig. 2.10. The voltage scan reverses the direction after the current maximum (peak) of the forward process has been passed. The backward scan gives signal in the opposite direction from the forward scan. This technique provides information about the properties and characteristics of the electrochemical process and also gives insight into any complicating side processes such as pre- and post-electron-transfer reactions as well as kinetic considerations.
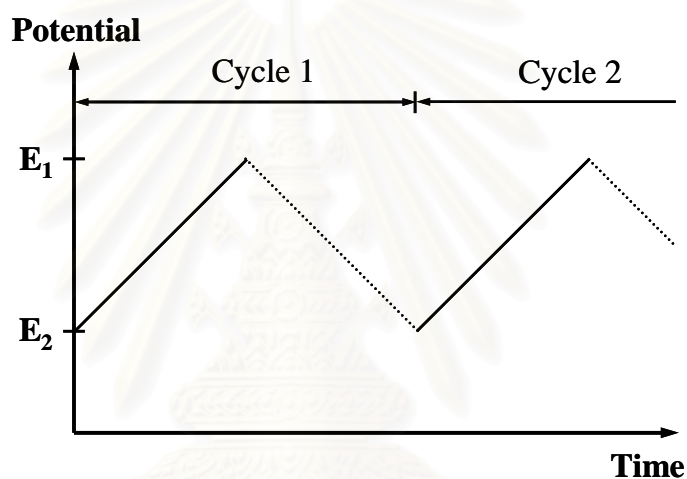
Figure 2.10 Potential-time profile used for cyclic voltammetry. Solid line represents forward scan and dashed line represents backward scan.

Fig. 2.11 illustrates the shape of a reversible cyclic voltammogram with an electrode of fixed area. The voltammogram is characterized by a peak potential, E_p, at which the current reaches its maximum value and that value is called the peak current, i_p. The $i_{p,a}$ and $E_{p,a}$ are anodic peak current and anodic peak potential , respectively. The $i_{p,c}$ and $E_{p,c}$ are cathodic peak current and cathodic peak potential, respectively.

The peak current is given by the Randles-Sevcik equation

$$i_p = 2.69\times10^5 n^{3/2} A D^{1/2} C v^{1/2} \qquad \text{at 25 °C} \qquad (2.11)$$

where i_p is in A, A (electrode area) is in cm^2, D (diffusion coefficient) is in cm^2 s^{-1}, C (concentration of electroactive species) is in mol cm^{-3}, and v (scan rate) is in V s^{-1}.
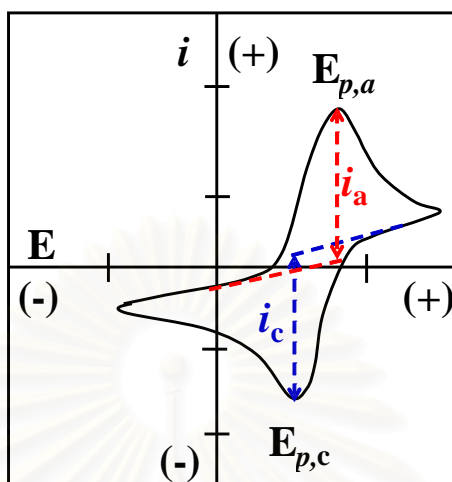
Figure 2.11 Typical reversible cyclic voltammetry with the initial sweep direction towards more positive potential.

The useful parameter of the voltammetric curve is the half-peak potential, $E_{p/2}$, which is the potential at which the registered current reaches half of its maximum value and is used to characterize a voltammogram. For a reversible process, $E_{1/2}$ is located halfway between E_p and $E_{p/2}$. The ratio of the peak current for the cathodic process relative to the peak current for the anodic process is equal to unity ($i_{p,c}/i_{p,a} = 1$). To measure the peak current for the cathodic process, the extrapolated baseline going from the foot of the cathodic wave to the extension of this cathodic current beyond the peak must be used as a reference, as illustrated in Fig. 2.11. The difference in the peak potentials between the anodic and cathodic processes of the reversible reaction is given by:

$$\left| \Delta E_p \right| = \left| \Delta E_{p,a} - \Delta E_{p,c} \right| = \frac{0.059}{n} \tag{2.12}$$

which provides a rapid and convenient means to determine the number of electrons involved in the electrochemical reaction. For a reversible system, i_p is a linear function of $v^{1/2}$, and E_p is independent of v.

2.4.2 Amperometry

Amperometry is an electrochemical technique for the measurement of current when a fixed potential is applied on a working electrode. Heterogeneous electron transfer reactions, i.e., the oxidation and reduction of electroactive substance, take place on the working electrode. The reaction is considered as a set of equilibrium involving the diffusion of the reactant to the electrode, the reaction at the electrode, and the diffusion of the product away from the electrode surface into the bulk solution.

All amperometric determination ultimately depends upon Faraday's law,

$$Q = nFN \tag{2.13}$$

where Q is the number of coulombs used in converting N moles of material, n is the number of electron equivalent lost or gained in the transfer process per mole of material, and F is Faraday's constant. Q is respect to current, i, by

$$\frac{dQ}{dt} = i = nFA\frac{dN}{dt} \tag{2.14}$$

and mass transfer is given by

$$\frac{dN}{dt} = -D\left(\frac{dC_{x,t}}{dx}\right)_{x=0} \tag{2.15}$$

Under controlled hydrodynamic conditions, the rate of the whole process is controlled by diffusion mass transfer. The diffusion current, i_d is directly proportional to the concentration of the electroactive substance, C:

$$i_d = nFAD\frac{C}{\delta} \tag{2.16}$$

where δ is thickness of the diffusion layer (being constant at a given convection). Low detection limit and wide linear measuring range are the main advantages of amperometry techniques.

2.5 Electrochemical cells

The three electrode system consisting of working, reference, and counter electrodes is commonly used for voltammetric, and amperometric techniques. The current or charge from the occurring reaction is measured at the electrochemical cell where the three electrodes are placed.

The placement of the electrodes is an important factor for the cell performance. The electrodes should be arranged in a way that: (i) provides a symmetrical electric field and uniform current distribution across the working electrode surface and (ii) minimizes the ohmic potential (iR_u) drop between the working and the reference electrodes.

The first requirement can be satisfied by having a symmetrical arrangement of the working and counter electrodes. Planar electrodes placed parallel to each other, or cylindrical or spherical working electrodes placed in the center of concentric counter electrode are the suitable arrangements. The requirement of minimal iR_u drop can be achieved by placing the tip of the reference electrode close to the working electrode. While the iR_u drop between the reference and counter electrodes is corrected by the potentiostat, the iR_u drop between the reference and working electrodes remains uncompensated, and therefore the actual working electrode potential can be in error. Althrough the iR_u drop is usually small, the use of Luggin capillary, a device that effectively allows the placing of the reference electrode tip very close to the working electrode surface, is advisable for accurate work. As a general rule, it is recommended that the reference electrode should be placed close to the working electrode in a line between the working and counter electrodes.

The design of the cell and the materials used in its construction must be chosen according to the nature of the sample and the experiments. Cells are usually constructed from glass or quartz. Advantages such as cost, high chemical resistance, impermeability, and transparency make glass the most convenient and satisfactory material. For work with substances that react with glass, a range of polymers such as Teflon, Kel-F, Nylon, and polyethylene are suitable.

In its simplest form, an electrochemical cell is a beaker or similar container, with a plastic top which allows insertion of the three electrodes as displayed in Fig. 2.12. There is normally a fourth hole to allow the introduction of a nitrogen gas line. Purging the solution with nitrogen to eliminate oxygen is usually necessary, particularly for the monitoring of processes at negative potentials.

Figure 2.12 Schematic diagram of electrochemical cell. WE, CE, and RE are working, counter, and reference electrodes, respectively. N_2 is nitrogen gas.

2.6 Working electrode

The performance of the voltammetric procedure is strongly influenced by the material of the working electrode. The working electrode should provide high signal-to-noise characteristic, as well as reproducible response. Thus, its selection depends primarily on two factors: the redox behavior of the target analyte and the background current over the potential region required for the measurement. Other considerations include the potential, electrical conductivity, surface reproducibility, mechanical properties, cost, availability, and toxicity. A range of materials have been applied as working electrodes for electroanalysis.   The most popular materials are those involving mercury, carbon, and noble metals (particularly platinum and gold). This research will focus on using carbon and metal electrodes.

2.6.1 Carbon electrode

Carbon exists in various conductive forms and its electron transfer kinetics depends on structure and surface preparation. Electrochemical reactions at carbon are normally slower than those of metallic electrodes. Carbon is the most commonly used electrode material in electroanalytical chemistry and it is available in a variety of microstructures: graphite, glassy carbon, carbon fiber, nanotube, amorphous powders, and diamond. They are all sp^2 carbons, except the diamond electrode which contains sp^3 carbons.

2.6.1.1 Glassy carbon (GC)

Glassy carbon (GC), also referred to as vitreous carbon, is the most commonly used carbon electrode for electroanalysis. It is available in a variety of architectures including rods, disks, and plates. GC is hard and microstructurally isotropic (same properties in all directions). The manufacture of GC consists of carbonization by heating phenol/formaldehyde polymers or polyacrylonitrile between 1,000°C and 3,000°C under pressure. Two peaks are present in the Raman spectrum for GC at 1,350 and 1,580 cm^{-1} with the ratio of the two peaks reflecting the extent of microstructural disorder. Since GC has some amorphous characteristics, as in Fig. 2.13, it is not always homogeneous. Typical 1,350-to-1,580 cm^{-1} peak intensity ratios are in the range of 1.3-1.5. The material possesses a complex surface chemistry consisting of various types of carbon–oxygen functional groups at the graphitic-edge-plane sites.
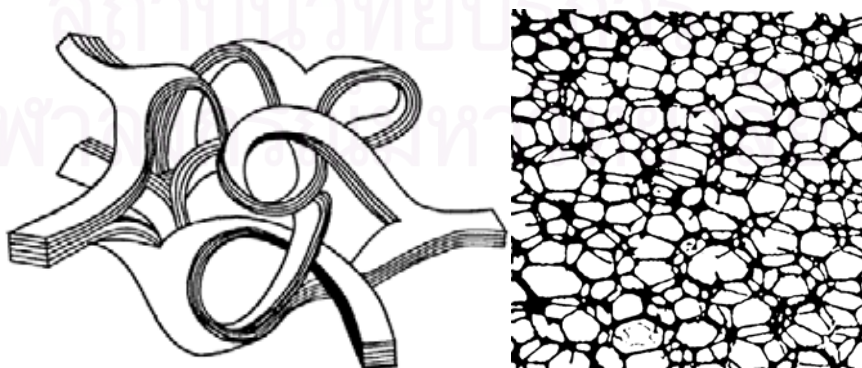
Figure 2.13 Representation of the ribbon structure of GC and the open-pore structure of vitreous carbon foam (adapted from [30])

2.6.1.2 Screen-printed carbon (SPC)

Screen-printing technology is a technique often used in the fabrication of electrodes for the development of disposable electrochemical biosensors [31]. A screen printed electrode is a planar device based on multiple layers of a graphite-powder-based ink printed on a polyimide, plastic, epoxy or alumina ceramic substrates. Graphite's structure is shown in Fig. 2.14. The advantages of designable techniques, adapted from microelectronics, have made screen-printing technology one of the most important technique for fabrication of single-use biosensors in the market of handheld instruments. The main advantages of the screen printed electrode include simplicity, versatility, modest cost, portability, ease of operation, reliability, small size, and mass production capabilities, which lead to its development in various applications in the electroanalytical field.
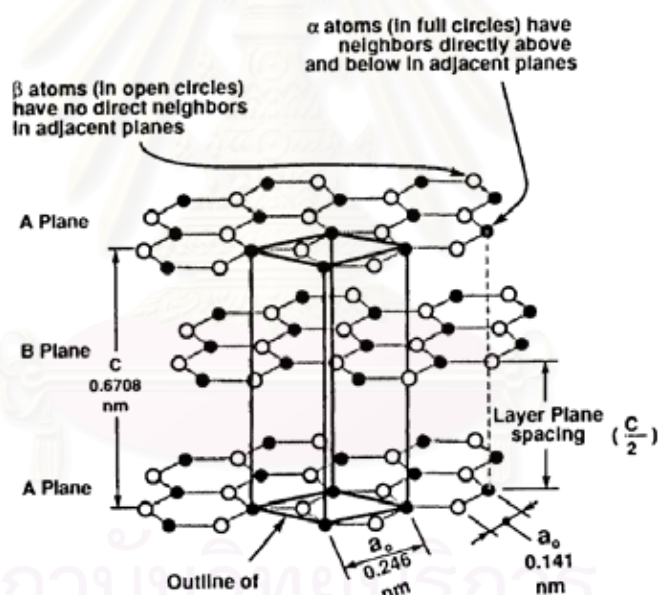
Figure 2.14 Crystal structure of graphite showing ABAB stacking sequence and unit cell (adapted from [30])

2.6.1.3 Boron-doped diamond (BDD) **[15, 29]**

Electrically conducting diamond is a new type of carbon electrode material that is beginning to find widespread use in electroanalysis. The material possesses superior properties than other forms of carbon including (i) low and stable background current over a wide potential range, (ii) wide working potential

window in aqueous media, (iii) relatively rapid electron-transfer kinetics for several redox systems without conventional pretreatment, (iv) weak molecular adsorption, (v) dimensional stability and high corrosion resistance, and (vi) optical transparency. The material is now available from several commercial sources and is not overly expensive, as commonly perceived. An SEM image of boron-doped crystalline diamond is shown in Fig. 2.15.
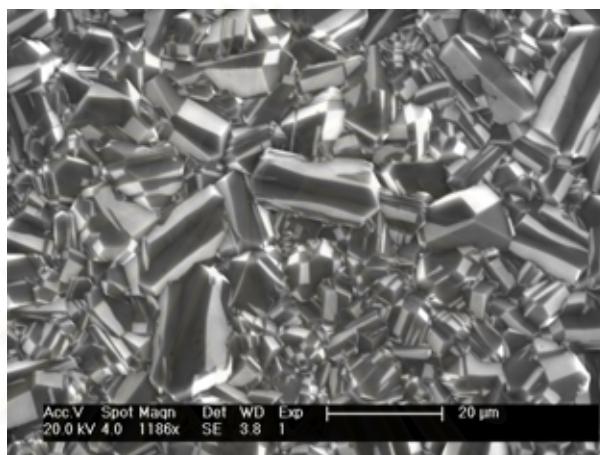
Figure 2.15 SEM image of a boron-doped crystalline diamond thin film grown on Si

Diamond is often grown as a thin film on a conducting substrate, such as highly doped Si, Mo, W, or Ti, using microwave plasma, hot-filament, or combustion flame-assisted CVD methods. The most common method is microwave plasma CVD because of the commercial availability of such reactor systems. While the mechanisms of film growth are somewhat different among each methods, all of them serve to activate a carbonaceous source gas producing a growth precursor in close proximity to the substrate surface. A typical CVD reactor consists of the growth chamber and equipment associated with the particular activation method (e.g., microwave power source) as well as various accessories such as mass flow controllers for regulating the source gases, a throttle exhaust value and controller for regulating the system pressure, a pumping system, temperature measurement capability, and the gas handling system for supplying the source gases. A block diagram of a typical CVD system is shown in Fig. 2.16. In the case of microwave assisted CVD, the microwave energy from the generator is pointed to, and focused within, a quartz cavity producing a spherically shaped, glow-discharge plasma directly above the substrate. The substrate can be positioned either outside of (few

mm), or immersed within, the intense discharge region. The plasma is where the reactive species involved in the diamond growth are formed. The key deposition parameters are the source gas composition, microwave power, system pressure, and substrate temperature.
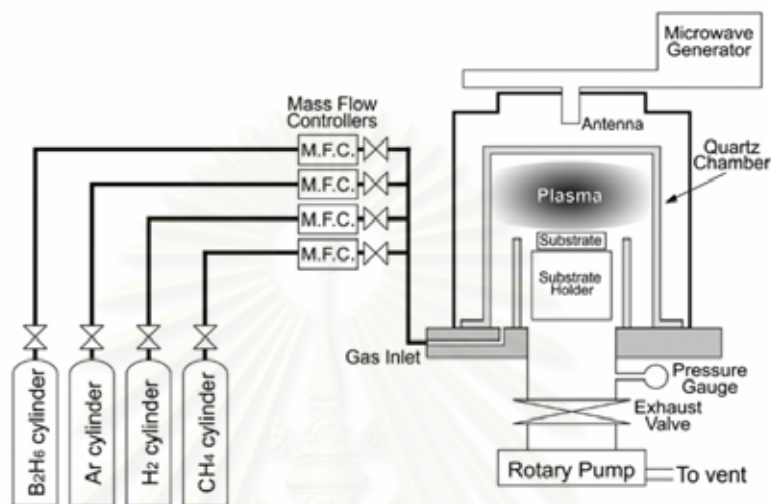
Figure 2.16   Block diagram of a typical microwave plasma CVD reactor (adapted from [29])

Diamond is one of nature's best electrical insulators. In order to have sufficient electrical conductivity for electroanalytical measurements (<10 S cm^{-1}), diamond films must be doped. The most common dopant is boron with doping levels in the $1 \times 1,019$ cm^{-3} range or greater, being the norm. The introduction of boron imparts *p*-type electrical properties to the film. Other dopants have also been used, such as nitrogen, phosphorous, and sulfur, but all of them suffer from either low solubility or high activation energy. The boron can be added to the source gas mixture in the form of B_2H_6 or $B(CH_3)_3$. B_2H_6 is the preferred gas because $B(CH_3)_3$ adds not only boron, but also extra carbon to the source gas mixture. This extra carbon can alter the film morphology and decrease the film quality. The electrically active boron is that which substitutionally inserts into the growing carbon lattice. The films are rendered electrically conducting through incorporation of boron dopant atoms during deposition even though the electrical conductivity depends in a complex manner on lattice hydrogen, defects, and dangling bonds, in addition to the boron doping level. For example, films can be doped as high as $1,021$ cm^{-3} with little alteration of the

morphology or microstructure. Typical film resistivities are $<0.05\ \Omega$ cm, carrier concentrations are $1{,}019$ cm^{-3} or greater, and carrier mobilities are in the range of 0.1-10 cm^2 V^{-1} s^{-1}. So far, there have been a few studies of how to activate diamond electrodes for electron transfer. Actually, one of the interesting features of this electrode material is the fact that pretreatment is usually not required to achieve an "activated" electrode. The most active surface tends to be the hydrogen-terminated one.

2.6.2 Metal electrodes

While a wide choice of noble metals is available, platinum and gold are the most widely used metallic electrodes. Such electrodes offer a very favorable electron-transfer kinetics and large anodic potential range. In contrast, the low hydrogen overvoltage of these electrodes limit the cathodic potential window (to the -0.2 to -0.5 V region, depending upon the pH). Another problem is the high background current associated with the formation of surface-oxide or adsorbed hydrogen layers. The surface-layers problem is less severe in non-aqueous media where noble metals are often an ideal choice.

2.7 Non-conducting polymers [29]

Deposited on electrode surface, non-conducting polymers are not involved in electron transfer reactions and therefore partially or totally passivate the surface. However, these polymers are useful in constructing permselective films. These films are deposited on substrate surface by the same methods as other polymers: dip-coating, spin-coating, drop-casting, or electropolymerization. The most elegant and useful approach to construct a highly selective modified electrode using a non-conducting polymer film is molecular imprinting.

The distinguishing feature of molecularly imprinted polymer films stems from the addition of a recognition molecule to the polymerization solution. During the reaction of a monomer, the recognition molecule becomes trapped within the newly formed polymer. After polymerization, the recognition molecule is removed, resulting

in structural voids with the structure that is complementary to the recognition molecule. Although imprinted polymer modified electrodes can be made using a nonconductive polymer template, the imprinting process is a general method. Any type of polymer can, in principle, be used.

The synthetic protocols needed to produce imprinted polymers have become significant is sues. However, successful construction of an imprinted polymer modified electrode is extremely rewarding: obtaining sites having affinities comparable to antibodies may be possible. Unlike current biorecognition elements, the selectivity of the imprinted layer remains high in a variety of environments. This stability results from the robust nature of the polymeric material. Recently, combinatorial approaches are being utilized for optimization of synthetic protocols in order to overcome synthetic challenges of creating these films**.**

2.8 Conducting polymers [28, 29, 32]
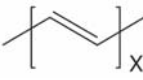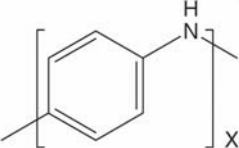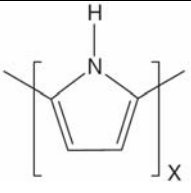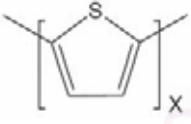
Electronically conducting polymers (such as polypyrrole, polythiophene, and polyaniline) have attracted considerable attention due to their ability to switch reversibly between the positively charged conductive state and a neutral (essentially insulating) form as well as their capibility to incorporate and expel anionic species (from and to the surrounding solution) upon oxidation or reduction:

$$P^0 + A^- \longrightarrow P^+A^- + e^{-1}$$

(2.17)
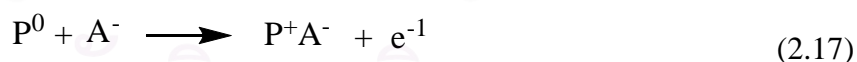
where P and A^- represent the polymer and the dopant anion, respectively. The lattice of polymer serves to maintain the electrical neutrality, that is, to counterbalance the positive charge of the polymer backbone. The electrical conductivity of these films, which originates from the electronic structure of their polymeric backbone (i.e., electron hopping involving the delocalized π electrons), varies with the applied potential. The structure of common conducting polymers and their conductivity ranges (from undoped to doped states) are displayed in Table 2.2. The redox charges (equation 2.9) are not located at a specific center, but rather delocalized over a number of conducting polymer groups.

Conducting polymers show unusual electrochemical properties such as high electrical conductivity, low ionization potential, high electronic affinities, and optical properties. These properties arise from only conjugated p-electron backbones in conducting polymers. There must be a high degree of overlapping of the polymer molecular orbital, which permits the formation of a delocated molecular wave function and partial occupation of the molecular orbital if there is free movement of electrons throughout the lattice.

Table 2.2 Simple conductive organic polymers (adapted from [28])

Structure	MW Monomer Unit	Conductivity (S cm^{-1}) of the oxidized polymer
Polyacetylene	26 (13)	3-1000
Polyaniline	91	0.001-5
Polypyrrole	65	0.3-100
Polythiophene	82	2-150

Conducting polymers exhibit intrinsic electronic conductivity ranging from about 10^{-14} to 10^{2} S cm^{-1} due to the extension of the doped state as shown in Table 2.2. In the neutral (undoped) state, these materials are only semi-conductive and electronic conductivity only appears when the material is doped with small-sized ions (e.g., when electrons or holes are injected into the super orbital). This kind of doping is normally produced by chemical or electrochemical oxidation of the monomer, in which the polymer chains acquire positive charges and the electrical neutrality of the

resulting material is preserved by the incorporation of small counter ions from the electrolyte solution.

The mechanism of electropolymerization of conductive polymers can be best explained by using polypyrrole as an example, as shown in Fig. 2.17.
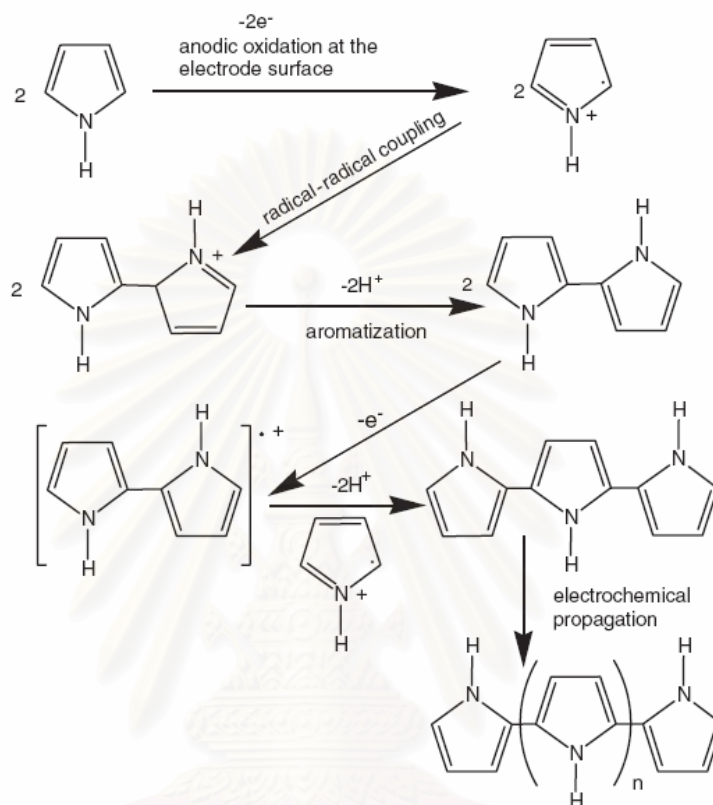
Figure 2.17 Mechanism of electropolymerization of polypyrrole

2.9 Literature reviews

2.9.1 Substrates of ALP for amperometric immunosensors

Alkaline phosphatase (*o*-phosphoric monoester phosphohydrolase; ALP) [2] is a common enzyme label used in immunoassays. It is easily conjugated to haptens, antibodies, and other proteins. Moreover, ALP has a high turnover number and broad substrate specificity. Enzyme immunoassay is an analytical technique that relies on a specific immuno-interaction to quantitatively determine antibody or antigen present in an analyte by measuring the activity of an enzyme label conjugated to either the antibody or antigen [1]. The main advantage of using enzyme labels is

the remarkable signal amplification that may be gained from the high turnover of enzyme product molecules for each enzyme label.

Different substrates for ALP have been investigated in different detection systems such as spectrophotometry using fosfestrol [33], fluorescence using 8-quinolyl phosphate [17] and 2-carboxy-1-naphthyl phosphate [18], chemiluminescence using lumiphos [16], bioluminescence using adenosine-3´-phosphate-5´-phosphosulfate [19], and electrochemical detector using phenyl phosphate [6].

In electrochemical immunosensors, an ALP enzyme is used to generate organic electroactive products most of which can be detected and quantified. This detector is generally sensitive and rapid for the redox reaction of the product of the enzyme hydrolysis of an ALP substrate. Several substrates for electroanalysis have been studied in immunoassays involving these enzymes such as catechol monophosphate [20], 3-indoyl phosphate (IP) [9, 21, 22, 34], hydroquinone diphosphate (HQDP) [14], 4-nitrophenol phosphate (NPP) [4, 10, 35], *p*-aminophenyl phosphate (APP) [3-5, 7, 11, 12, 36], 1-naphthyl phosphate (NTP) [8, 12, 13], phenyl phosphate (PheP) [4, 11, 14, 37], and 2-phospho-L-ascorbic acid (AAP) [5, 7, 23]. During the enzymatic process, these substrates are converted to electrochemical active species such as catechol, indigo carmine (IC), hydroquinone (HQ), 4-nitrophenol (NP), 4-aminophenol (AP), 1-naphthol (NT), phenol (Phe), and L-ascorbic acid (AA).

2.9.2 Conducting polymer based for amperometric immunosensors

The major challenge when using conducting polymers in the design of immunosensors with electrochemical transducers is to understand the mechanism of the electron transfer in a configuration that usually runs parallel to the charging of a double layer at the electrode surface and the mass transport processes at the polymer interface [38]. Over the last decade, biosensors have attracted much global attention and plenty of active research throughout the world is being dedicated to the development of new and novel immunosensors. Immunosensors have found many applications in every sphere of life. They find their use in diagnosis, biotechnology, genetic engineering, and environmental monitoring. A crucial step in the design of immunosensors is the immobilization of immunoreagents onto the electrode surface.

This immobilization determines the quality of the immunosensor, mostly the reproducibility. Some strategies for the immobilization of immunoreagents on solid surfaces include physical adsorption [9, 13], entrapment in polymer matrix [36, 39, 40], and covalent attachment [36, 41, 42]. The previously conducting polymers were constructed for electrochemical immunosensors, which are described in the literature summarized below.

Tsuji and co-workers [43] constructed highly sensitive amperometric enzyme immunosensors for human immunoglobulin G (IgG), prepared on the basis of electrogenerated polytyramine (PTy, tyramine = p-(2-aminoethyl)-phenol) modified electrodes. This electrode provided a large surface area with little non-specific adsorption of proteins. By means of the competitive enzyme immunoassay technique using glucose oxidase (GOD) labeled IgG, IgG was determined from the oxidation current of H_2O_2 generated by the GOD reaction.

Darain research group constructed the immunosensors for detection of rabbit IgG [44] and carp (*Carassius auratus*) Vitellogenin (Vtg) [45]. A conducting polymer, poly-terthiophene carboxylic acid, was the basis of these immunosensors and formed by electropolymerization on the surface of an SPC electrode. The group started from rabbit IgG detection and applied to carp Vitellogenin detection. Both of immunosensors polymer bases were constructed using the same method, followed by horseradish peroxidase (HRP) and streptavidin covalently binding with the polymer on the electrode. Biotinylated antibodies were then immobilized on the electrode surface using avidin−biotin coupling. These sensors were based on the competitive assay between free and labeled antigen for the available binding sites of antibody. GOD was used as a label. In the presence of glucose, H_2O_2 formed by the analyte-enzyme conjugate was reduced by the enzyme channeling via HRP bonded on the electrode. The catalytic current was monitored amperometrically at -0.35 V vs. Ag/AgCl.

Ordonez and Fabregas [46] reported the preparation of polysulfone membrane for amperometric immunosensors monitoring at -0.1V vs. SCE. This immunosensor based on a porous conducting polymer-graphite-polysulfone electrode has been developed using a phase inversion technique for the determination of anti-rabbit IgG (anti-RIgG) and was based on the competitive assay between free and

labeled anti-RIgG for the available binding sites of immobilized rabbit IgG (RIgG). The immunological reaction was detected by using an enzymatic-labeling procedure (HRP enzyme) combined with the amperometric detection using H_2O_2 as a substrate and hydroquinone as a mediator. The immunosensor showed good reproducibility and high stability for a period of one week.

Dong et al. [36] constructed an electrochemical immunosensor using an electropolymerized pyrrolepropylic acid (PPA) film with high porosity and hydrophilicity. High density of carboxyl groups of PPA was used to covalently attach to protein probes, leading to significantly improved the detection sensitivity compared with the conventional entrapment method. As a model, anti-mouse IgG was covalently immobilized or entrapped in the PPA film and used in a sandwich-type alkaline phosphatase-catalyzing amperometric immunoassay with *p*-aminophenyl phosphate as a substrate.

Zhang et al. [42] described a simple, potentially low-cost, amperometric enzyme-amplified sandwich-type immunoassay for IgG monitoring. The assay utilizes a screen-printed carbon electrode on which a redox hydrogel and avidin were co-electrodeposited. To neutralize nonspecifically binding positively charged microdomains of the avidin, two polyanions, poly(acrylic acid-*co*-maleic acid) and poly(acrylic acid), were applied. These polyanions bound to cysteine, lysine, or arginine functions of the avidin by electrostatical force as well as Michael addition. The electrode was then made specific for the analyte, for which rabbit IgG was chosen, by conjugating the film bound avidin to biotin-labeled anti-rabbit IgG. After exposure to the test solution and the capture of rabbit IgG, the sandwich was completed by conjugation of HRP-labeled anti-rabbit IgG. Electrical contact between the HRP and the electrode-bound hydrogel resulted in the formation of an electrocatalyst for the electroreduction of H_2O_2 to water. The application of the poly(acrylic acid-*co*-maleic acid) and the poly(acrylic acid) reduced the nonspecific adsorption-associated noise.

Ionescu et al. [47] developed a novel copolymer modified amperometric immunosensor for the detection of cholera antitoxin (anti-CT) by the electropolymerization of pyrrole–biotin and pyrrole–lactitobionamide monomers on Pt and GC electrodes. For the detection of cholera antitoxin, they used three

enzymatic marker detection systems based on HRP-labeled rabbit IgG antibodies, biotinylated polyphenol oxidase (PPO-B), and biotinylated glucose oxidase (GOD-B). The comparison of the electro-enzymatic performances of these three configurations with different substrates clearly resulted in the sensitive amperometric immunosensor of anti-CT using the hydroquinone/H_2O_2 system.

In this research, the development of conductive polymer modified electrode is shown to offer substantial improvements in the stability and sensitivity of MIgG immunosensor. Poly-*o*-ABA was used as the basis of covalent bonding between primary antibody and electrode surface. Previously, the electropolymerized *o*-ABA synthesis at Au [24], Pt [48], and GC [49, 50] were reported.

2.9.3 BDD material immunosensor

Compared to other electrode materials, BDD has many outstanding properties such as physicochemical stability, wide electrochemical potential window, low background current, semimetallic electronic behavior, and chemical sensitivity [15, 51]. These versatile properties make BDD an excellent candidate for electrochemical use coupled with biochemical applications [52, 53]. On the other hand, immunosensing, a combination of specific immunoreaction with sensitive optical or electrochemical transduction, has attracted great attention due to its high sensitivity and specificity [54-56]. However, immobilization of a biomolecule or protein at BDD requires surface activation procedures since the inert nature of the original diamond surface does not allow BDD to have a stable and covalent bond with any molecule [57-59]. Surface linkers such as carboxyl groups and amine groups are needed to perform covalent bonding between BDD and the proteins.

Many studies have used multiple steps for photochemically linking a vinyl group of allylamine [60], 2,2,2-trifluorine-*N*-9′-decenil acetamide [61], or 10-aminodec-1-ene [62-64] to the diamond surface to introduce a homogeneous layer of amine groups which serve as binding sites for protein or DNA attachment. Coffinier and co-workers [65, 66] used site-specific α-oxo semicarbazone ligation for peptide conjugation. The active surface was prepared from the aminated surface, using NH_3 plasma treatment or photochemical reaction of aminopropyltriethoxysilane at the oxidized BDD surface, followed by the chemical reaction of the terminal amino

groups with triphosgene and Fmoc-protected hydrazine. Zhang et al. [67] used direct amination on polycrystalline diamond to produce functionalized surfaces for DNA. The amination was conducted by UV irradiation of diamond in ammonia gas to generate amine groups directly. Ushizawa et al. and Huang and Chang [68, 69] reported that the oxidative-acid-treated diamond surface succeeded to bond covalently with protein and DNA. Zhou and Zhi [70] combined chemical and electrochemical modifications of BDD film with 4-nitrobenzenediazonium tetrafluoroborate to produce aminophenyl-modified BDD, followed by immobilizing tyrosinase covalently at the BDD surface via carbodiimide coupling.

Polymerization at the BDD electrode can provide freely accessible carboxyl groups, which can also be used as the base of a biosensor. Gu group [71, 72] reported the impedimetric sensing of DNA hybridization on a polyaniline/polyacrylate (PANI/PAA)-modified BDD electrode. An ultrathin film of PANI/PAA copolymer was electropolymerized onto the diamond surfaces to provide carboxylic groups for conjugation to DNA sensing probes.

However, to the best of our knowledge, only one report existed on the development of the BDD immunosensor [63]. The researchers investigated the electrical properties of the antibody-antigen modified diamond and silicon surfaces using electrical impedance spectroscopy (EIS). Photochemical functionalization of silicon and diamond surfaces provides these surfaces with organic monolayers terminated with primary amine groups, which can then be used to covalently link antibodies to silicon and diamond surfaces.

Therefore, in this research, the BDD immunosensor was studied and developed for mouse IgG determination by the construction of conductive poly-*o*-ABA for changing BDD surfaces to carboxyl groups. This functional group was used for covalent bonding with primary antibodies.

CHAPTER III

EXPERIMENTAL

Electrochemical instruments set-up, chemicals, materials, and electrode modification are explained thoroughly in this chapter.

3.1 Instruments

3.1.1 Electrode preparations

The instruments for fabrication of BDD and SPC electrodes are listed in Table 3.1.

Table 3.1 List of instruments for electrode preparations

Instruments	Details
Microwave plasma chemical vapor deposition system	Astex Corp., Japan
Semi-automatic screen printer	Model SPM/B, MPM, Franklin, MA

3.1.2 Electrochemical measurement for products of ALP substrates

The products of ALP substrates were determined at GC disk, Au disk, and SPC electrodes by using many instruments. All of them are listed in Table 3.2.

Table 3.2 List of instruments for the electrochemical measurement for products of ALP substrates

Instruments	Details
μAutolab III analysis system with GPES 4.9 software	Eco Chemie B. V., The Netherlands
Conventional three-electrode electrochemical cell	1.5 mL, Home made
Ag/AgCl reference electrode	BAS, Japan
Platinum wire	Goodfellow, USA
Gold disk electrode	Au disk; 2 mm (i.d.), CH Instruments, USA
Glassy-carbon disk electrode	GC disk; 3 mm (i.d.), CH Instruments, USA
Screen-printed carbon electrode	SPC; Home made
Micro stir bar	2 (i.d.) $\times$ 7 (l) mm, Cole-Parmer, Japan

3.1.3 The base of covalent bonding in immunoassay system

Two approaches, self-assembled monolayers (SAMs) of thiol and electropolymerization of *o*-ABA polymer, were used to prepare a base of covalent bonding between the electrode and the primary antibody. All instruments for this work are listed in Tables 3.2 and 3.3.

Table 3.3 List of instruments for the base of covalent bonding in the immunoassay system

Instruments	Details
Glassy carbon plate electrode	GC plate; Tokai Carbon, Tokyo, Japan
Potentiostat	Hokuto Denko, HSV-100,Japan
Boron-doped diamond	BDD; Home made
Silicone rubber gasket	5 mm (i.d.), Japan

3.1.4 Characterization of poly-*o*-ABA

All instruments for this work are shown in Tables 3.4.

Table 3.4 List of instruments for the characterization of poly-*o*-ABA

Instruments	Details
X-ray photoelectronic spectroscopy equipped with an MgKa X-ray source	XPS; Voltage 10 kV and emission 10 mA, JPS-9000MC, JEOL, Japan
Scanning electron microscopy	SEM; JSM-5400, JEOL, Japan

3.1.5 Electrode immunosensors

All instruments for this the fabrication of the immunosensor are displayed in Table 3.5.

Table 3.5 List of instruments for the fabrication of electrode immunosensor

Instruments	Details
Glass ring	0.8 cm (i.d.), home made
Micro pipette	200 μL

3.2 Chemicals

3.2.1 Electrode preparations

The chemicals involved in the fabrication of BDD and SPC electrodes are listed in Table 3.6.

Table 3.6 List of chemicals for the electrode preparations

Chemicals	Suppliers
Methanol	Wako Chemical Company, Japan
Acetone	Wako Chemical Company, Japan
Boron trioxide, B_2O_3, extra pure	Wako Chemical Company, Japan
Hydrogen peroxide, H_2O_2	Wako Chemical Company, Japan
Carbon ink	Ercon, G-449(I), Wareham, MA
Insulator	Ercon, E6165-116 Blue Insulayer, Wareham, MA
Sulfuric acid 95%, H_2SO_4	Sigma, USA

3.2.2 Electrochemical measurement for products of ALP substrates

The chemicals used in this work are listed Table 3.7. All materials were prepared by deionized (DI) water ($R \geq 18.2$ MΩ-cm).

Table 3.7 List of chemicals for the electrochemical measurement for products of ALP substrates

Chemicals	Suppliers
1-Naphthol (NT), C_6H_7OH	Sigma, USA
L-ascorbic acid (AA), $C_6H_8O_6$	Sigma, USA
Phenol (Phe), C_6H_5OH	Sigma, USA
Indigo carmine (IC), $C_{16}H_8N_2Na_2O_8S_2$	Sigma, USA
Hydroquinone (HQ), C_6H_4-1,4-$(OH)_2$	Aldrich, USA
4-Nitrophenol (NP), $O_6NC_6H_4OH$	Aldrich, USA
4-Aminophenol (AP), $H_2NC_6H_4OH$	Fluka,USA
Tris-hydrochloride (Tris)	Sigma, USA
Acetic acid, CH_3CO_2H	Aldrich,USA
Sodium acetate, CH_3CO_2Na	Aldrich, USA

3.2.3 The base of covalent bonding in immunoassay system

11-Mercaptoundecanoic acid (C11, $HS(CH_2)_{10}CO_2H$), and 6-mercapto-1-hexanol (C6, $HSCH_2(CH_2)_4CH_2OH$) were obtained from Aldrich and Fluka, USA, respectively. The *o*-aminobenzoic acid (*o*-ABA, $2-(H_2N)C_6H_4CO_2H$) used for electropolymerization was obtained from Sigma, USA.

3.2.4 Electrode immunosensors

All chemicals for this work are shown in Table 3.8.

Table 3.8 List of chemicals for the fabrication of electrode immunosensors

Chemicals	Suppliers
Sodium chloride , NaCl	Sigma
Potassium chloride, KCl	Wako
Tween 20	Sigma
1-Ethyl-3-(3-dimethyl aminopropyl) carbodiimide (EDAC)	Sigma
N-hydroxysulfosuccinimide (NHS)	Sigma
Ethanolamine-HCl	Sigma
MES monohydrate (MES), $C_6H_{13}NO_4S \cdot H_2O$	Fluka
Bovine serum albumin fraction V (BSA)	Sigma
IgG from mouse (MIgG)	Sigma, St. Louis, MO, USA
Anti-mouse IgG from goat (GaMIgG)	Sigma, St. Louis, MO, USA
Anti-mouse IgG conjugated alkaline phosphatase (GaMIgG-ALP)	Sigma, St. Louis, MO, USA
N_2 gas	For mixing in solution
2-Phospho-L-ascorbic acid trisodium salt (AAP), $C_6H_6Na_3O_9P.$ xH_2O,	Fluka

3.3 Chemical preparations

3.3.1 Electrode preparations

3.3.1.1 Mixture of carbon and boron sources for CVD

A mixture of acetone and methanol (9:1, v/v) as the carbon source and B_2O_3 as the boron source was used. 1.09 g of B_2O_3 was added in a mixture of 72-mL acetone and 8-mL methanol. The mixture solution was sonicated until it was a clear.

3.3.1.2 0.1 M H_2SO_4

1.41 mL of concentrated H_2SO_4 was diluted to 250 mL by Milli-Q water.

3.3.1.3 0.2 M H_2SO_4

2.81 mL of concentrated H_2SO_4 was diluted to 250 mL by Milli-Q water.

3.3.1.4 Piranha solution

A piranha solution was prepared by mixing 9 mL of concentrated H_2SO_4 and 3 mL of H_2O_2 (30% v/v) in a beaker. The solution was freshly prepared before used. *Safety note*: the piranha solution should be handled with extreme caution.

3.3.2 Electrochemical measurement for products of ALP substrates

3.3.2.1 1 M NaOH

4.0 g of NaOH was weighed, and dissolved into 100 mL of Milli-Q water. This solution was prepared to adjust the pH of the buffer.

3.3.2.2 0.5 M Tris buffer solution (pH 8.5)

78.80 g of Tris was weighed and dissolved with 1,000 mL of Milli-Q water. The solution was adjusted to a pH of 8.5 with 1 M NaOH.

3.3.2.3 0.1 M Acetate buffer solution (pH 4.6)

0.1 M acetic acid (5.6 mL of glacial acetic acid in 500 mL of Milli-Q water) and 0.1 M solution of sodium acetate (13.61 g of sodium acetatetrihydrate in 500 mL of Milli-Q water) were prepared. The solutions were mixed and adjusted to a pH of 4.6 with pH meter.

3.3.2.4 10 mM stock solution of IC

46.6 mg of IC was weighed, dissolved in 0.5 M Tris buffer solution (pH 8.5), transferred to a 10-mL volumetric flask, and made a volume of 10 mL with 0.5 M Tris buffer solution (pH 8.5).

3.3.2.5 10 mM stock solution of HQ

11.0 mg of HQ was weighed, dissolved in 0.5 M Tris buffer solution (pH 8.5), transferred to a 10-mL volumetric flask, and made a volume of 10 mL with 0.5 M Tris buffer solution (pH 8.5).

3.3.2.6 10 mM stock solution of NP

13.9 mg of NP was weighed, dissolved in 0.1 M acetate buffer solution (pH 4.6), transferred to a 10-mL volumetric flask, and made a volume of 10 mL with 0.1 M acetate buffer solution (pH 4.6).

3.3.2.7 10 mM stock solution of AP

10.9 mg of AP was weighed, dissolved in 0.5 M Tris buffer solution (pH 8.5), transferred to a 10-mL volumetric flask, and made a volume to 10 mL with 0.5 M Tris buffer solution (pH 8.5).

3.3.2.8 10 mM stock solution of NT

14.5 mg of NT was weighed, dissolved in 0.5 M Tris buffer solution (pH 8.5), transferred to a 10-mL volumetric flask, and made a volume to 10 mL with 0.5 M Tris buffer solution (pH 8.5).

3.3.2.9 10 mM stock solution of Phe

9.4 mg of Phe was weighed, dissolved in 0.5 M Tris buffer solution (pH 8.5), transferred to a 10-mL volumetric flask, and made a volume of 10 mL with 0.5 M Tris buffer solution (pH 8.5).

3.3.2.10 10 mM stock solution of AA

17.6 mg of AA was weighed, dissolved in 0.5 M Tris buffer solution (pH 8.5), transferred to a 10-mL volumetric flask, and made a volume of 10 mL with 0.5 M Tris buffer solution (pH 8.5).

3.3.3 The base of covalent bonding in immunoassay system

3.3.3.1 1 M H_2SO_4

5.62 mL of concentrated H_2SO_4 was diluted to 100 mL by Milli-Q water.

3.3.3.2 50 mM o-ABA

10.3 mg of *o*-ABA was weighed into a 1.5-mL PTFT tube and mixed with 1.5 mL of 1 M H_2SO_4 for solubility. The mixture was sonicated until it was clear.

3.3.3.3 Mixtures of 1 mM C11 : C6 SAM

(1) 2.1836 g of 11-mercaptoundecanoic acid (C11) was weighed, dissolved in ethanol, transferred in a 10-mL volumetric flask, and then made a volume of 10 mL with ethanol.

(2) 1.41 mL of 6-mercapto-1-hexanol (C6) was diluted to 10 mL with ethanol.

The solutions of (1) and (2) were mixed at the ratios of 1:9, 2:8, 3:7, 4:6, 6:4, and 8:2.

3.3.4 Electrode immunosensors

3.3.4.1 0.1 M Tris buffer solution (pH 7.4)

15.76 g of Tris was weighed and then dissolved in 1,000 mL of Milli-Q water. The solution was adjusted to a pH 7.4 by 1 M NaOH.

3.3.4.2 Washing buffer solution

This solution is Tris buffer pH 7.4 containing 0.1 M NaCl, 0.005 M KCl, and 0.1% (v/v) Tween-20. Firstly, 0.1% (v/v) Tween-20 solution (0.5 mL of Tween 20 in 500 mL of 0.1 M Tris buffer pH 7.4) was prepared. Then, 2.9220 g of NaCl and 0.1864 g of KCl were weighed and dissolved in 500 mL of 0.1% (v/v) Tween-20 solution.

3.3.4.3 Blocking buffer

This solution is 1% (w/v) BSA in washing buffer solution. 0.1 g of BSA was weighed and dissolved in 10 mL of washing buffer solution. The solution was freshly prepared before used everyday.

3.3.4.4 20 mM PBS buffer (pH 8.6)

1.7418 g of K_2HPO_4 was weighed, and dissolved in 500 mL of Milli-Q water.

3.3.4.5 100 mM MES buffer (pH 6.0)

10.6625 g of MES was weighed, and dissolved in 500 mL of Milli-Q water. The solution was adjusted to a pH of 6.0 with 1 M NaOH.

3.3.4.6 50 mM AAP (substrate)

24.1 mg of AAP was weighed into a 1.5-mL PTFT tube and dissolved in 1.5 mL of Milli-Q water. This solution was prepared freshly everyday.

3.4 Electrode preparations

3.4.1 The Au electrode

The Au disk electrodes were first polished with alumina (0.05 μm) prior to use. The electrodes were soaked in freshly prepared piranha solution for an hour and rinsed with Milli-Q water. The cleaned Au disk electrodes were scanned with a cyclic potential between 0.0 and 1.6 V in 0.2 M H_2SO_4 repetitively until the characteristic gold peak was observed [73].

3.4.2 The SPC electrode

The SPC electrodes were manufactured by a semi-automatic screen printer using a carbon ink and alumina ceramic plates. The electrodes were cured for 1 hour at 200°C. A layer of insulator was then printed onto a portion of the conducting lines, exposing a rectangular (1.5 mm × 6.0 mm) working electrode area. The SPC electrodes were pretreated with 0.1 M H_2SO_4 by applying an anodic current of 25 μA for 300 s.

3.4.3 The GC electrode

3.4.3.1 The GC disk electrode was polished to a mirror-like surface with 0.05 μm alumina slurries and then rinsed with Milli-Q water prior to use.

3.4.3.2 The GC plate electrode was cut into 1×1 cm^2, polished to a mirror-like surface with 0.05 μm α-alumina on filter paper, and then sonicated prior to use two times with isopropanol and one time with Milli-Q water.

3.4.4 The BDD electrode

The BDD thin film was deposited on Si (111) wafers in a microwave plasma chemical vapor deposition system using a mixture of acetone and methanol (9:1, v/v) as the carbon source and B_2O_3 as a boron source. The details of the preparation are described elsewhere [51]. The boron doped in diamond film is approximately 10^4 ppm of B/C molar ratio. Hydrogen (99.99%) was used as the carrier gas during deposition. The C/H ratio in the source gas was estimated to be

0.03 ± 0.01. Film deposition was carried out using a microwave power of 5 kW. The growth rate was ca. 3-4 μm h^{-1}, with a thickness of approximately 20 mm being achieved after 6 hours.
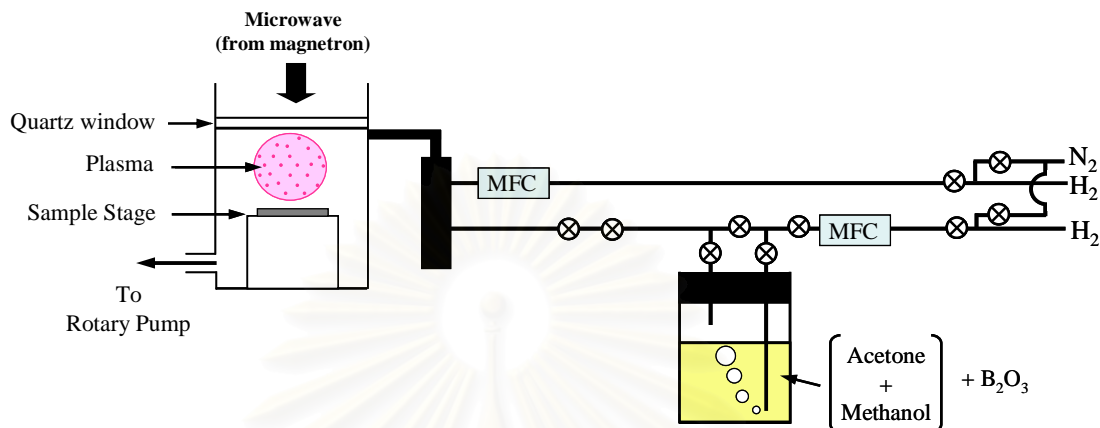
Figure 3.1 Schematic of a microwave plasma reactor for CVD diamond film growth

BDD thin film was cut into 1×1 cm^2, soaked in freshly prepared piranha solution for an hour, and rinsed with Milli-Q water.

3.5 Electrochemical measurement for products of ALP substrates

3.5.1 Cyclic voltammetric measurement

The equipments for cyclic voltammetric cell are as shown in Fig. 3.2. The working electrode (WE) was GC disk, Au disk, or SPC electrodes. The counter (CE) and reference (RE) electrodes were Pt wire and Ag/AgCl, respectively. WE, CE, and RE were contained in a glass cell and connected with a μAutolab III analysis system using the GPES 4.9 software. A 0.5 M Tris buffer solution (pH 8.5) was used as the supporting electrolyte for IC, HQ, AP, Phe, NT, and AA whereas a 0.1 M acetate buffer solution (pH 4.6) was used for NP. The working concentration of each seven products of ALP substrates was 100 μM. The potential scan of each substrates is shown in Table 3.9. The responses of different substances on different electrode materials were detected by cyclic voltammetry with a scan rate of 100 mV s^{-1} and the

corresponding voltammograms were recorded as current vs. potential curves. Electrochemical measurements were performed at room temperature.
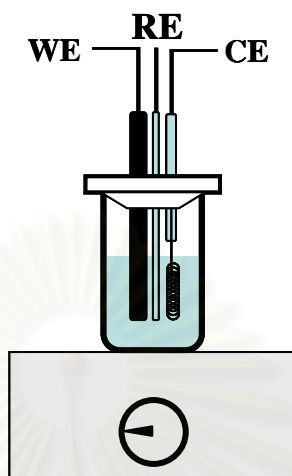
Figure 3.2 Electrochemical cell of cyclic voltammetric technique consisting of WE, CE, and RE

Table 3.9 Potential window scan for seven products of ALP substrates by cyclic voltammetric measurement at GC disk, SPC, and Au disk electrodes

Products of ALP substrates	Potential window scan (V)		
	GC disk electrode	SPC electrode	Au disk electrode
IC	-0.7 to 0.7	-0.7 to 0.7	-0.7 to 0.7
HQ	-0.3 to 0.3	-0.6 to 0.6	-0.3 to 0.4
NP	-1.0 to 1.4	-0.8 to 1.4	-0.8 to 1.4
AP	-0.5 to 0.8	-0.5 to 0.8	-0.3 to 0.35
NT	-0.2 to 0.8	-0.2 to 0.8	-0.2 to 0.8
Phe	0.0 to 0.8	0.0 to 0.8	0.0 to 0.8
AA	-0.4 to 0.8	-0.4 to 0.8	-0.2 to 0.5

3.5.2 Amperometric measurement

The equipment setting for hydrodynamic amperometric measurements is shown in Fig. 3.3. Similar set-up to cyclic voltammetric measurement was used except that magnetic bar was present. Amperometric measurements were performed

under stirring in 990 µL of the same electrolyte used in cyclic voltammetric measurements. The anodic potentials and cathodic potentials of seven products of ALP substrates were applied to the GC disk, Au disk, and SPC WEs as shown in Table 3.10. After the background current reached steady state, the 10 µL of stocked solutions of each ALP substrate were added, and the corresponding current responses were recorded as a function of time.
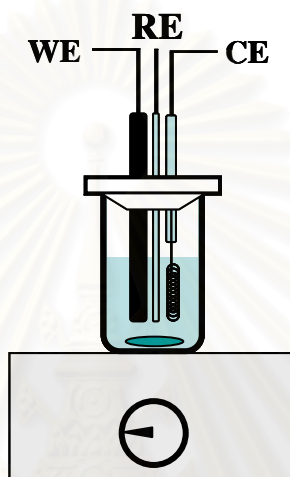
Figure 3.3 Electrochemical cell of amperometric technique consisting of WE, CE, and RE

Table 3.10 The applied potential for seven products of ALP substrates by amperometric measurement at GC disk, Au disk, and SPC electrodes

Products of ALP substrates	Applied potential (V)					
	GC disk electrode		SPC electrode		Au disk electrode	
	Anodic	Cathodic	Anodic	Cathodic	Anodic	Cathodic
IC	+0.50	-0.40	+0.50	-0.40	+0.50	-0.40
HQ	+0.10	-0.10	+0.30	-0.20	+0.10	-0.10
NP	+1.10	-0.70	+1.10	-0.70	+1.10	-0.70
AP	+0.20	-	+0.15	-	+0.20	-
NT	+0.35	-	+0.35	-	+0.35	-
Phe	+0.65	-	+0.70	-	+0.65	-
AA	+0.40	-	+0.50	-	+0.40	-

3.6 The base of covalent bonding in immunoassay system

3.6.1 Self-assembled monolayers (SAMs) of thiol

The Au disk electrodes were cleaned as described in 3.4.1.   After cleaning, 50 μL of a mixture of 1 mM C11:C6 (1:9) SAM was dropped onto the clean/dried Au disk electrodes surface and kept overnight for the co-assembly process. After that, they were washed twice with ethanol, dried with N_2 gas, and followed in the next step of immobilization.

3.6.2 Electropolymerization of poly-*o*-ABA electropolymerization

The GC disk, Au disk, SPC, GC plate, and BDD electrodes were set up in electrochemical cells as shown in Fig. 3.2 (for GC disk, Au disk, and SPC electrodes) and Figs. 3.4 and 3.5 (for GC plate and BDD electrodes). Then, the electrodes were electropolymerized in the potential range 0 to 0.97 V with 50 mM *o*-ABA in 1 M H_2SO_4 by cyclic voltammetry at the scan rate of 40 mV s^{-1} for 10 cycles. The working area of GC plate and BDD electrodes were controlled by a silicone rubber gasket of 5 mm diameter.   After electropolymerization, they were washed twice with Milli-Q water, dried with N_2 gas, and followed in the next step of immobilization

cell
gasket
electrode
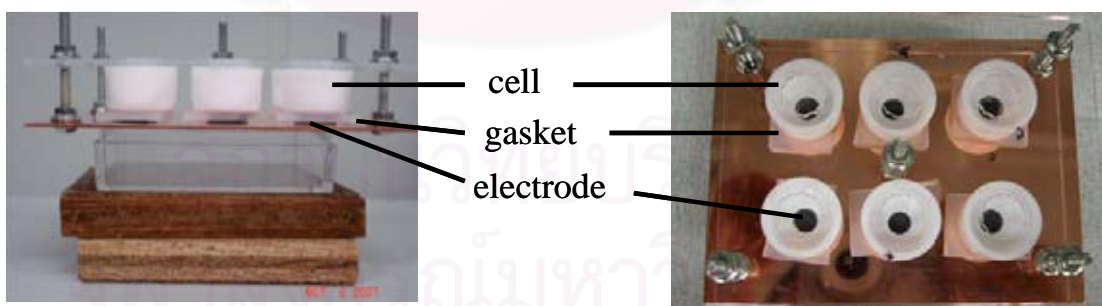
Figure 3.4   The composite of electrochemical cell setting for immunoassay and electrochemical detection
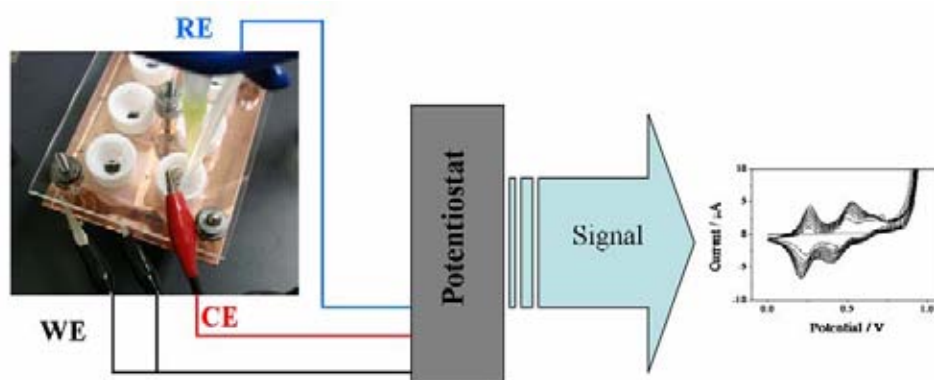
Figure 3.5 The electrochemical cell and equipments setting for cyclic voltammetric detection

3.7 Electrode immunosensors

3.7.1 Electrode immobilization

The modified electrodes were subsequently coated with 50 μL of NHS/EDAC solution (1/1 mg in 100μL of 100 mM PBS buffer, pH 7.22) for 30 minutes and then the solution was removed. A drop of 50 μL of 40 ppm GaMIgG was applied to each of the modified electrodes. After 120 minutes of incubation, the solution was removed and 50 μL of 1 M ethanolamine solution was drop cast onto each modified immunosensor and incubated for 30 minutes. After taking out of the solution, the modified electrodes were washed three times with a washing buffer solution.

3.7.2 Sandwich type immunoassay at modified immunosensors

The immunosensors were first added with the desired amount of the target MIgG using blocking solution for dilution (for control the absence of the target) at room temperature for 60 minutes. After washing with a washing buffer solution, the immunosensor was finally incubated with GaMIgG-ALP for 60 minutes and washed three times with the washing buffer solution afterward.

3.7.3 The immunosensor detection

3.7.3.1 GC Disk, Au Disk, and SPC electrodes

The equipments were set up as shown in Fig. 3.3. Amperometric measurements were performed in 900 μL of a 0.1 M Tris buffer solution (pH 8.5) by applying a potential of +0.4 V (for GC disk and Au disk) and +0.5 V (for SPC) on the modified electrode immunosensors at room temperature. A 100 μL aliquot of 30 mM substrate (AAP) was added to the stirred solution once the background current reached a steady state and the corresponding current vs. time curve was recorded.

3.7.3.2 GC Plate and BDD electrodes

The sandwiched immunosensors of GC plate and BDD electrodes in electrochemical cells were set up as shown in Fig. 3.6. Amperometric experiments were performed in 900 μL of a 0.1 M Tris buffer solution (pH 8.5) by applying a potential of +0.4 V at the sandwich IgG modified immunosensor at room temperature. A 100 μL aliquot of 30 mM AAP, as a substrate, was added to the stirred solution with bubble N_2 gas once the background current reached a steady state and the corresponding current vs. time curve was recorded.
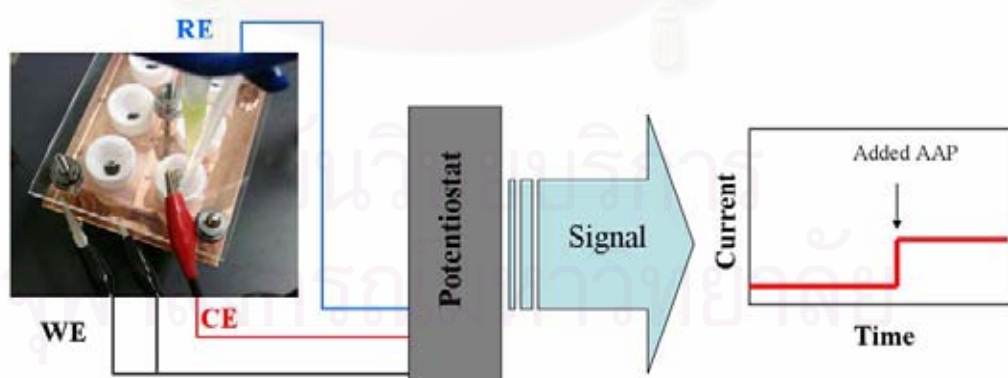
Figure 3.6 The electrochemical cell and equipments setting for amperometric detection

3.8 Characterization of poly-*o*-ABA at BDD electrodes

3.8.1 Scanning electron microscopy (SEM)

Scanning electron microscopy (SEM) images of the poly-*o*-ABA modified BDD electrodes were obtained by using JSM-5400 at the operating voltage of 20 kV. Bare BDD and poly-*o*-ABA modified BDD electrodes were characterized and compared.

3.8.2 X-ray photoelectronic spectroscopy (XPS)

X-ray photoelectronic spectra were obtained by using JPS-9000MC equipped with an MgKa X-ray source at the voltage of 10 kV and the emission of 10 mA. Bare BDD and poly-*o*-ABA modified BDD electrodes were characterized and compared.

3.9 Poly-*o*-ABA modified BDD immunosensors for MIgG determination in a mouse serum

The BDD poly-*o*-ABA modified immunosensors were prepared by the method of 3.6 and 3.7 for measurements of MIgG in a mouse serum. The mouse serum was diluted 50,000 times. Two methods, standard addition and external standard, were used to quantify MIgG in the mouse serum. For standard addition method, three standard MIgG concentrations were spiked into the diluted serum sample and the responses collected at poly-*o*-ABA modified immunosensors using the method of 3.7.3.2. For external standard method, five standard MIgG concentrations were measured and the calibration curve was constructed to obtain the relationship between concentration and current density. The diluted serum sample was measured at poly-*o*-ABA modified BDD immunosensor and the measured current density was used to calculate the quantity of MIgG in the serum sample. The mean values of two slopes and MIgG amounts from the two methods were compared using student's t-test. Differences were considered to be statistically significant when p values were <0.05. Statistical analysis was performed using OriginPro 7.5.

CHAPTER IV

RESULTS AND DISCUSSION

4.1 Electroanalysis of products of ALP substrates

Under alkaline conditions, ALP hydrolyses the phosphate ester ($RHPO_4^-$) functional group of its substrates (IP, HQDP, NPP, APP, NTP, PheP, and AAP) to the respective alcoholic (ROH) products (IC, HQ, NP, AP, NT, Phe, and AA), as shown in equation (4.1). These products can be electrochemically detected via equation (4.2).

Enzyme reaction:

$$RHPO_4^- + H_2O \xrightarrow{\text{ALP}} ROH + H_2PO_4^- \tag{4.1}$$

Electrochemical reaction:

$$ROH \longrightarrow R{=}O + ne^- + nH^+ \tag{4.2}$$
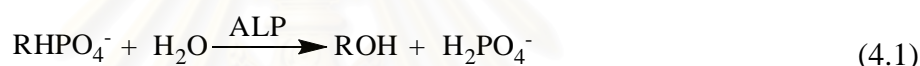
An ideal substrate of ALP should not appear to produce any electrochemical signal at the same potential as its dephosphorylated form (product, ROH). The electrochemical behaviors of seven most commonly used products named: IC, HQ, NP, AP, NT, Phe, and AA (the structures shown in Fig. 4.1), were examined by cyclic voltammetry and amperometry at unmodified GC disk, SPC, and Au disk electrodes. Fig. 4.2-4.4 display the corresponding cyclic voltammograms (Figs. 4.2-4.4A) and amperograms (Figs. 4.2-4.4B) for all the products on GC disk, SPC, and Au disk electrodes. These data indicate that the different products have different electrochemical behaviors on the same electrode material, and the same product also shows different behaviors on different electrode materials. Their potential peaks and current density peaks are shown in Tables 4.1 and 4.2.
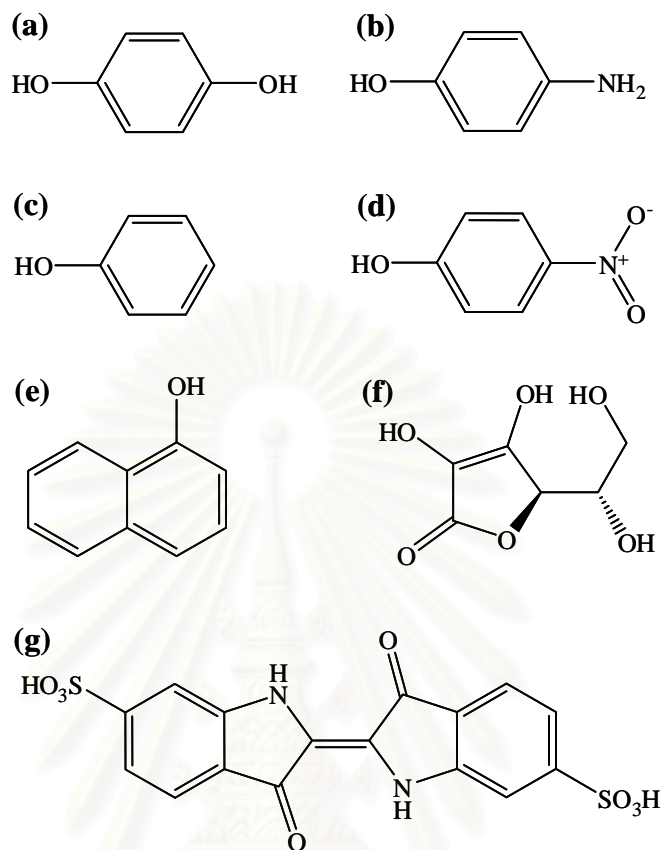
Figure 4.1 Structures of the seven products of ALP substrates: (a) hydroquinone, (b) 4-aminophenol, (c) phenol, (d) 4-nitrophenol, (e) 1-naphthol, (f) L-ascorbic acid, and (g) indigo carmine
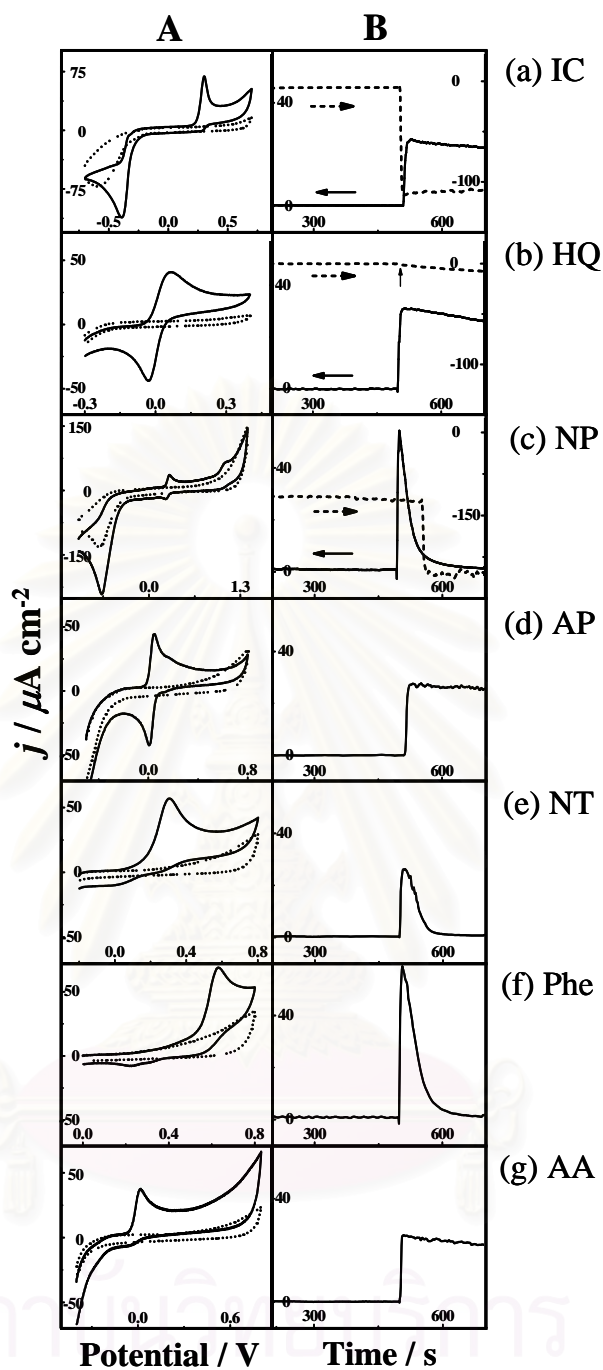
Figure 4.2 A) Cyclic voltammograms (solid lines: 100 μM products of substrates; dotted lines: background) at the scan rate of 100 mV s^{-1} and B) amperograms (solid lines: anodic current; dashed lines: cathodic current) of different products of substrates at GC disk electrode. The electrolyte for (a), (b), and (d)-(g) was 0.5 M Tris buffer solution (pH 8.5); and for (c) was 0.1 M acetate buffer solution (pH 4.6). The potentials applied for anodic amperometry (solid lines) were (a) +0.50 V, (b) +0.10 V, (c) +1.10 V, (d) +0.20 V, (e) +0.35 V, (f) +0.65 V, and (g) +0.40 V, and for cathodic amperometry (dashed lines) were (a) -0.40 V, (b) -0.10 V, and (c) -0.70 V.
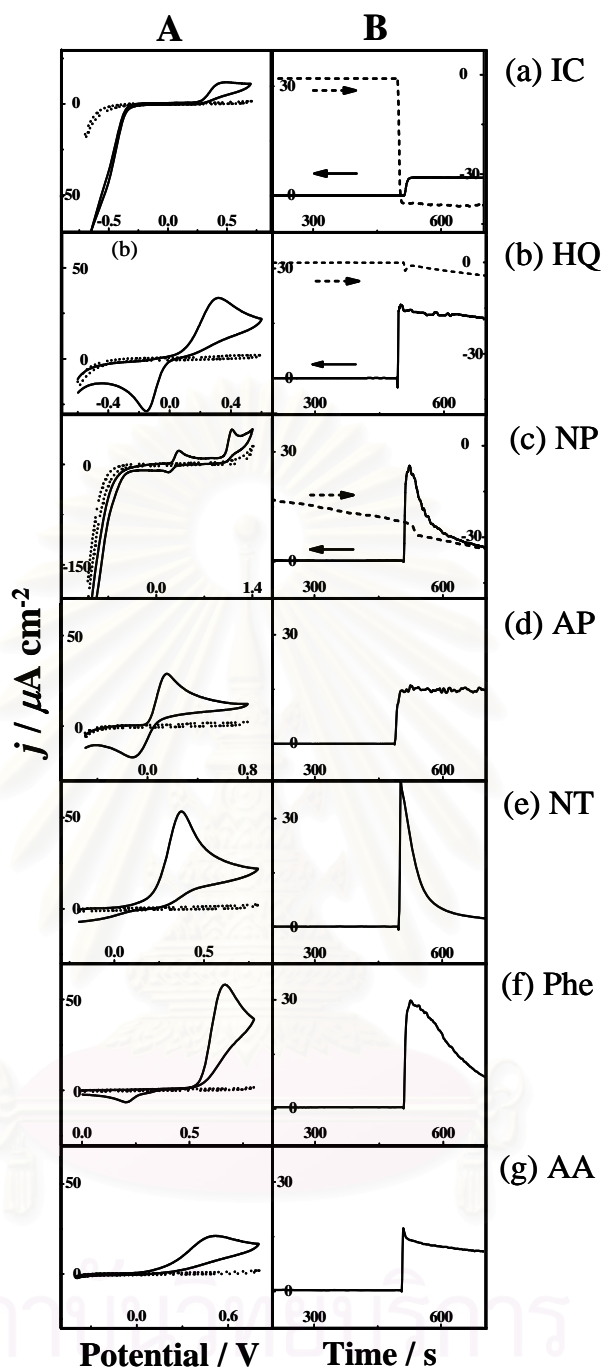
Figure 4.3 A) Cyclic voltammograms (solid lines: 100 μM products of substrates; dotted lines: background) at the scan rate of 100 mV s^{-1} and B) amperograms (solid lines: anodic current; dashed lines: cathodic current) of different products of substrates at SPC electrode. The potentials applied for anodic amperometry (solid lines) were (a) +0.50 V, (b) +0.30 V, (c) +1.10 V, (d) +0.15 V, (e) +0.35 V, (f) +0.70 V, and (g) +0.50 V, and for cathodic amperometry (dashed lines) were (a) -0.40 V, (b) -0.20 V, and (c) -0.70 V. The other conditions were the same as Fig. 4.2.
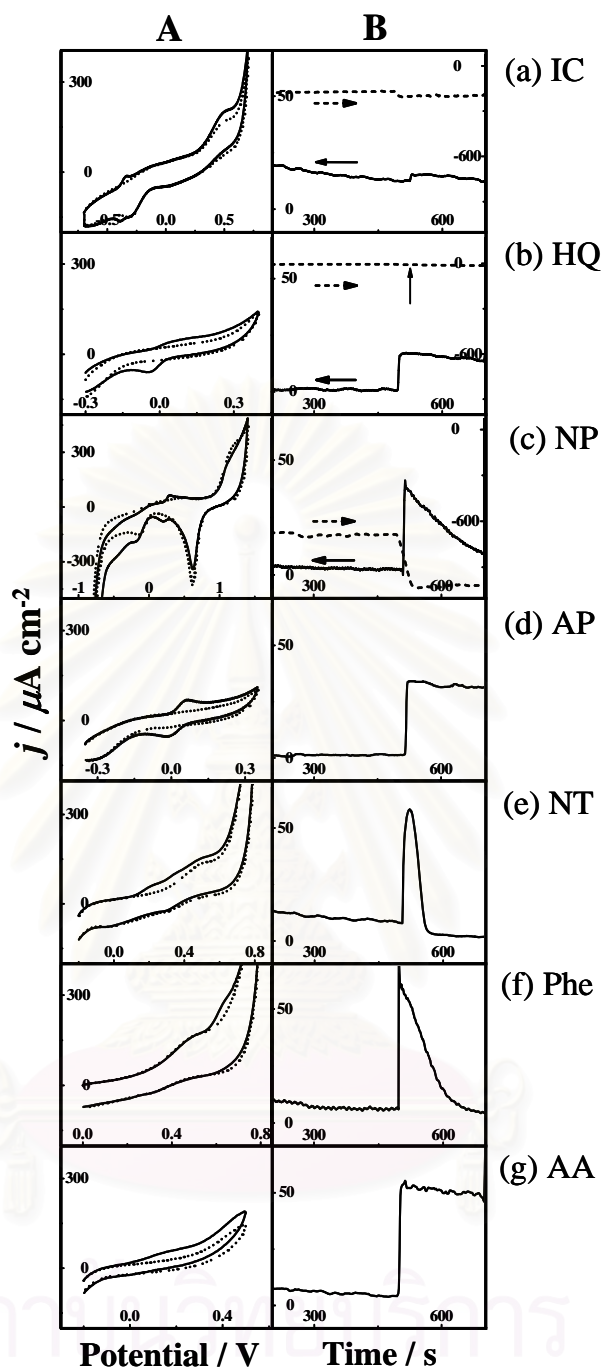
Figure 4.4 A) Cyclic voltammograms (solid lines: 100 μM products of substrates; dotted lines: background) at the scan rate of 100 mV s^{-1} and B) amperograms (solid lines: anodic current; dashed lines: cathodic current) of different products of substrates at Au disk electrode. The other conditions were the same as Fig. 4.2.

Table 4.1 The potential peaks and current density peaks for seven products of ALP substrates by cyclic voltammetric measurement at GC disk, SPC, and Au disk electrodes

Products of ALP substrates	GC disk electrode				SPC electrode				Au disk electrode			
	Anodic		Cathodic		Anodic		Cathodic		Anodic		Cathodic	
	E (V)	j (μA cm^{-2})	E (V)	j (μA cm^{-2})	E (V)	j (μA cm^{-2})	E (V)	j (μA cm^{-2})	E (V)	j (μA cm^{-2})	E (V)	j (μA cm^{-2})
IC	0.30	62.50	-0.39	-61.64	0.44	11. 43	-0.50	-44.88	0.50	32.16	-0.38	-19.11
HQ	0.06	38.79	-0.03	-40.96	0.32	32.00	-0.16	-28.00	0.10	18.79	-0.04	-35.80
NP	1.07	25.00	-0.68	-108.74	1.10	47.00	-0.70	-52.00	1.10	33.00	-0.60	-122.00
AP	0.04	41.40	0.01	-39.0	0.15	28.89	-0.12	-17.00	0.07	40.01	-0.01	-32.00
NT	0.31	52.95	-	-	0.34	53.00	-	-	0.23	30.11	-	-
Phe	0.63	50.21	-	-	0.66	58.11	-	-	0.64	66.07	-	-
AA	0.01	34.19	-	-	0.49	21.00	-	-	0.20	30.10	-	-

Table 4.2 The applied potentials and the current density height for seven products of ALP substrates by amperometric measurement at GC disk, SPC, and Au disk electrodes

Products of ALP substrates	GC disk electrode				SPC electrode				Au disk electrode			
	Anodic		Cathodic		Anodic		Cathodic		Anodic		Cathodic	
	E (V)	j (μA cm^{-2})	E (V)	j (μA cm^{-2})	E (V)	j (μA cm^{-2})	E (V)	j (μA cm^{-2})	E (V)	j (μA cm^{-2})	E (V)	j (μA cm^{-2})
IC	+0.50	24	-0.40	-100	+0.50	5	-0.40	-38	+0.50	3	-0.40	-35
HQ	+0.10	29	-0.10	-6	+0.30	17	-0.20	-1	+0.10	15	-0.10	-
NP	+1.10	-	-0.70	-130	+1.10	-	-0.70	-4	+1.10	-	-0.70	-347
AP	+0.20	25	-	-	+0.15	14	-	-	+0.20	32	-	-
NT	+0.35	-	-	-	+0.35	-	-	-	+0.35	-	-	-
Phe	+0.65	-	-	-	+0.70	-	-	-	+0.65	-	-	-
AA	+0.40	24	-	-	+0.50	12	-	-	+0.40	46	-	-

Basically, IC (Figs. 4.2-4.4(a)), HQ (Figs. 4.2-4.4(b)), NP (Figs. 4.2-4.4(c)), and AP (Figs. 4.2-4.4(d)) show both anodic and cathodic peaks in their cyclic voltammograms. The cathodic peaks of IC (Figs. 4.2-4.4A(a)) and NP (Figs. 4.2-4.4A(c)) at the potentials of -0.39 and -0.68 V (for GC), -0.50 and -0.70 V (for SPC), and -0.38 and -0.60 V (for Au), respectively, gave very high current as shown in solid lines. The electrolyte gave a hydrogen evolution at about -0.7 V. The HQ cyclic voltammograms showed quasi-reversible shapes at all of three electrodes. For SPC and Au electrodes, AP showed quasi-reversible behavior. However, using GC as a working electrode, AP exhibited reversible behavior where AP gave the ratio of $i_{p,c}/i_{p,a}$ close to 1 (0.95) and the peak separation was nearly 0.59/n V (0.6/n V). HQ and AP underwent the reactions in equations (4.3) and (4.4), respectively.

$$\text{Hydroquinone (HQ)} \underset{+2e^-, +2H^+}{\overset{-2e^-, -2H^+}{\rightleftharpoons}} \text{Benzoquinone} \tag{4.3}$$

$$\text{4-Aminophenol (AP)} \underset{-2e^-, -2H^+}{\overset{+2e^-, +2H^+}{\rightleftharpoons}} \text{Quinonemine} \tag{4.4}$$
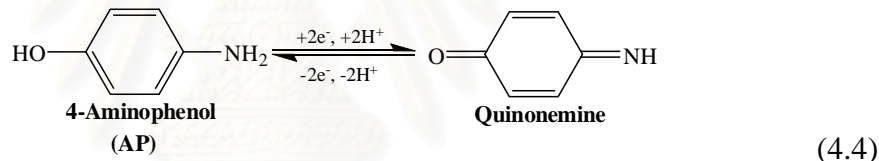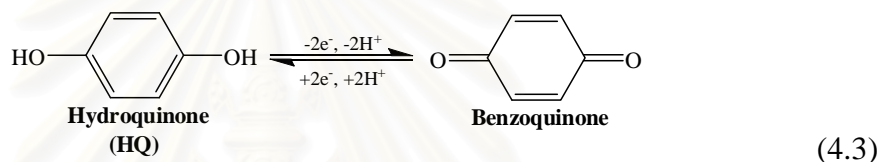
Normally, in an ALP reaction, IP substrate generated indigo blue (IB) by enzymatic hydrolysis as shown reaction in equation (4.5). IB is less soluble in aqueous solution. Therefore, fuming sulphuric acid was added in the solution to form soluble IC which can be investigated by electrochemical detection (equation (4.6)) [4]. Since the alkaline condition is required for the reaction of ALP, it is complicated to detect IP using electrochemical technique. Also, ALP can be exhibited the good reaction in base solution (pH 8-10). Therefore, fuming sulphuric acid is not suitable for ALP reaction.

$$3\text{-Indoxyl phosphate (IP)} \xrightarrow[-PO_3^{2-}]{ALP} \text{Indigo blue (IB)} \xrightarrow{H_2SO_4} \text{Indigo carmine (IC)} \tag{4.5}$$

$$\text{Indigo carmine (IC)} \underset{-2e^-, -2H^+}{\overset{+2e^-, +2H^+}{\rightleftharpoons}} \text{Leucoindigo carmine} \tag{4.6}$$
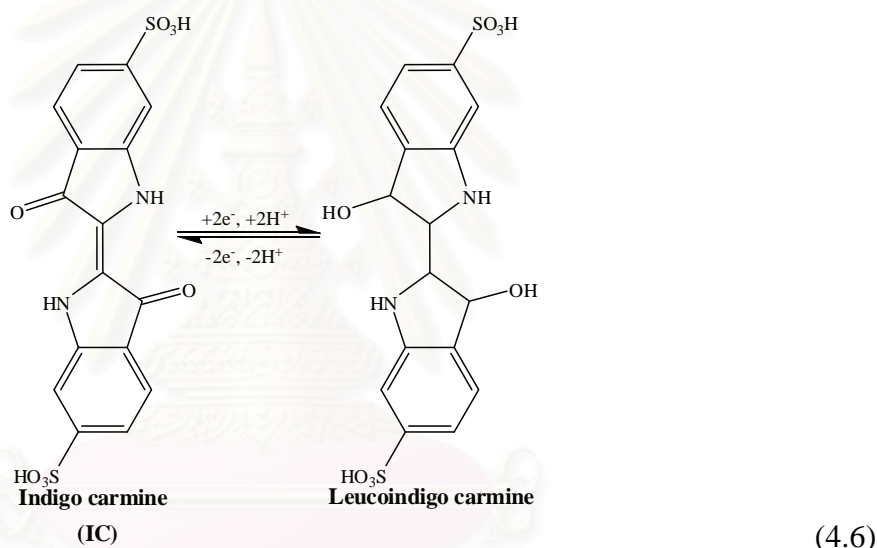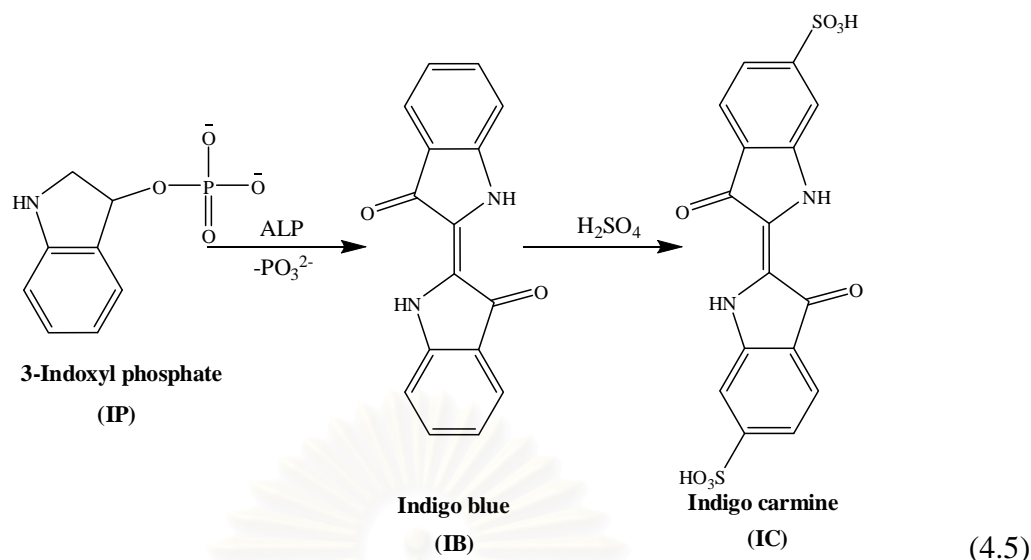
In contrast, NP (Figs. 4.2-4.4(c)) NT (Figs. 4.2-4.4(e)), Phe (Figs. 4.2-4.4(f)), and AA (Figs. 4.2-4.4(g)) display a well-defined anodic peak of cyclic voltammogram corresponding to the literatures [4, 5, 7, 10-14]. Phe, NP, and NT cyclic voltammograms display a poor redox reversibility in all oxidation studies, as same as the voltammograms showed in previous work [4]. The NP and NT electrochemical reactions were similar to the Phe reaction shown in equation (4.7) and their amperometric responses quickly decayed to zero (or base-line current density) due to electrode fouling, as shown in Figs. 4.2-4.4B(c), Figs. 4.2-4.4B(e), and Figs. 4.2-4.4B(f) for NP, NT, and Phe, respectively. The NP, NT, and Phe electrooxidation reactions caused the accumulation of electroinactive species or polymer formation at the electrode surface, leading to passivation of the electrode. Electrode passivation or

fouling can pose problems for the development and application of electrochemical immunosensors. For AA (Figs. 4.2-4.4A(g)), cyclic voltammograms showed an anodic peak at 20 mV, 500 mV, and 200 mV for GC disk, SPC, and Au disk, respectively. This irreversible reaction was consistent with previous studies [5, 7]. Figs. 4.2-4.4B(g) demonstrates the nearly constant amperometric responses of AA, indicating that less passivation occurring at all of the electrodes. The electrochemical reaction of AA is showed in equation (4.8).
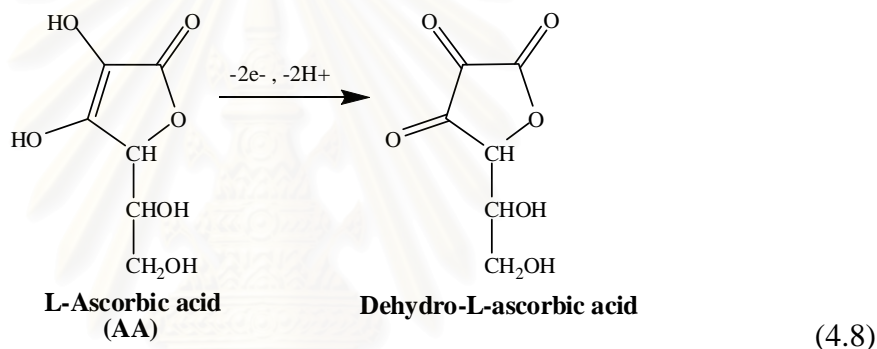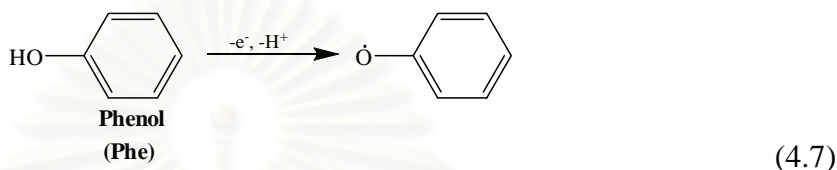
$$\text{Phenol (Phe)} \xrightarrow{-e^-, -H^+} \dot{O}\text{-phenyl} \tag{4.7}$$

$$\text{L-Ascorbic acid (AA)} \xrightarrow{-2e^-, -2H^+} \text{Dehydro-L-ascorbic acid} \tag{4.8}$$

Most electrochemical immunoassay methods are based on the application of a constant potential to an electrode transducer and the measurement of the current generated by the oxidation of enzyme hydrolysis products. Thus, amperometric detection was performed to evaluate the behavior of these products. When NP, NT and Phe solutions were added, the responses rapidly decayed due to the electrode fouling. These results were similar to the results reported in the literatures [7, 25]. In contrast, the HQ, AP, and AA amperograms in Figs. 4.2-4.4B(b), Figs. 4.2-4.4B(d), and Figs. 4.2-4.4B(g) displayed nearly constant anodic current signals after HQ, AP, and AA solutions were added to the electrolytes for amperometric measurement, implying less significant electrode passivation. The electrode was reused for 3 times of the measurements nearly without loss of sensitivity. The sensitivities for determination of HQ, AP, and AA at GC disk, SPC, and Au disk electrodes were to be 0.29 ± 0.02, 0.17 ± 0.01, and 0.15 ± 0.01 μA cm^{-2} μM^{-1} for HQ; 0.25 ± 0.00, 0.14 ± 0.02, and 0.32 ± 0.01 μA cm^{-2} μM^{-1} for AP; and 0.24 ± 0.02, 0.12 ± 0.02, and 0.47 ± 0.01 μA

cm^{-2} μM^{-1}, respectively. For ALP enzyme reaction, HQ, AP, and AA are generated from HQP, APP, and AAP substrates, respectively. An AAP substrate was commercially available, inexpensive, and non-fouling at the electrodes whereas AA product was non-toxic, chemically stable, and highly sensitive for response at the electrodes [5, 7, 23]. Compared with the non-commercially available HQDP and the costly APP, AAP was chosen as the enzyme substrate for the immunoassay experiments.

4.2 Characterization of poly-*o*-ABA using electropolymerization

Poly-*o*-ABA was modified onto GC disk, Au disk, SPC, GC plate, and BDD electrodes by cyclic voltammetric electropolymerization. The cyclic voltammogram for characterization of *o*-ABA polymer at BDD electrode is shown in Fig. 4.5. The voltammograms at the other electrodes were also analogous to those of BDD electrode. Fig. 4.5 shows cyclic voltammograms of 50 mM *o*-ABA scanning from 0 to 0.97 V (vs. Ag/AgCl) at BDD electrode with a scan rate of 40 mV s^{-1}. Previously, similar electropolymerization of *o*-ABA at Au [24], platinum [48], and GC [49, 50] electrodes were reported. In the first cycle, an irreversible anodic peak at 0.80 V was obtained. It is believed that the peak is related to the oxidation of *o*-ABA to free radical at the surface of the electrode (equation (4.9)). A protonic peak at 0.44 V and the de-doping processing at 0.23 V are shown in the cathodic scan [24].
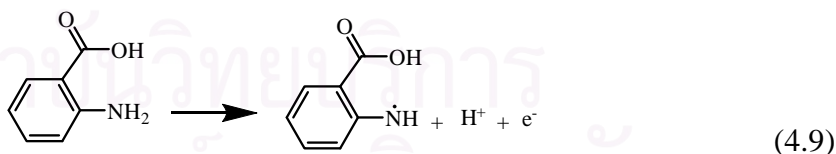
$$(4.9)$$

After the first scan, cyclic voltammograms gave two distinct redox processes. The first couple appeared at $E_{p_{a,1}} = 0.26$ V and $E_{p_{c,1}} = 0.21$ V, with the peak separation (ΔE_p) close to 50 mV. The second couple was observed at $E_{p_{a,2}} = 0.51$ V and $E_{p_{c,2}} = 0.41$ V with ΔE_p of 100 mV. The second through tenth cycles appeared with increasing currents, indicating that the polymer film had grown. After the tenth cycle, the current increased very slowly. Therefore, the 10-cycle voltammetry was fixed for

the optimum condition of *o*-ABA electropolymerization. The peaks are similar to those reported by Wang et al. [24]. They fabricated the self-doped conducting polyaniline by electrochemical polymerization of aniline and *o*-ABA and investigated the carboxyl groups by *in situ* electrochemistry and surface plasmon resonance spectroscopy (SPR). Benyoucef et al. [48] synthesized the homo-polymer of *o*-, *m*-, and *p*-ABA at Pt electrodes by electrochemical cyclic scanning of the potential and characterized their polymers with *in situ* FTIRS. Assuming that the *o*-ABA was coupled by a head-to-tail for polymeric chain growing in the main path, the postulated equations were given by equations (4.10) and (4.11) [24, 48], and the polymer structure is also show in Fig. 4.6.

(4.10)

(4.11)
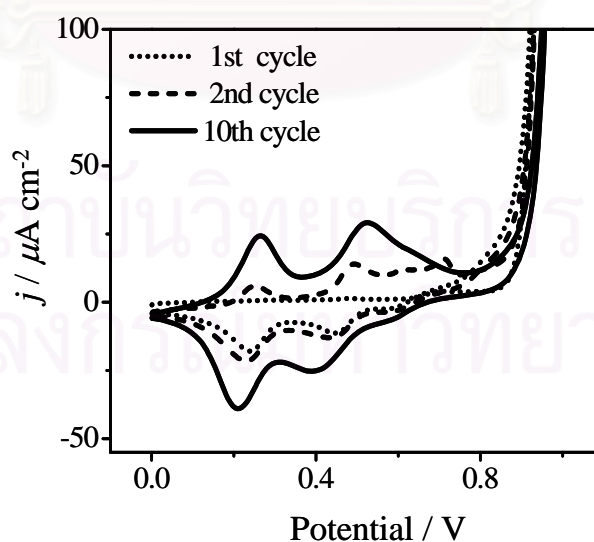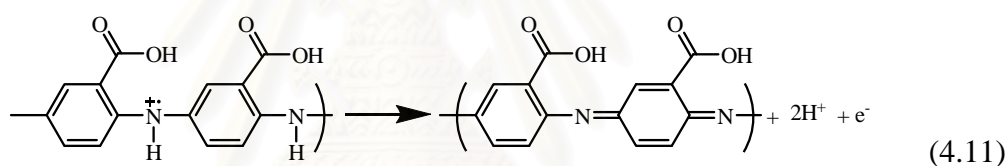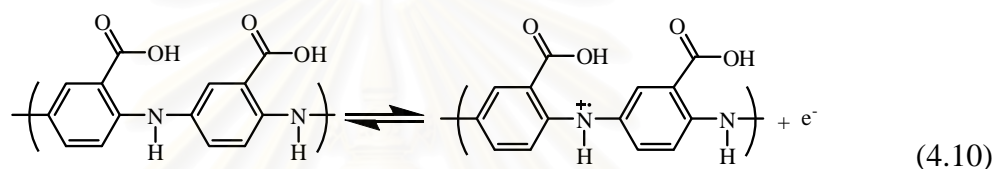
Figure 4.5 Cyclic voltammograms of the first cycle (dotted line), the second cycle (dashed line), and the tenth cycle (solid line) of *o*-ABA polymerization at BDD electrode with the scan rate of 40 mV s^{-1}
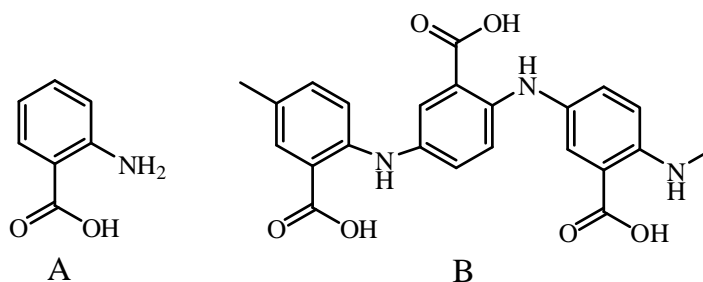
Figure 4.6 Structures of A) *o*-aminobenzoic acid (*o*-ABA) and B) poly-*o*-aminobenzoic acid (poly-*o*-ABA)

SEM image of BDD, Fig. 4.7, shows a half of the bright color of the unmodified BDD surface (Fig. 4.7A) and the other half of the dark color of the poly-*o*-ABA modified BDD surface (Fig. 4.7B).
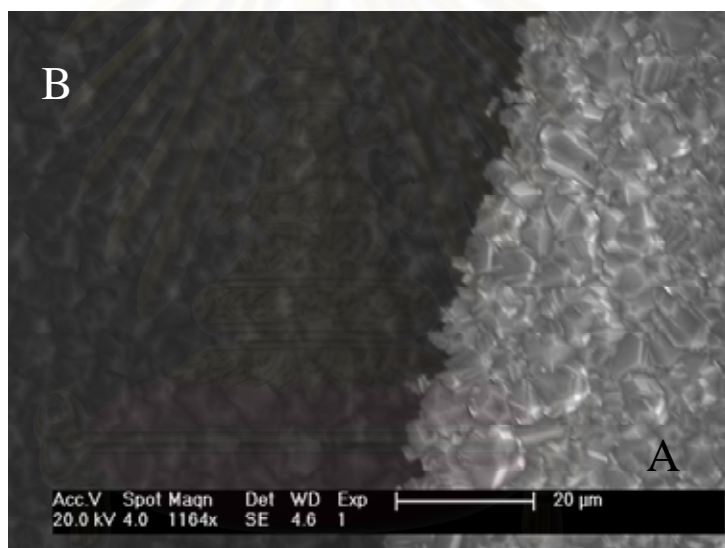
Figure 4.7 SEM image of BDD electrode A) before (bright color) and B) after (dark color) modified by poly-*o*-ABA

XPS was used to analyze the chemical composition of the BDD surface, C1s and N1s regions, before and after poly-*o*-ABA electropolymerization. Fig 4.8A shows the decreasing of the bulk C1s peak at about 283.7 eV after the polymer-coated BDD was generated. The C1s component at binding energy of ~288 eV is characteristic of the COOH group of poly-*o*-ABA modified at the BDD surface [74]. This spectrum component was small, but appeared clearly in comparison with the spectrum of the unmodified BDD. The N1s spectrum in Fig 4.8B shows the presence

of poly-*o*-ABA. The spectrum is the same as the N1s spectrum of polyaniline because the *o*-ABA is one of an aniline derivative. The ratio of C1s peak of COOH groups to N1s of poly-*o*-ABA (COOH/N) is about 1:1. This result confirmed the postulation of poly-*o*-ABA formation that one COOH group and one N might come from a monomer of *o*-ABA.
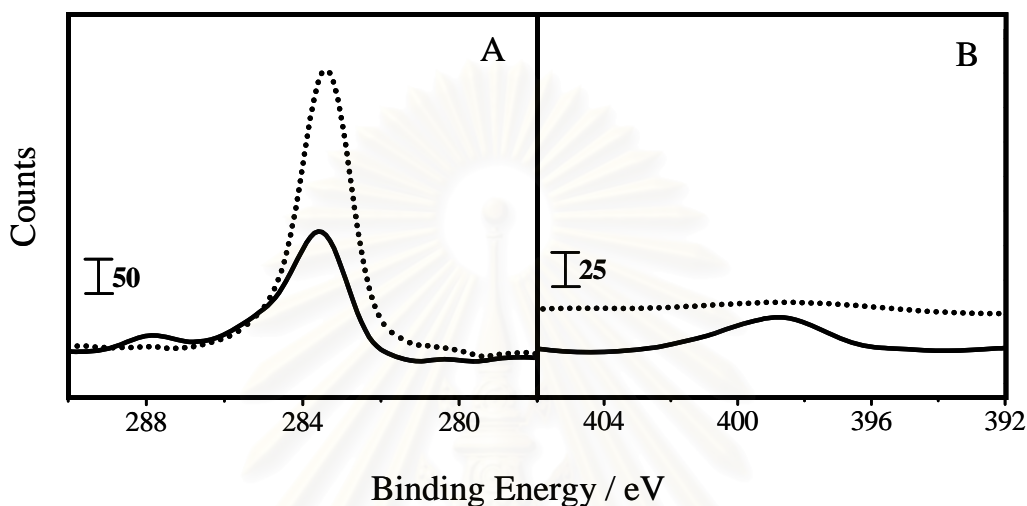
Figure 4.8 XPS of A) C1s and B) N1s spectra of BDD before (dotted lines) and after (solid lines) modified by poly-*o*-ABA

4.3 Comparison of SAM/Au disk and poly-*o*-ABA/Au disk immunosensors for MIgG determination

In this research, the sandwich immunoassay was used for fabrication of immunosensors. This assay involved immobilization of the primary antibody GaMIgG, capture of the target MIgG, association of GaMIgG-ALP, and finally using AAP as a substrate, which gave the best product signal among 7 ALP substrates as described in section 4.1. Enzymatically generated by ALP, AA is an electroactive species that can produce electrochemical oxidation signal being related to the quantity of MIgG. The enzymatic reaction of ALP and the electrochemical oxidation of AA are shown in equations (4.12) and (4.8), respectively [23].

2-Phospho-L-ascorbic acid
(AAP)

L-Ascorbic acid
(AA)

$$\text{(4.12)}$$

L-Ascorbic acid
(AA)

Dehydro-L-ascorbic acid

$$\text{(4.8)}$$
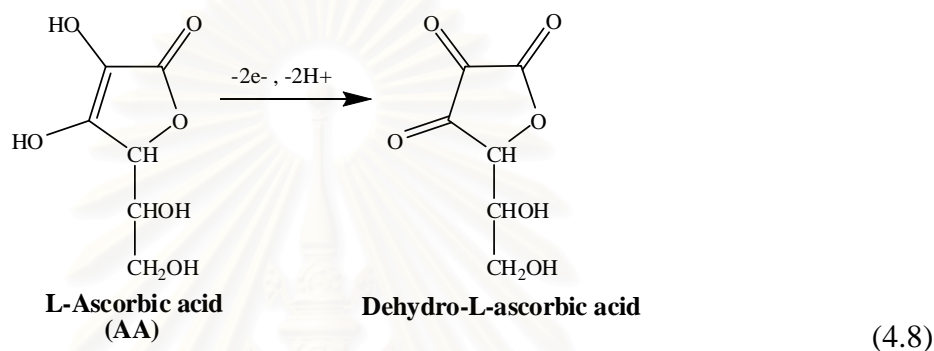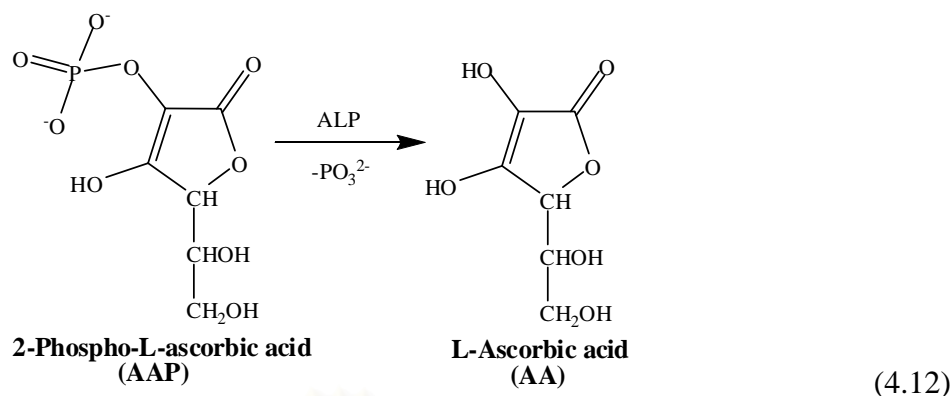
Two types of Au disk electrode immunosensors, SAM/Au disk and poly-*o*-ABA/Au disk immunosensors, were studied. SAM and poly-*o*-ABA were bases for covalent bonding between the electrode surface and the primary antibody (GaMIgG) for sandwich immunoassay.

4.3.1 SAM/Au disk immunosensor

Basically, Au is very good for using with SAM of thiols as the basis of the covalent bonding immunosensor because there is strong bonding between the Au surface and thiol groups introducing COOH groups to the Au surface. A mix SAM of 11-mercaptoundecanoic acid (C11) and 6-mercapto-1-hexanol (C6) was used for the base of the immunosensor. The structures of C11 and C6 and a schematic of the SAM/Au disk immunosensor are shown in Fig. 4.9 and 4.10, respectively. The preparation of the MIgG SAM/Au immunosensors was optimized by a variety of C11-to-C6 ratios (1:9, 2:8, 3:7, 4:6, 6:4, and 8:2) and the current density response of those immunosensors are shown in Fig. 4.11A. The highest ratio of target (T; 1,000 ng mL^{-1} MIgG) to control (C; 0 ng mL^{-1} MIgG) was obtained when using C11-to-C6 ratio of 1:9, as shown in Fig 4.11B. At this ratio, C6 efficiently minimized non-specific adsorption and C11 provided enough binding for GaMIgG at the same time.
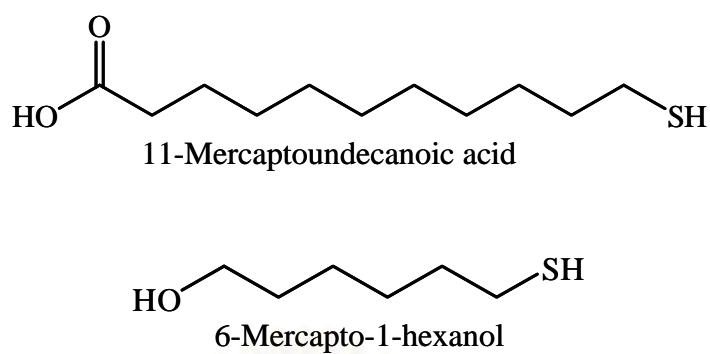
Figure 4.9 Structures of 11-mercaptoundecanoic acid (C11) and 6-mercapto-1-hexanol (C6)
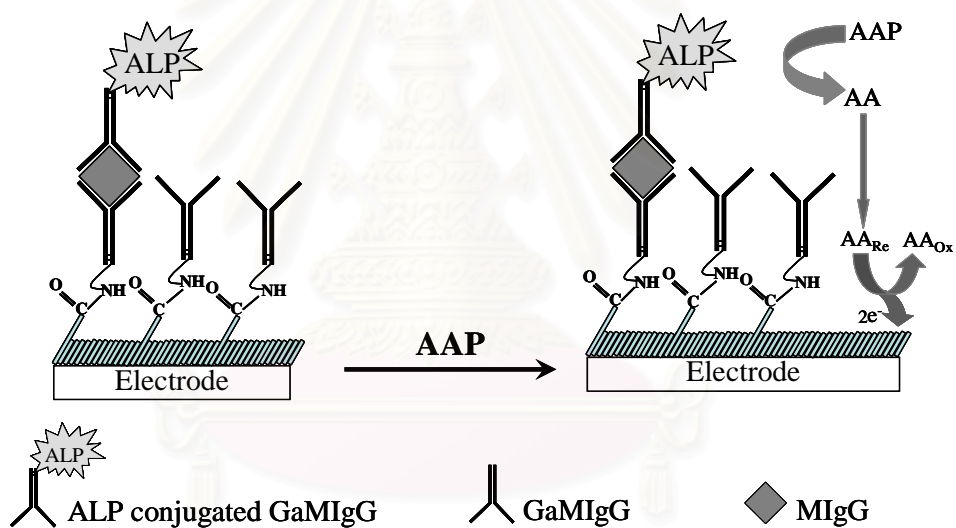
Figure 4.10 Schematic of the amperometric enzyme immunosensor based on the SAM modified electrode
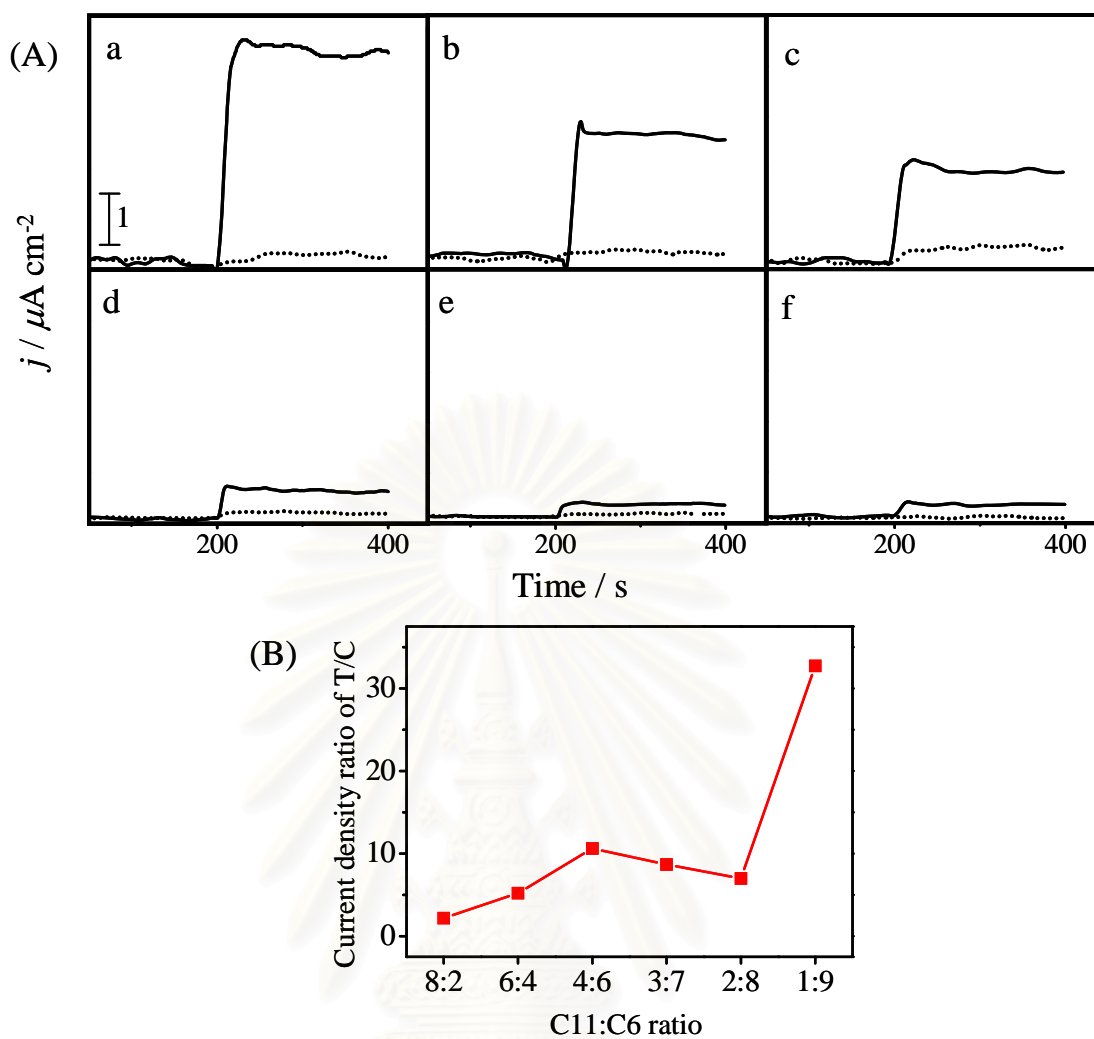
Figure 4.11   A) Amperometric responses of 1,000 ng mL^{-1} (Target, T; solid lines) and 0 ng mL^{-1} MIgG (Control, C; dotted lines) onto SAM/Au with the C11:C6 ratios of (a) 1:9, (b) 2:8, (c) 3:7, (d) 4:6, (e) 6:4, and (f) 8:2 in 0.5 M Tris buffer solution (pH 8.5) at +0.40 V vs. Ag/AgCl.

B) The relationship of current density ratios of T:C with various C11:C6 ratio of SAM/Au immunosensors that presented in Fig. 4.11A.

4.3.2 Poly-*o*-ABA /Au disk immunosensor

Determination of MIgG (the target protein) using a sandwich-type immunoassay by disposable poly-*o*-ABA modified electrode was developed. The schematic is shown in Fig. 4.12.
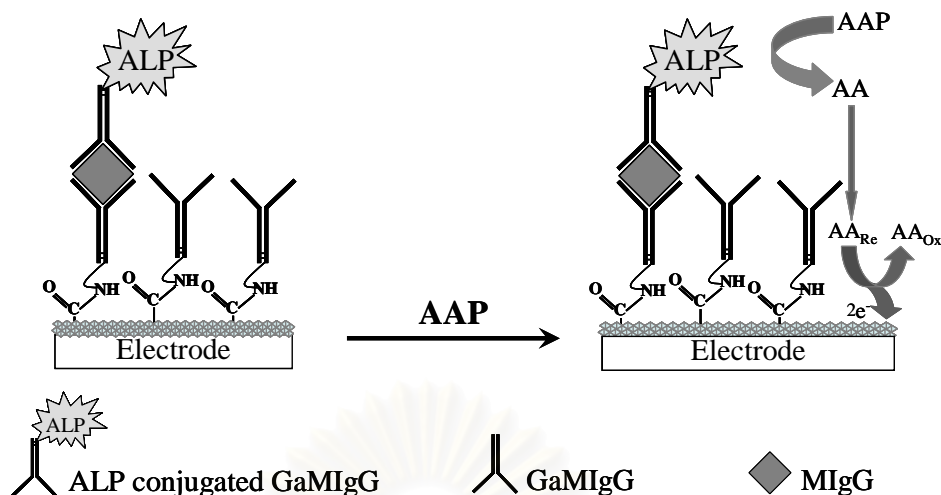
Figure 4.12 Schematic of the amperometric enzyme immunosensor based on the poly-*o*-ABA modified electrode

In Fig 4.12, the sandwich immunoassay method was applied for the immunosensor system. The GaMIgG was bound covalently to the COOH groups at the surface of the poly-*o*-ABA modified electrodes. To link the GaMIgG to the carboxyl surface, NHS/EDAC was added to modify carboxyl groups to N-hydrosuccinimide esters, which bonds covalently with amines on the antibodies in a natural pH aqueous solution at ambient temperature [75]. The incubation times for GaMIgG, MIgG, and GaMIgG-ALP were optimized. The optimum incubation time of 120 minutes at room temperature was fixed in solutions containing GaMIgG (40 μg mL^{-1}), followed by the incubation in ethanolamine solution for 30 minutes for blocking and quenching the active functional group that remained on the surface of poly-*o*-ABA. Then, the 60-minute incubation of different concentrations of target MIgG (including control solution without MIgG) and then the last 60 minutes for incubation in solutions containing the GaMIgG-ALP were obtained.

The amperometric immunosensor was operated by adding 0.5 M Tris buffer electrolyte solution (pH 8.5) to a cell consisting of immunosensor, Ag/AgCl, and Pt wire as working, reference, and counter electrodes, respectively. A potential of 0.4 V, under stirring, was applied to the immunosensor until the baseline of background was stable before the addition of AAP substrate to the solution. The optimized concentration of AAP for the saturated reaction with ALP conjugated immunosensor was 3 mM. Due to the oxidation of AA generated by the enzyme

reaction, the current increase caused an immediate response and reached steady state very fast. Result of poly-*o*-ABA/Au disk immunosensor is shown in Fig 4.13A. The current densities of 1,000 ng mL^{-1} (T; solid line) and 0 ng mL^{-1} (C; dotted line) MIgG were 4.19 and 0.13 μA cm^{-2}, respectively.

Amperometric responses of poly-*o*-ABA/Au disk (Fig. 4.13A) and SAM/Au disk (Fig. 4.13B) were compared under the same condition of sandwich immobilization, detection, and target concentration. Results showed T:C ratios of 33 and 297 for SAM/Au disk and poly-*o*-ABA/Au disk immunosensors, respectively.

Therefore, using poly-*o*-ABA conductive polymer provided higher sensitivity than using SAM for the base Au immunosensor because electron transfer on conductive polymer is very good by froming π electron backbone of the polymer structure on the electrode surface is very good. In comparison, layers of SAM and biomolecules make electron transfer more difficult and lead to the blocking of direct electron transfer between the electroactive species and an electrode.
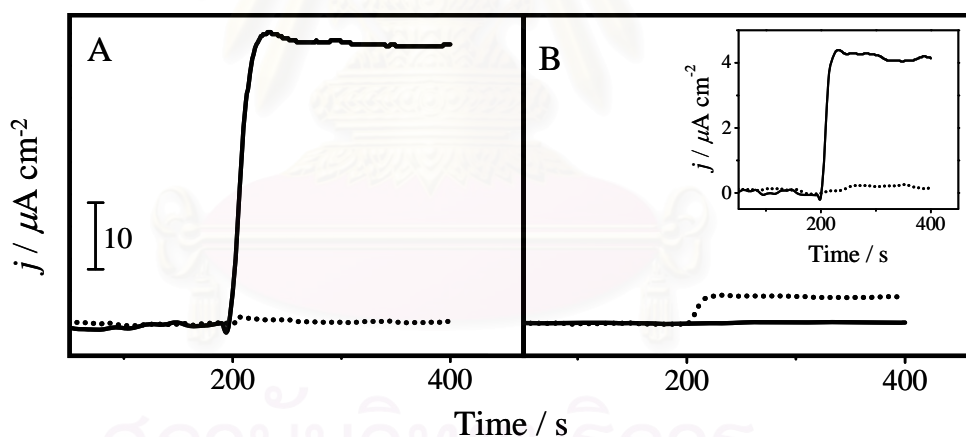
Figure 4.13 Amperometric responses of 1,000 ng mL^{-1} MIgG (solid lines) and 0 ng mL^{-1} MIgG (dotted lines) at A) poly-*o*-ABA/Au, and B) SAM/Au immunosensors in 0.5 M Tris buffer solution (pH 8.5) at +0.40 V vs. Ag/AgCl. Inset of B) shows the amperometric responses zooming for SAM/Au immunosensor

4.4 Poly-*o*-ABA at Au disk, GC disk, and SPC immunosensors for MIgG determination

4.4.1 Electrochemical studies of AAP and AA at Au disk, GC disk, and SPC electrodes

Cyclic voltammograms of 500 μM AA and 500 μM AAP were obtained at bare Au disk, GC disk, and SPC electrodes; AA produced irreversible oxidation at 0.2, 0.4, and 0.5 V in 0.5 M Tris buffer (pH 8.5) at bare Au disk, GC disk, and SPC electrodes, respectively (Fig 4.12). As shown in dashed lines of Fig. 4.12, no electrochemical process was observed for AAP, substrate of ALP, under the same conditions. Therefore, AAP did not appear to produce any electrochemical signal at the same potential as its product (AA), implying the ability to be ALP substrate for the immunosensor.
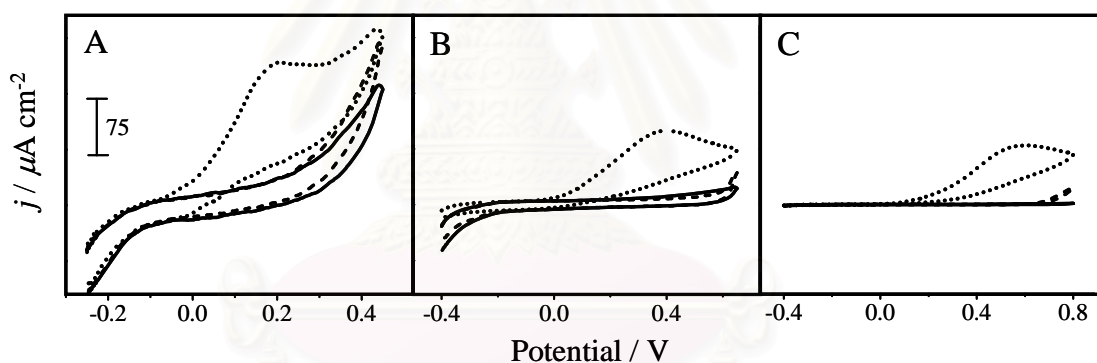
Figure 4.14 Cyclic voltammograms of 0.5 M Tris buffer (pH 8.5) electrolyte (solid lines), 500 μM AAP (dashed lines), and 500 μM AA (dotted lines) on bare working electrodes of A) Au disk, B) GC disk, and C) SPC electrodes at scan rate 100 mV s^{-1}

4.4.2 Optimization of immunoassay

The poly-*o*-ABA GC disk and poly-*o*-ABA SPC immunosensors were fabricated in the same manner as the poly-*o*-ABA Au disk immunosensor in section 4.3.2.

The preparation of the MIgG immunosensor on the poly-*o*-ABA/SPC electrode was studied to reveal the necessity of pre-treatment step with the applied current of 25 μA for 300 s and the curing temperature for SPC electrode preparation

before poly-*o*-ABA electropolymerization was varied from 200, 250, and 300°C. The best curing temperature was selected from the highest current response and the reversible potential separation for cyclic voltammogram of 1 mM $K_4Fe(CN)_6/K_3Fe(CN)_6$ solution. The maximum response was found at SPC electrodes with a curing temperature of 200°C after pre-treatment with the anodic current of 25 μA for 300 s. The pre-treatment and non pre-treatment of SPC electrodes were compared by the immunoassay process as shown in Fig 4.15. Fig. 4.15 shows the amperometric responses of AA generated from AAP by ALP enzyme on MIgG immunosensors based on poly-*o*-ABA/SPC at the potential of 0.50 V. After, the pre-treatment, the SPC electrode surface has hydrophilic property, so it can be electropolymerized better than the non pre-treated SPC electrode.
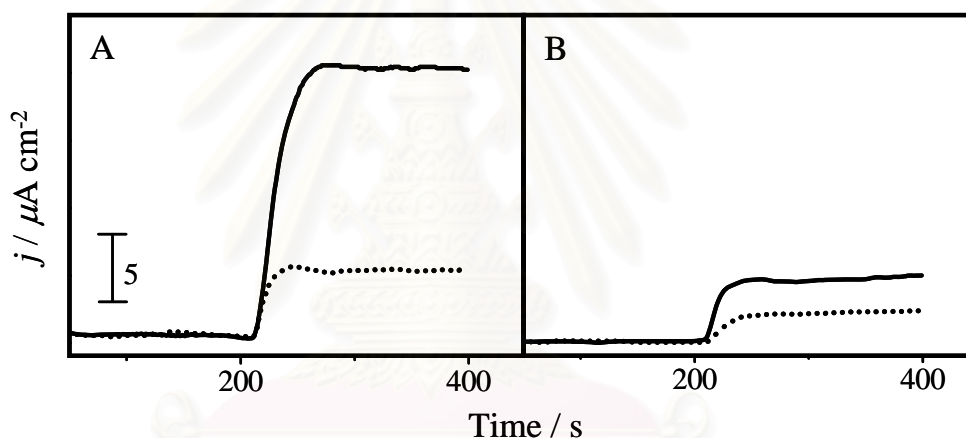
Figure 4.15 Amperometric responses of 1,000 ng mL^{-1} (solid lines) and 0 ng mL^{-1} MIgG (dotted lines) at poly-*o*-ABA/SPC with A) pre-treatment using 25 μA for 300 s and B) non pre-treatment in 0.5 M Tris buffer solution (pH 8.5) at +0.50 V vs. Ag/AgCl

Figs. 4.16A-C compare the amperometric responses of AA generated from AAP by ALP enzyme on MIgG immunosensors based on poly-*o*-ABA/GC disk, poly-*o*-ABA/SPC, and poly-*o*-ABA/Au disk electrodes at the potentials of 0.40, 0.50, and 0.40 V, respectively. The suitable potentials of their electrode immunosensors were obtained from hydrodynamic voltammetric measurement at each immunosensor by adding AAP in the electrolyte solution at various applied potentials of 0.1 to 0.6 V. Displayed in solid lines of Fig. 4.16A-C, the current densities for 1,000 ng mL^{-1} target MIgG at the poly-*o*-ABA/GC disk, poly-*o*-ABA/SPC, and poly-*o*-ABA/Au disk

immunosensors were 33.10, 22.49, and 43.50 μA cm^{-2}, respectively. The dotted lines in Fig. 4.16A-C representing the control corresponding to the current density at zero concentration of MIgG were 0.33, 5.88, and 0.15 μA cm^{-2}, respectively. We found that MIgG immunosensor on poly-*o*-ABA/Au disk gave the highest current density of response, with a T:C ratio of approximately 297, which implied that the poly-*o*-ABA on the Au surface would produce a surface with the least non-specific adsorption. Thus, we used this immunosensor as an MIgG sensor in the subsequent experiments. For the behavior of larger molecule as a substrate may exhibit slower turnover in the enzymatic reaction and may also exhibit slower diffusion through the biolayer towards the electrode surface. Using small molecule like AAP, it can generate to AA very quickly once it was added into the Tris buffer solution, showing a stable current within 30 s at all three immunosensors.
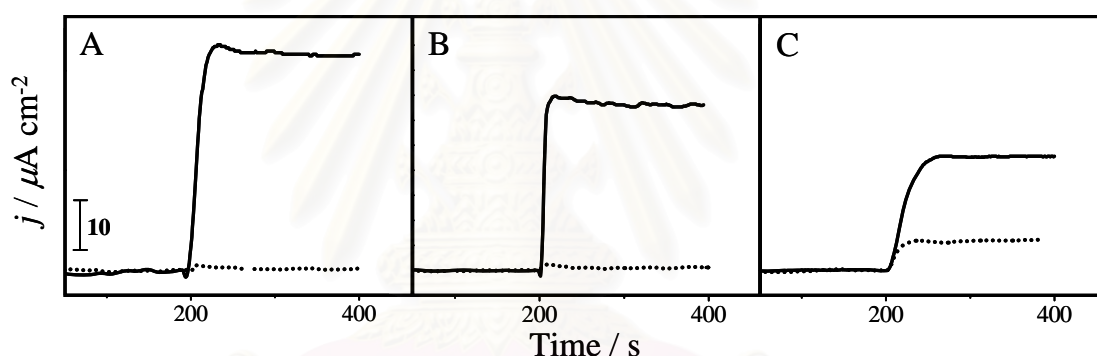
Figure 4.16 Amperometric responses of 1,000 ng mL^{-1} (solid lines) and 0 ng mL^{-1} MIgG (dotted lines) at A) poly-*o*-ABA/Au disk, B) poly-*o*-ABA/GC disk, and C) poly-*o*-ABA/SPC immunosensors in 0.5 M Tris buffer solution (pH 8.5) at A) and B) +0.40 V and C) +0.50 V vs. Ag/AgCl

4.4.3 Calibration curve of poly-*o*-ABA/Au disk immunosensor

The poly-*o*-ABA/Au disk immunosensing system displays the most sensitive response to the MIgG detection when compared with GC disk and SPC immunosensors. Fig. 4.17 presents amperograms of various MIgG concentrations. Measurements were performed in triplicate using three different immunosensors. The inset graph shows the dynamic range of the relationship between the average of current density responses (n=3) and MIgG concentration. It can be seen that the

dynamic range is from 3 to 200 ng mL^{-1} (R^2 = 0.9905), the sensitivity is 0.1401 μA cm^{-2} (ng mL^{-1})$^{-1}$, SD < 2 (n=3), and the detection limit is 1 ng mL^{-1}.
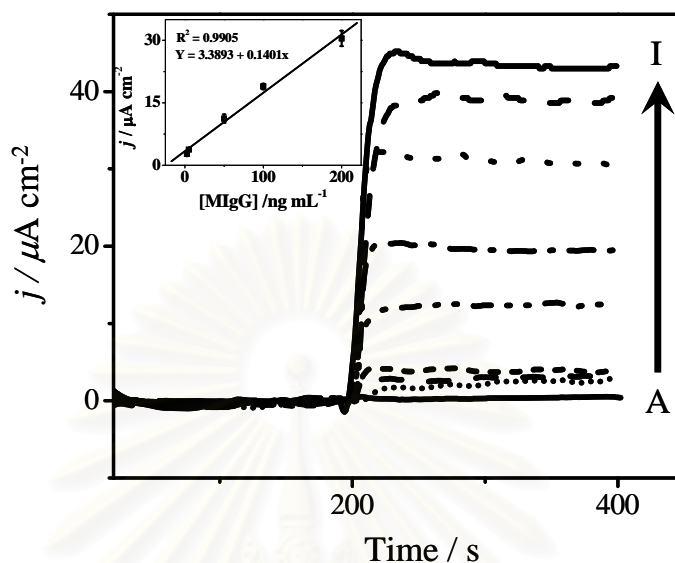
Figure 4.17 Amperograms of 0, 1, 3, 5, 50,100, 200, 500, and 1,000 ng mL^{-1} MIgG (A to I) at poly-*o*-ABA/Au disk immunosensor in 0.5 M Tris buffer solution (pH 8.5) at +0.40 V vs. Ag/AgCl. Inset shows the linear range of 3 to 200 ng mL^{-1} MIgG.

4.5 Poly-*o*-ABA at BDD and GC plate immunosensors for MIgG determination

4.5.1 Electrochemical studies of AAP and AA at GC plate and BDD electrodes

Cyclic voltammograms of 100 μM AA and 3 mM AAP in 0.1 M Tris buffer pH 8.5 solutions at BDD and GC plate before and after poly-*o*-ABA modification are shown in Figs. 4.18 and 4.19, respectively. The anodic peak potentials of AA before and after poly-*o*-ABA modification were obtained at 0.28 and 0.44 V for BDD and 0.01 and 0.42 V for GC plate. After the modification, all of anodic peaks were shifted positively as ~0.16 V for both oxidation of AA and AAP at BDD, and 0.41 and 0.17 V for AA and AAP oxidation at GC plate, respectively. A plausible possibility is that, after electropolymerization, the -COOH groups (negatively charged species) that covered at the electrode surfaces provide

electrostatic repulsion to AA and AAP. Therefore, higher potential is required for the sufficient kinetics of the electron transfer. Influence of BDD termination on the oxidation of negatively charged molecules has been reported [55, 76]. The noticeable point is that the anodic current of AA at both BDD and GC plate before and after the modification with poly-*o*-ABA showed almost the same current, indicating good electron transfer with poly-*o*-ABA as a conductive polymer. The poly-*o*-ABA is a carboxyl-group-functionalized polyaniline and its structure has π electron backbones for electron transfer [24, 32, 48-50, 77]. This is a great point to apply for immunosensor because the surface polymer needs to provide -COOH groups for conjugation with protein by covalent bonding and should also perform good electron transfer for AA oxidation at the same time. A summary of anodic potentials and current responses of AA and AAP at the BDD and GC plate before and after poly-*o*-ABA modification is given in Table 4.3.

AAP at the concentration of 3 mM was selected for the investigation as it is the optimum substrate concentration. The difference in anodic peak potential between 100 μM AA and 3 mM AAP after poly-*o*-ABA modification was about 0.4 V which should be enough to avoid the interference for the AA signal generated from the enzymatic reaction.
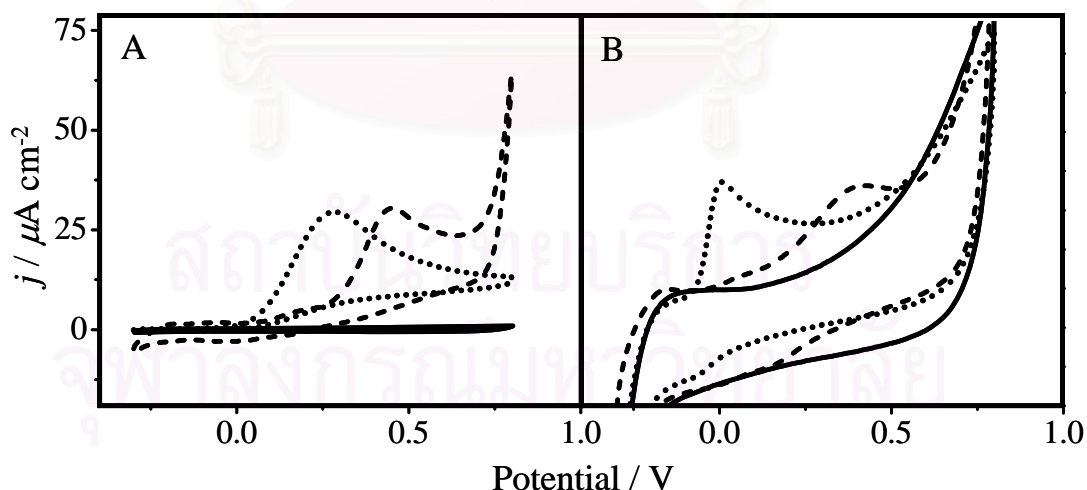
Figure 4.18 Cyclic voltammograms of electrolyte (0.1 M Tris buffer solution, pH 8.5; solid lines) and 100 μM AA at A) BDD and B) GC plate electrodes before (dotted lines) and after (dashed lines) modified by poly-*o*-ABA at the scan rate of 50 mV s^{-1}
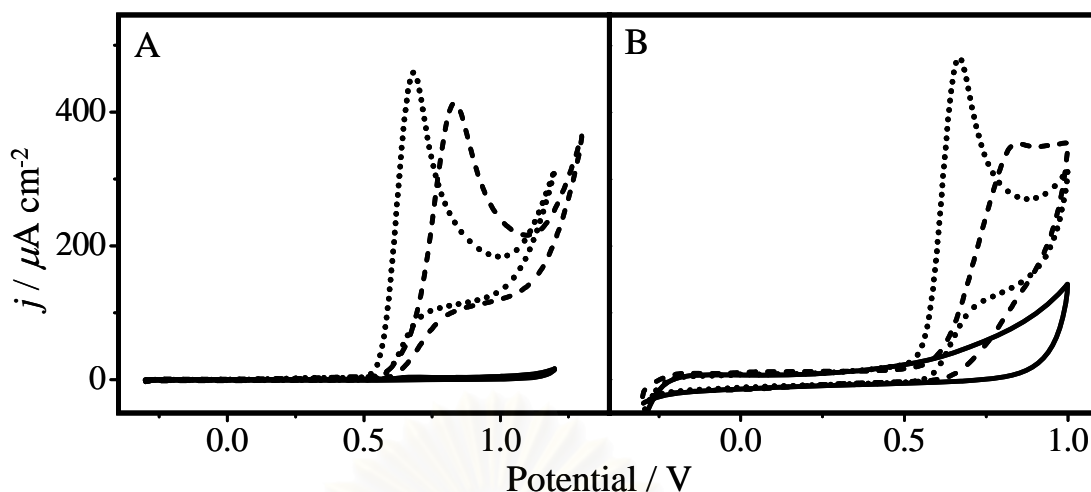
Figure 4.19 Cyclic voltammograms of electrolyte (0.1 M Tris buffer solution, pH 8.5; solid lines) and 3 mM AAP at A) BDD and B) GC plate electrodes before (dotted lines) and after (dashed lines) modified by poly-*o*-ABA at scan rate of 50 mV s^{-1}

Table 4.3 Summary of potentials and current responses for the oxidation of AA and AAP at BDD and GC plate before and after electropolymerized by poly-*o*-ABA

Type of electrode	Chemical	Bare electrode		Poly-*o*-ABA modified electrode	
		Potential peak (V)	*j* of peak (μA cm^{-2})	Potential peak (V)	*j* of peak (μA cm^{-2})
BDD	AA	0.28	30.48	0.44	29.60
	AAP	0.68	459.30	0.84	414.64
GC plate	AA	0.01	36.33	0.42	37.22
	AAP	0.67	480.41	0.84	354.08

4.5.2 Optimization of immunosensor system

Amperometric detection was used for the immunosensors. The hydrodynamics of AA at poly-*o*-ABA modified BDD and GC plate electrodes were investigated at the potential from 0.2 to 0.6 V. The highest current peaks were observed at 0.4 V for both electrodes. Therefore, for further experiments, an applied potential of 0.4 V was set up to detect AA in the immunoassay system.

Blocking the surface is one of the most important steps to minimize and to control non-specific binding. A shown in Fig. 4.20, the electrode current density for non-specific adsorption, in the absence of target MIgG and after being washed in multiple steps, was ~1.12 μA cm^{-2}. Apparently, the poly-o-ABA can decrease the physically non-specific adsorption by covering the surface with a thin film of polymer. The covalent attachment of poly-o-ABA reduces the non-specific binding to 0.33 μA cm^{-2}, which is about 4 times lower than the value when the polymer is absent. The use of BSA in the concentration range of 0-5% as blocking agent was also investigated. It was found that the use of 1% BSA could decrease the current density of non-specific adsorption to 0.24 μA cm^{-2} whereas more than 1% BSA gave almost the same current density as the 1% BSA. Therefore, in the next experiments, 1% BSA was fixed for blocking non-specific adsorption.
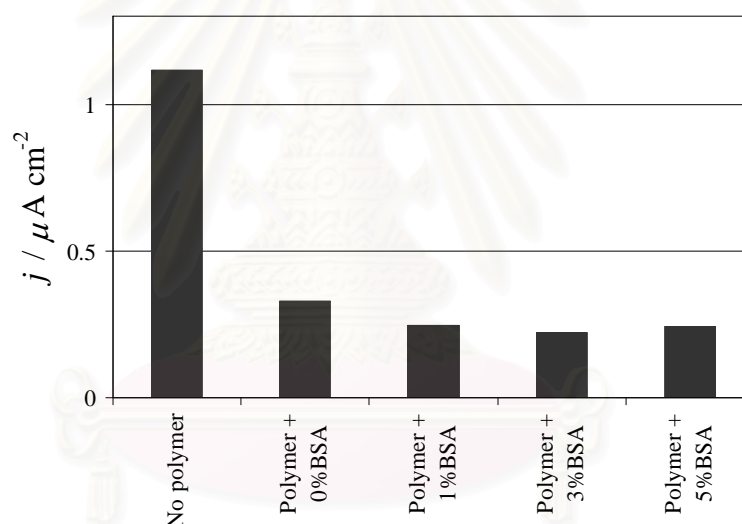
Figure 4.20 A relationship between the current density response and various conditions for control of immunosensors

Fig. 4.21 shows the amperometric responses of poly-o-ABA/BDD and poly-o-ABA/GC plate immunosensors at the potential of 0.40 V. Represented by the solid lines, the current density in target of 1,000 ng mL^{-1} MIgG were 23.50 and 16.13 μA cm^{-2} whereas, displayed by the dotted lines, the corresponding controls were 0.24 and 1.00 μA cm^{-2} for poly-o-ABA/BDD and poly-o-ABA/GC plate immunosensors, respectively. That results showed the T:C ratios as 97.92 and 16.13 for poly-o-ABA/BDD, and poly-o-ABA/GC plate immunosensors, respectively. Therefore, the poly-o-ABA/BDD immunosensor is better.
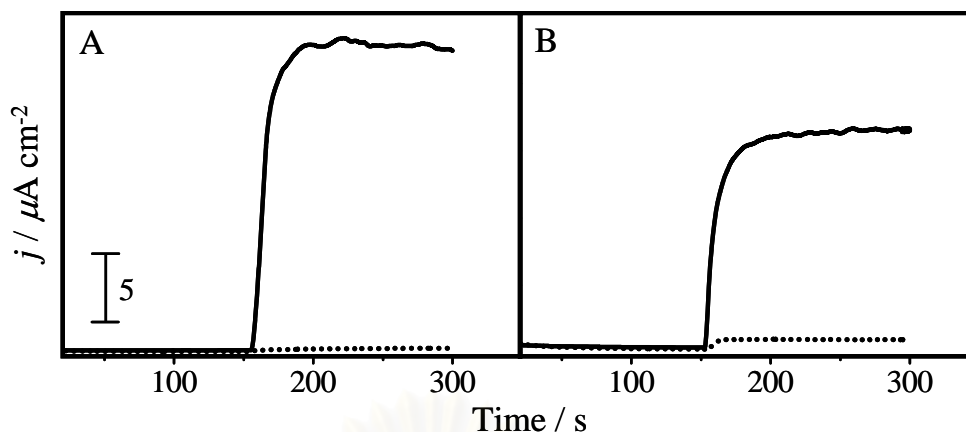
Figure 4.21 Amperometric responses of 1,000 ng mL^{-1} (solid lines) and 0 ng mL^{-1} MIgG (dotted lines) at A) poly-*o*-ABA/BDD and B) poly-*o*-ABA/GC plate immunosensors in 0.1 M Tris buffer solution (pH 8.5) at +0.40 V vs. Ag/AgCl

4.5.3 Reproducibility

Reproducibility of the immunoassay was expressed in terms of percentage of relative standard deviation (% RSD) of six different immunosensors under the same condition and concentration (intra-assay) as well as four different days of three replicate immunosensors in each day (inter-assay). High reproducibility was shown by collecting current signal of 100 ng mL^{-1} MIgG for replicate analysis in the intra-assay (*n*=6) and inter-assay (*n* =4) with % RSD values of 2.60 and 5.36 for poly-*o*-ABA/BDD immunosensors, and 6.84 and 9.07 for poly-*o*-ABA/GC plate immunosensors, respectively. The % RSD of poly-*o*-ABA/BDD immunosensor lower than poly-*o*-ABA/GC plate immunosensor, meaning that the poly-*o*-ABA/BDD immunosensor has higher reproducibility than the poly-*o*-ABA/GC plate immunosensor.

Table 4.4 Reproducibility study for poly-*o*-ABA/BDD and poly-*o*-ABA/GC plate immunosensors

Type of immunosensor	% RSD	
	Inter-assay (n=4)	Intra-assay (n=6)
poly-*o*-ABA/BDD	5.36	2.60
poly-*o*-ABA/GC plate	9.07	6.84

4.5.4 Detection limit and correlation

Fig. 4.22 shows the amperograms of MIgG using the poly-*o*-ABA/BDD and poly-*o*-ABA/GC plate immunosensor systems. The linear calibration curves are shown in the insets. The poly-*o*-ABA/BDD immunosensor is able to measure MIgG concentrations ranging from 1 to 1,000 ng nL^{-1}. The analytical performance of BDD immunosensor is compared with poly-*o*-ABA/GC plate immunosensor and summarized in Table 4.5. The linear range (LR) of poly-*o*-ABA/GC plate immunosensor was 10 to 500 ng mL^{-1}. The detection limits of poly-*o*-ABA/BDD and poly-*o*-ABA/GC plate were found to be 0.30 ng mL^{-1} (2 pM) and 3.50 ng mL^{-1} (23.3 pM) (3SD; calculation), respectively. High correlation can be obtained as shown by r^2 >0.999.
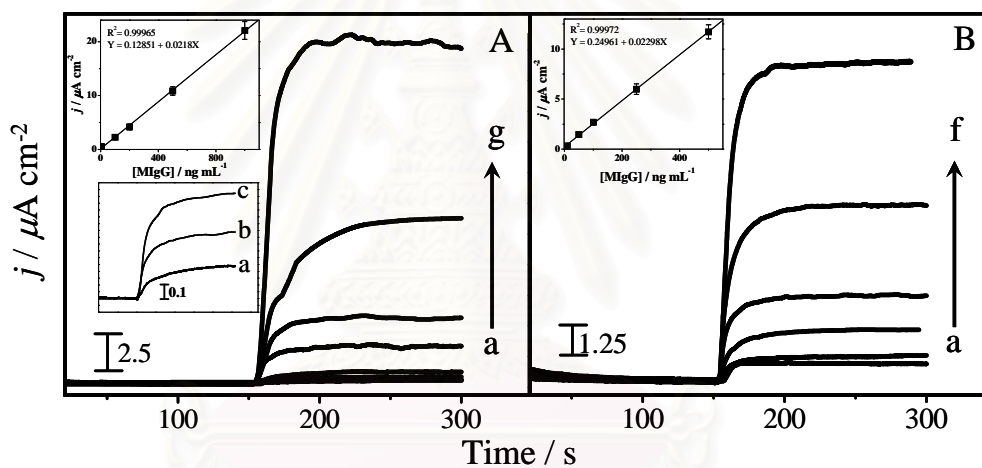
Figure 4.22 Amperograms of products (AA) after the addition of substrates (AAP) of ALP in Tris buffer solution (pH 8.5) at A) poly-*o*-ABA/BDD and B) poly-*o*-ABA/GC plate immunosensors by various target MIgG concentrations (0, 1, 5, 100, 200, 500, and 1,000 ng mL^{-1}; (a) to (g)) at the applied potential of 0.4 V. Insets in the top represent calibration plot showing the correspondence between the changes in anodic peak current after subtracting the control current (0 ng mL^{-1} ; absence of MIgG) and the concentration of MIgG and inset in the lower of (A) is zooming amperograms of (a) to (c) at poly-*o*-ABA/BDD immunosensors.

Table 4.5. Analytical performance of poly-*o*-ABA/BDD and of poly-*o*-ABA/GC plate immunosensors

Type of immunosensor	Mean of control (n=15) (μA cm^{-2} ±SD)	LOD (3SD; ng mL^{-1})	LR (ng mL^{-1})	R^2
poly-*o*-ABA/BDD	0.2471 ±0.045	0.30	1-1,000	0.99965
poly-*o*-ABA/GC plate	0.7104 ±0.119	3.50	10-500	0.99972

4.6 Comparison with other methods

Table 4.6 summarizes the MIgG determination at BDD immunosensor compared to immunosensors fabricated GC plate and Au disk using this system and other immunosensor systems. It can be observed that using the poly-*o*-ABA BDD immunosensor with amperometric detection provides a significantly low detection limit (0.3 ng mL^{-1}). To investigate the stability of the immunosensor, the electrode was stored in PBS at 4°C for an extended period of time. The sensor was evaluated over a period of 14 days of storage without loss of activity.

Table 4.6 Comparison of electroanalytical data for the determination of MIgG

Solid state based immunoassay	Enzyme label	Substrate	Method for detection	Linear Range	LOD (ng mL^{-1})	Stability	Ref
poly-*o*-ABA /BDD	ALP	AAP	Amperometry	1-1,000 ng mL^{-1}	0.3	2 weeks	[a]
poly-*o*-ABA /GC plate	ALP	AAP	Amperometry	10-500 ng mL^{-1}	3.5	-[b]	[a]
poly-*o*-ABA /Au disk	ALP	AAP	Amperometry	3-200 ng mL^{-1}	1	-	[a]
iridium oxide /Glass substrate	ALP	HQDP[c]	Amperometry	0-165 ng mL^{-1}	3	5 weeks	[78]
iridium oxide /APTES[c] /Glass substrate	ALP	HQDP[c]	Amperometry	5-50 ng mL^{-1}	2	-	[79]
SAM /Au (RMD[e])	ALP	PAPP[f]	Cyclic voltammetry	5-100 ng mL^{-1}	0.009	-	[80]
Dynabeads	ALP	PAPP[f]	GC-RDE[g] Amperometry	50-5,000 ng mL^{-1}	-	-	[81]
A 96-well plate	ALP	ANP[h]	Amperometry	0.01-100 µg ml^{-1}	6	-	[82]
carbon nanotubes /Fe /Al$_2$O$_3$ /SiO$_2$ /Si substrate	-	-	EIS[i]	range up to a 100 µg mL^{-1}	200	-	[83]

[a] This proposed method ; [b] no report, [c] hydroquinone diphosphate ; [d] (3-aminopropyl)triethoxysilane; [e] recessed microdisk; [f] 4-aminophenyl phosphate ; [g] glassy carbon rotating disk electrode; [h] 4-amino-1-naphthylphosphate ; and [i] electrochemical impedance spectroscopy

4.7 Poly-*o*-ABA modified BDD immunosensors for MIgG determination in a mouse serum

The poly-*o*-ABA modified BDD immunosensor was also applied to measure MIgG in a real sample of mouse serum. The external standard and standard addition curves are shown in Fig. 4.23. The mouse serum was diluted 50,000 times which is the interval dilution of the commercial MIgG ELISA test kit. The external standard was determined using five different MIgG concentrations (n=3) for a calibration curve. The standard addition was investigated by spiking three difference MIgG standard concentrations (n=2) into the diluted mouse serum. Recoveries of 80-100% were achieved for the poly-*o*-ABA modified BDD immunosensor that as show in Table 4.7. MIgG concentrations in the serum were found to be 174.30 and 189.34 ng mL^{-1} from external standard and standard addition at the 0.05 level, respectively. The population mean is not significantly different from the test mean (181.82). Moreover, a sample t-test was used to analyze the slopes of two methods, external standard and standard addition methods.   Both slopes were satisfactory at the 0.05 level, and that the population mean was not significantly different from the test mean (0.02055). These results indicate that the poly-*o*-ABA modified BDD immunosensor has high specificity and sensitivity for real samples of MIgG.
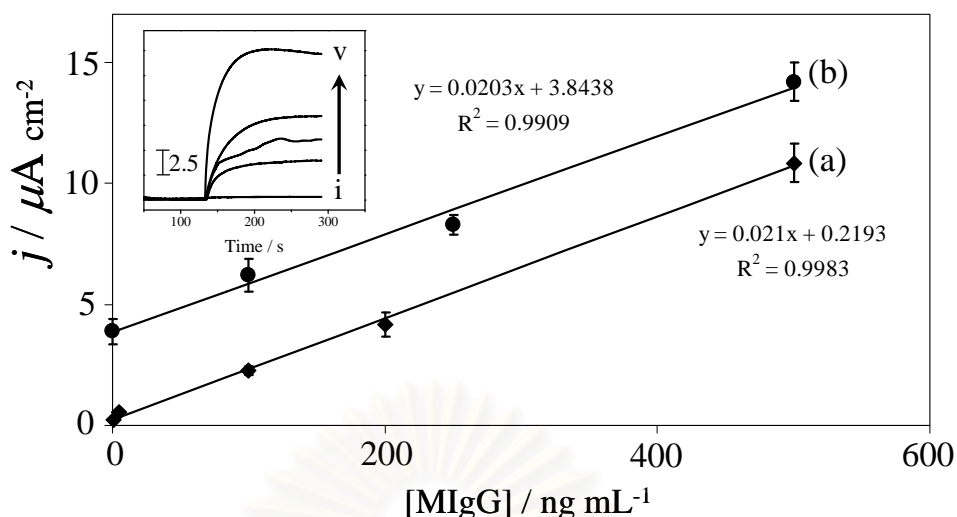
Figure 4.23 Comparison of two MIgG measurement methods in a mouse serum by (a) external standard and, (b) standard addition. Inset shows (i) control (Tris buffer), (ii) mouse serum diluted 50,000 times, (iii) mouse serum diluted 50,000 times in addition of 100 ng mL^{-1} standard MIgG, (iv) mouse serum diluted 50,000 times in addition of 250 ng mL^{-1} standard MIgG, (v) mouse serum diluted 50,000 times in addition to 500 ng mL^{-1} standard MIgG

Table 4.7 Standard addition of MIgG spiked in mouse serum

Concentration of standard MIgG spiked in mouse serum (ng mL^{-1})	Mean (n=2) (ng mL^{-1}; ±SD)	% RSD	% Recovery
100	100.23 (±4.08)	4.07	100.23
250	200.20 (±14.89)	7.43	80.08
500	481.51 (±38.09)	7.91	96.30

CHAPTER V

CONCLUSIONS AND FUTURE PERSPECTIVE

5.1 Conclusions

Having a variety of substrates, alkaline phosphatase (ALP) can be used as an effective label for sensitive immunoelectrochemical assays. Seven products of the ALP substrates, which are IC, HQ, NP, AP, NT, Phe, and AA have been comparatively examined by means of cyclic voltammetry and amperometry. Since AA gave the large and stable signal, along with having an inexpensive substrate, it was selected for the development of immunosensors at GC disk, Au disk, and SPC electrodes. Using mouse IgG (MIgG) as a model analyte, sandwich-type amperometric immunosensors based on all the electrodes were constructed. Cyclic voltammetric technique was simply employed to electropolymerize o-aminobenzoic acid (o-ABA) onto the electrode surfaces. Characterized by SEM and XPS, the modified surface provided freely accessible carboxyl groups as the binding sites for immunosensor base. Anti-mouse IgG (GaMIgG), the model antibody, was covalently immobilized at the poly-o-ABA modified electrode whereas MIgG was the target antigen for the detection. As the enzyme label, ALP was conjugated with GaMIgG to form a sandwich-type immunoassay. 2-phospho-L-ascorbic acid (AAP) was chosen as the substrate of ALP. Conversion of AAP to AA by ALP will give the electrochemical signal directly related to the quantity of the target antigen. This research found that the poly-o-ABA modified Au disk immunosensor gave the most favorable response (linear range: 3-200 ng mL^{-1}) with good sensitivity and reproducibility (SD<2; n=3) for MIgG sensor as well as low non-specific adsorption.

This immunoassay system was applied to BDD, the new electrode material. Similar to the other electrodes, the sandwich-type enzyme-amplified electrochemical immunosensor based on BDD was successfully prepared. Stable and selective MIgG sensing was shown by the GaMIgG poly-o-ABA modified BDD. This system was compared with the poly-o-ABA modified GC plate immunosensor. The detection

limit and the linear range were 0.3 ng mL^{-1} and 1-1000 ng mL^{-1} for the poly-*o*-ABA modified BDD immunosensor, and 3.50 ng mL^{-1} and 10-500 ng mL^{-1} for the poly-*o*-ABA modified GC plate immunosensor. From these results, it can be concluded that the poly-*o*-ABA modified BDD immunosemnsor provided the lower detection limit and wider linear range in comparison with the poly-*o*-ABA modified GC plate.

In addition, the poly-*o*-ABA modified BDD immunosensor was applied to measure MIgG in a real sample of mouse serum. External standard and standard addition methods were used. The recovery yields of 80-100% were achieved for the poly-*o*-ABA modified BDD immunosensor. MIgG concentrations in the serum were found to be 189.34 and 174.30 ng mL^{-1} via the external standard and standard addition methods, indicating that the poly-*o*-ABA modified BDD immunosensor had high specificity and sensitivity towards the MIgG real sample.

5.2 Future perspective

This developed method is versatile, offers enhanced performance including the possibility of *in vivo* detection by BDD microelectrode, and can be easily extended to other protein detection.

REFERENCES

1. Brajter-Toth, A.; and Chambers, J. Q. Electroanalytical methodes for biological meterials. New York: Marcel Dekker, INC. 2002.

2. Cleland, W. W.; and Hengge, A. C. Enzymatic mechanisms of phosphate and sulfate transfer. Chemical Reviews 106 (2006): 3252-3278.

3. Kwon, S. J.; Kim, E.; Yang, H.; and Kwak, J. An electrochemical immunosensor using ferrocenyl-tethered dendrimer. Analyst 131 (2006): 402-406.

4. Rosen, I.; and Rishpon, J. Alkaline phosphatase as a label for a heterogeneous immunoelectrochemical sensor : an electrochemical study. Journal of Electroanalytical Chemistry 258 (1989): 27-39.

5. Gyurcsanyi, R. E.; Bereczki, A.; Nagy, G.; Neuman, M. R.; and Lindner, E. Amperometric microcells for alkaline phosphatase assay. Analyst 127 (2002): 235-240.

6. Kreuzer, M. P.; O'Sullivan, C. K.; and Guilbault, G. G. Alkaline phosphatase as a label for immunoassay using amperometric detection with a variety of substrates and an optimal buffer system. Analytica Chimica Acta 393 (1999): 95-102.

7. Moore, E. J.; Pravda, M.; Kreuzer, M. P.; and Guilbault, G. G. Comparative study of 4-aminophenyl phosphate and ascorbic acid 2-phosphate, as substrates for alkaline phosphatase based amperometric immunosensor. Analytical Letters 36 (2003): 303-315.

8. Chikae, M.; Kerman, K.; Nagatani, N.; Takamura, Y.; and Tamiya, E. An electrochemical on-field sensor system for the detection of compost maturity. Analytica Chimica Acta 581 (2007): 364-369.

9. Diaz-Gonzalez, M.; Gonzalez-Garcia, M. B.; and Costa-Garcia, A. Immunosensor for Mycobacterium tuberculosis on screen-printed carbon electrodes. Biosensors and Bioelectronics 20 (2005): 2035-2043.

10. Fanjul-Bolado, P.; Gonzalez-Garcia, M. B.; and Costa-Garcia, A. Flow screen-printed amperometric detection of p-nitrophenol in alkaline phosphatase-based assays. Analytical and Bioanalytical Chemistry 385 (2006): 1202-1208.

11. Hart, J. P.; Pemberton, R. M.; Luxton, R.; and Wedge, R. Studies towards a disposable screen-printed amperometric biosensor for progesterone. Biosensors and Bioelectronics 12 (1997): 1113-1121.

12. Pemberton, R. M.; Hart, J. P.; Stoddard, P.; and Foulkes, J. A. A comparison of 1-naphthyl phosphate and 4-aminophenyl phosphate as enzyme substrates for use with a screen-printed amperometric immunosensor for progesterone in cows' milk. Biosensors and Bioelectronics 14 (1999): 495-503.

13. Rao, V. K.; Sharma, M. K.; Pandey, P.; and Sekhar, K. Comparison of different carbon ink based screen-printed electrodes towards amperometric immunosensing. World Journal of Microbiology & Biotechnology 22 (2006): 1135-1143.

14. Wilson, M. S.; and Rauh, R. D. Hydroquinone diphosphate: an alkaline phosphatase substrate that does not produce electrode fouling in electrochemical immunoassays. Biosensors and Bioelectronics 20 (2004): 276-283.

15. Fujishima, A.; Einaga, Y.; Rao, T. N.; and Tryk, D. A. Diamond electrochemistry. Tokyo: Elsevier-BKC, 2004.

16. Tannous, B. A.; Verhaegen, M.; Christopoulos, T. K.; and Kourakli, A. Combined flash- and glow-type chemiluminescent reactions for high-throughput genotyping of biallelic polymorphisms. Analytical Biochemistry 320 (2003): 266-272.

17. Zhu, X. J.; and Jiang, C. Q. 8-Quinolyl phosphate as a substrate for the fluorimetric determination of alkaline phosphatase. Clinica Chimica Acta 377 (2007): 150-153.

18. Zhu, X. J.; Liu, Q. K.; and Jiang, C. Q. 2-Carboxy-1-naphthyl phosphate as a substrate for the fluorimetric determination of alkaline phosphatase. Analytica Chimica Acta 570 (2006): 29-33.

19. Arakawa, H.; Shiokawa, M.; Imamura, O.; and Maeda, M. Novel bioluminescent assay of alkaline phosphatase using adenosine-3'-phosphate-5'-phosphosulfate as substrate and the luciferin-luciferase reaction and its application. Analytical Biochemistry 314 (2003): 206-211.

20. Szydlowska, D.; Campas, M.; Marty, J. L.; and Trojanowicz, M. Catechol monophosphate as a new substrate for screen-printed amperometric biosensors with immobilized phosphatases. Sensors and Actuators B-Chemical 113 (2006): 787-796.

21. Diaz-Gonzalez, M.; Fernandez-Sanchez, C.; and Costa-Garcia, A. Indirect determination of alkaline phosphatase based on the amperometric detection of indigo carmine at a screen-printed electrode in a flow system. Analytical Sciences 18 (2002): 1209-1213.

22. Fanjul-Bolado, P.; Gonzalez-Garcia, M. B.; and Costa-Garcia, A. Voltammetric determination of alkaline phosphatase and horseradish peroxidase activity using 3-indoxyl phosphate as substrate - application to enzyme immunoassay. Talanta 64 (2004): 452-457.

23. Kokado, A.; Arakawa, H.; and Maeda, M. New electrochemical assay of alkaline phosphatase using ascorbic acid 2-phosphate and its application to enzyme immunoassay. Analytica Chimica Acta 407 (2000): 119-125.

24. Wang, Y. J.; and Knoll, W. In situ electrochemical and surface plasmon resonance (SPR) studies of aniline-carboxylated aniline copolymers. Analytica Chimica Acta 558 (2006): 150-157.

25. Gorczynski, R.; and Stanley, J. Clinical immunology. U.S.A.: Texas, 1999.

26. Mikkelsen, S. R.; and Corto´n, E. Bioanalytical chemistry. New Jersey: John Wiley & Sons, 2004.

27. Emon, J. M. V. Immunoassay and other bioanalytical techniques. FL: Taylor & Francis Group, 2007.

28. Bagotsky, V. S. Fundamentals of electrochemistry. New Jersey: John Wiley & Sons, 2006.

29. Zoski, C. G. Handbook of electrochemistry. UK: Elsevier, 2006.

30. Pierson, H. O. Handbook of carbon, graphite, diamond and fullerenes: properties, processing and applications. New Jersey: Noyes publications, 1993.

31. Tangkuaram, T.; Ponchio, C.; Kangkasomboon, T.; Katikawong, P.; and Veerasai, W. Design and development of a highly stable hydrogen peroxide biosensor on screen printed carbon electrode based on horseradish peroxidase bound with gold nanoparticles in the matrix of chitosan. Biosensors and Bioelectronics 22 (2007): 2071-2078.

32. Ahuja, T.; Mir, I. A.; Kumar, D.; and Rajesh. Biomolecular immobilization on conducting polymers for biosensing applications. Biomaterials 28 (2007): 791-805.

33. Tzanavaras, P. D.; Themelis, D. G.; and Karlberg, B. Rapid spectrophotometric determination of fosfestrol following on-line hydrolysis by alkaline phosphatase using flow injection and chasing zones. Analytica Chimica Acta 462 (2002): 119-124.

34. Martinez-Montequin, S.; Fernandez-Sanchez, C.; and Costa-Garcia, A. Voltammetric monitoring of the interaction between streptavidin and biotinylated alkaline phosphatase through the enzymatic hydrolysis of 3-indoxyl phosphate. Analytica Chimica Acta 417 (2000): 57-65.

35. Kim, H. J.; and Kwak, J. Electrochemical determination of total alkaline phosphatase in human blood with a micropatterned ITO film. Journal of Electroanalytical Chemistry 577 (2005): 243-248.

36. Dong, H.; Li, C. M.; Chen, W.; Zhou, Q.; Zeng, Z. X.; and Luong, J. H. T. Sensitive amperometric immunosensing using polypyrrolepropylic acid films for biomolecule immobilization. Analytical Chemistry 78 (2006): 7424-7431.

37. Sun, X. M.; Gao, N.; and Jin, W. R. Monitoring yoctomole alkaline phosphatase by capillary electrophoresis with on-capillary catalysis-electrochemical detection. Analytica Chimica Acta 571 (2006): 30-33.

38. Gerard, M.; Chaubey, A.; and Malhotra, B. D. Application of conducting polymer to biosensors. Biosensors and Bioelectronics 17 (2002): 345-359.

39. Santandreu, M.; Cespedes, F.; Alegret, S.; and Martinez-Fabregas, E. Amperometric immunosensors based on rigid conducting immunocomposites. Analytical Chemistry 69 (1997): 2080-2085.

40. Santandreu, M.; Sole, S.; Fabregas, E.; and Alegret, S. Development of electrochemical immunosensing systems with renewable surfaces. Biosensors and Bioelectronics 13 (1998): 7-17.

41. Garcinuno, R. M.; Fernandez, P.; Perez-Conde, C.; Gutierrez, A. M.; and Camara, C. Development of a fluoroimmunosensor for theophylline using immobilised antibody. Talanta 52 (2000): 825-832.

42. Zhang, Y.; and Heller, A. Reduction of the nonspecific binding of a target antibody and of its enzyme-labeled detection probe enabling electrochemical immunoassay of an Antibody through the 7 pg/mL-100 ng/mL (40 fM-400 pM) range. <u>Analytical Chemistry</u> 77 (2005): 7758-7762.

43. Tsuji, I.; Eguchi, H.; Yasukouchi, K.; Unoki, M.; and Taniguchi, I. Enzyme immunosensors based on electropolymerized polytyramine modified electrodes. <u>Talanta</u> 66 (2005): 15-20.

44. Darain, F.; Park, S.-U.; and Shim, Y.-B. Disposable amperometric immunosensor system for rabbit IgG using a conducting polymer modified screen-printed electrode. <u>Biosensors and Bioelectronics</u> 18 (2003): 773-780.

45. Darain, F.; Park, D. S.; Park, J.-S.; Chang, S.-C.; and Shim, Y.-B. A separation-free amperometric immunosensor for vitellogenin based on screen-printed carbon arrays modified with a conductive polymer. <u>Biosensors and Bioelectronics</u> 20 (2005): 1780-1787.

46. Ordonez, S. S.; and F`abregas, E. New antibodies immobilization system into a graphite-polysulfone membrane for amperometric immunosensors. <u>Biosensors and Bioelectronics</u> 22 (2007): 965-972.

47. Ionescu, R. E.; Gondran, C.; Cosnierc, S.; Gheber, L. A.; and Marks, R. S. Comparison between the performances of amperometric immunosensors for cholera antitoxin based on three enzyme markers. <u>Talanta</u> 66 (2005): 15-20.

48. Benyoucef, A.; Huerta, F.; Vazquez, J. L.; and Morallon, E. Synthesis and in situ FTIRS characterization of conducting polymers obtained from aminobenzoic acid isomers at platinum electrodes. <u>European Polymer Journal</u> 41 (2005): 843-852.

49. Cheng, W.; Jin, G.; and Zhang, Y. Electrochemical characteristics of poly(*o*-aminobenzoic acid) modified glassy-carbon electrode and its electrocatalytic activity towards oxidation of epinephrine. <u>Russian Journal of Electrochemistry</u> 41 (2005): 940-945.

50. Zhang, Y. Z.; Jin, G. Y.; Cheng, W. X.; and Li, S. P. Poly (*o*-aminobenzoic acid) modified glassy carbon electrode for electrochemical detection of dopamine in the presence of ascorbic acid. <u>Frontiers in Bioscience</u> 10 (2005): 23-29.

51. Yano, T.; Popa, E.; Tryk, D. A.; Hashimoto, K.; and Fujishima, A. Electrochemical behavior of highly conductive boron-doped diamond electrodes for oxygen reduction in acid solution. <u>Journal of the Electrochemical Society</u> 146 (1999): 1081-1087.

52. Suzuki, A.; Ivandini, T. A.; Yoshimi, K.; Fujishima, A.; Oyama, G.; Nakazato, T.; Hattori, N.; Kitazawa, S.; and Einaga, Y. Fabrication, characterization, and application of boron-doped diamond microelectrodes for in vivo dopamine detection. <u>Analytical Chemistry</u> 79 (2007): 8608-8615.

53. Murata, M.; Ivandini, T. A.; Shibata, M.; Nomura, S.; Fujishima, A.; and Einaga, Y. Electrochemical detection of free chlorine at highly boron-doped diamond electrodes. <u>Journal of Electroanalytical Chemistry</u> 612 (2008): 29-36.

54. Yagi, I.; Ishida, T.; and Uosaki, K. Electrocatalytic reduction of oxygen to water at Au nanoclusters vacuum-evaporated on boron-doped diamond in acidic solution. <u>Electrochemistry Communications</u> 6 (2004): 773-779.

55. Ivandini, T. A.; Rao, T. N.; Fujishima, A.; and Einaga, Y. Electrochemical oxidation of oxalic acid at highly boron-doped diamond electrodes. <u>Analytical Chemistry</u> 78 (2006): 3467-3471.

56. Watanabe, T.; Ivandini, T. A.; Makide, Y.; Fujishima, A.; and Einaga, Y. Selective detection method derived from a controlled diffusion process at metal-modified diamond electrodes. <u>Analytical Chemistry</u> 78 (2006): 7857-7860.

57. Bauer, C. G.; Eremenko, A. V.; EhrentreichForster, E.; Bier, F. F.; Makower, A.; Halsall, H. B.; Heineman, W. R.; and Scheller, F. W. Zeptomole-detecting biosensor for alkaline phosphatase in an electrochemical immunoassay for 2, 4-dichlorophenoxyacetic acid. <u>Analytical Chemistry</u> 68 (1996): 2453-2458.

58. Honda, N.; Inaba, M.; Katagiri, T.; Shoji, S.; Sato, H.; Homma, T.; Osaka, T.; Saito, M.; Mizuno, J.; and Wada, Y. High efficiency electrochemical immunosensors using 3D comb electrodes. <u>Biosensors and Bioelectronics</u> 20 (2005): 2306-2309.

59. Aguilar, Z. P.; Vandaveer, W. R.; and Fritsch, I. Self-contained microelectrochemical immunoassay for small volumes using mouse IgG as a model system. <u>Analytical Chemistry</u> 74 (2002): 3321-3329.

60. Zhou, Y. L.; Tian, R. H.; and Zhi, J. F. Amperometric biosensor based on tyrosinase immobilized on a boron-doped diamond electrode. <u>Biosensors and Bioelectronics</u> 22 (2007), 822-828.

61. Rubio-Retama, J.; Hernando, J.; Lopez-Ruiz, B.; Hartl, A.; Steinmuller, D.; Stutzmann, M.; Lopez-Cabarcos, E.; and Garrido, J. A. Synthetic nanocrystalline diamond as a third-generation biosensor support. <u>Langmuir</u> 22 (2006): 5837-5842.

62. Yang, W.; Auciello, O.; Butler, J. E.; Cai, W.; Carlisle, J. A.; Gerbi, J. E.; Gruen, D. M.; Knickerbocker, T.; Lasseter, T. L.; Russell, J. N.; Smith, L. M.; and Hamers, R. J. DNA-modified nanocrystalline diamond thin-films as stable, biologically active substrates. <u>Nature Materials</u> 1 (2002): 253-257.

63. Yang, W. S.; Butler, J. E.; Russell, J. N.; and Hamers, R. J. Direct electrical detection of antigen-antibody binding on diamond and silicon substrates using electrical impedance spectroscopy. <u>Analyst</u> 132 (2007): 296-306.

64. Yang, W. S.; and Hamers, R. J. Fabrication and characterization of a biologically sensitive field-effect transistor using a nanocrystalline diamond thin film. <u>Applied Physics Letters</u> 85 (2004): 3626-3628.

65. Coffinier, Y.; Szunerits, S.; Jama, C.; Desmet, R.; Melnyk, O.; Marcus, B.; Gengembre, L.; Payen, E.; Delabouglise, D.; and Boukherroub, R. Peptide immobilization on amine-terminated boron-doped diamond surfaces. <u>Langmuir</u> 23 (2007): 4494-4497.

66. Coffinier, Y.; Szunerits, S.; Marcus, B.,; Desmet, R.; Melnyk, O.; Gengembre, L.; Payen, E.; Delabouglise, D.; and Boukherroub, R. Covalent linking of peptides onto oxygen-terminated boron-doped diamond surfaces. <u>Diamond and Related Materials</u> 16 (2007): 892-898.

67. Zhang, G. J.; Song, K. S.; Nakamura, Y.; Ueno, T.; Funatsu, T.; Ohdomari, I.; and Kawarada, H. DNA micropatterning on polycrystalline diamond via one-step direct amination. <u>Langmuir</u> 22 (2006): 3728-3734.

68. Huang, L. C. L.; and Chang, H. C. Adsorption and immobilization of cytochrome c on nanodiamonds. <u>Langmuir</u> 20 (2004): 5879-5884.

69. Ushizawa, K.; Sato, Y.; Mitsumori, T.; Machinami, T.; Ueda, T.; and Ando, T. Covalent immobilization of DNA on diamond and its verification by diffuse reflectance infrared spectroscopy. Chemical Physics Letters 351 (2002): 105-108.

70. Zhou, Y. L.; and Zhi, J. F. Development of an amperometric biosensor based on covalent immobilization of tyrosinase on a boron-doped diamond electrode. Electrochemistry Communications 8 (2006): 1811-1816.

71. Gu, H. R.; di Su, X.; and Loh, K. P. Electrochemical impedance sensing of DNA hybridization on conducting polymer film-modified diamond. Journal of Physical Chemistry B 109 (2005): 13611-13618.

72. Gu, H. R.; Su, X. D.; and Loh, K. P. Conductive polymer-modified boron-doped diamond for DNA hybridization analysis. Chemical Physics Letters 388 (2004). 483-487.

73. Berggren, C.; Stalhandske, P.; Brundell, J.; and Johansson, G. A feasibility study of a capacitive biosensor for direct detection of DNA hybridization. Electroanalysis 11 (1999): 156-160.

74. Ferro, S., Dal Colle, M., and De Battisti, A. Chemical surface characterization of electrochemically and thermally oxidized boron-doped diamond film electrodes. Carbon 43 (2005): 1191-1203.

75. Johnsson, B.; Lofas, S.; and Lindquist, G. Immobilization of proteins to a carboxymethyldextran-modified gold surface for biospecific interaction analysis in surface plasmon resonance sensors. Analytical Biochemistry 198 (1991): 268-277.

76. Ivandini, T. A.; Sarada, B. V.; Rao, T. N.; and Fujishima, A. Electrochemical oxidation of underivatized-nucleic acids at highly boron-doped diamond electrodes. Analyst 128 (2003): 924-929.

77. Ramanathan, K.; Pandey, S. S.; Kumar, R.; Gulati, A.; Murthy, A. S. N.; and Malhotra, B. D. Covalent immobilization of glucose oxidase to poly(o-amino benzoic acid) for application to glucose biosensor. Journal of Applied Polymer Science 78 (2000): 662-667.

78. Wilson, M. S.; and Nie, W. Electrochemical multianalyte immunoassays using an array-based sensor. Analytical Chemistry 78 (2006): 2507-2513.

79. Wilson, M. S. Electrochemical immunosensors for the simultaneous detection of two tumor markers. Analytical Chemistry 77 (2005): 1496-1502.

80. Aguilar, Z. P.; Vandaveer, W. R.; and Fritsch, I. Self-contained microelectrochemical immunoassay for small volumes using mouse IgG as a model system. <u>Analytical Chemistry</u> 74 (2002): 3321-3329.

81. Wijayawardhana, C. A.; Halsall, H. B.; and Heineman, W. R. Micro volume rotating disk electrode (RDE) amperometric detection for a bead-based immunoassay. <u>Analytica Chimica Acta</u> 399 (1999): 3-11.

82. Masson, M.; Runarsson, O. V.; Johannson, F.; and Aizawa, M. 4-amino-1-naphthylphosphate as a substrate for the amperometric detection of alkaline phosphatase activity and its application for immunoassay. <u>Talanta</u> 64 (2004): 174-180.

83. Yun, Y.; Bange, A.; Heineman, W. R.; Halsall, H. B.; Shanov, V. N.; Dong, Z. Y.; Pixley, S.; Behbehani, M.; Jazieh, A.; Tu, Y.; Wong, D. K. Y.; Bhattacharya, A.; and Schulz, M. J. A nanotube array immunosensor for direct electrochemical detection of antigen-antibody binding. <u>Sensors and Actuators B-Chemical</u> 123 (2007): 177-182.
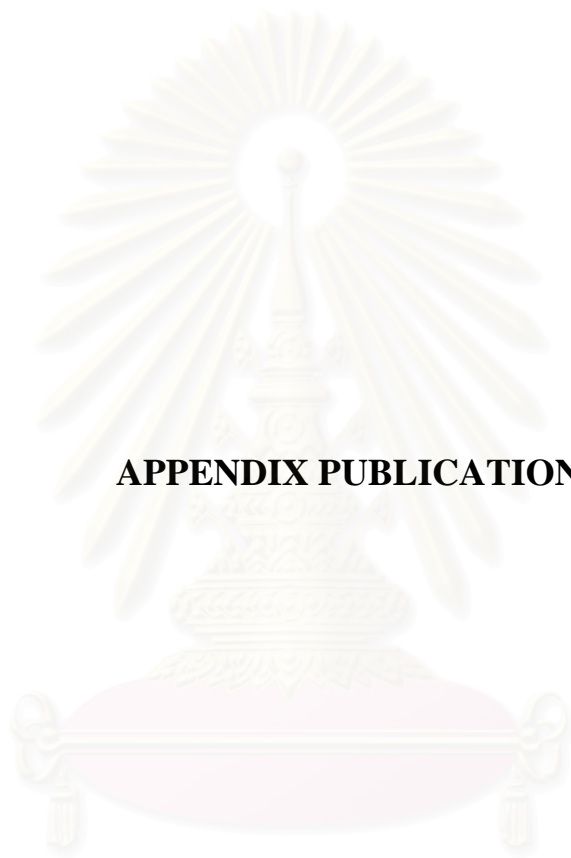
APPENDIX PUBLICATION

Development of Amperometric Immunosensor Using Boron-Doped Diamond with Poly(o-aminobenzoic acid)

Anchana Preechaworapun,[†,‡] Tribidasari A. Ivandini,[†,§] Akane Suzuki,[†] Akira Fujishima,[⊥] Orawon Chailapakul,*,[‡] and Yasuaki Einaga*,[†]

Department of Chemistry, Keio University, 3-14-1 Hiyoshi, Yokohama 223-8522, Japan, Sensor Research Unit, Department of Chemistry, Faculty of Science, Chulalongkorn University, Patumwan, Bangkok 10330, Thailand, Department of Chemistry, Faculty of Mathematics and Science, University of Indonesia, Kampus Baru UI Depok, Jakarta 16-424, Indonesia, and Kanagawa Academy of Science and Technology, KSP, 3-2-1 Sakado, Kawasaki 213-0012, Japan

An alternative method of a protein immunosensor has been developed at boron-doped diamond (BDD) electrode material. In order to construct the base of the immunosensor, o-aminobenzoic acid (o-ABA) was electropolymerized at an electrode by cyclic voltammetry. The poly-o-ABA-modified BDD was characterized by scanning electron microscopy (SEM) and X-ray photoelectron spectroscopy (XPS). The XPS result found that carboxyl groups were formed at the electrode surface. The carboxyl groups were then used to covalently attach protein probes. The amperometric sensing of mouse IgG (MIgG) was selected as the model at the poly-o-ABA-modified BDD to compare to the poly-o-ABA-modified glassy carbon (GC) at the same condition. An antimouse IgG from goat (GaMIgG) was covalently immobilized at a poly-o-ABA-modified BDD electrode which used a sandwich-type alkaline phosphatase (ALP) catalyzing amperometric immunoassay with 2-phospho-L-ascorbic acid (AAP) as substrate. The ALP enzyme conjugated at the immunosensor can generate AAP to the electroactive species of ascorbic acid (AA), which can be determined by amperometric detection. The signal was found to be proportional with the quantity of MIgG. The limits of detection (LODs) of 0.30 (3 SD) and 3.50 ng mL^{-1} (3 SD) for MIgG at BDD and GC electrodes were obtained. It also was found that the dynamic range of 3 orders of magnitude (1–1000 ng mL^{-1}) was obtained at BDD, whereas at GC, the dynamic range was more narrow (10–500 ng mL^{-1}). The method was applied to a real mouse serum sample that contains MIgG.

Boron-doped diamond (BDD) has many outstanding properties when compared to other electrode materials, such as its physicochemical stability, wide electrochemical potential window, low background current, semimetallic electronic behavior, and chemical sensitivity.[1–3] These versatile properties make BDD an excellent candidate for electrochemical use coupled with biochemical applications.[4–6] On the other hand, immunosensing, a combination of specific immunoreaction with sensitive optical or electrochemical transduction, has attracted great attention due to its high sensitivity and specifically.[7–9] However, immobilization of a biomolecule or protein at BDD requires surface activation procedures since the inert nature of the original diamond surface could not allow BDD to have a stable and covalent bond with any molecule.[10–12] The presence of surface linkers, such as carboxyl groups or amine groups, is needed to perform covalent bonding with the proteins.

Many studies have used multiple steps for photochemically linking such as a vinyl group of allylamine,[13] 2,2,2-trifluorine-N-9'-decenil acetamide,[14] or 10-aminodec-1-ene[15–17] to link at the diamond to introduce a homogeneous layer of amine groups which

(1) Fujishima, A.; Einaga, Y.; Rao, T. N.; Tryk, D. A. *Diamond Electrochemistry*; Elsevier-BKC: Tokyo, 2004.
(2) Yano, T.; Tryk, D. A.; Hashimoto, K.; Fujishima, A. *J. Electrochem. Soc.* 1998, 145, 1870–1876.
(3) Koppang, M. D.; Witek, M.; Blau, J.; Swain, G. M. *Anal. Chem.* 1999, 71, 1188–1195.
(4) Chiku, M.; Kamiya, A.; Ivandini, T.A.; Fujishima, A.; Einaga, Y. *J. Electroanal. Chem.*, in press.
(5) Murata, M.; Shibata, M.; Namura, S.; Ivandini, T. A.; Fujishima, A.; Einaga, Y. *J. Electroanal. Chem.* 2008, 612, 29–36.
(6) Suzuki, A.; Ivandini, T. A.; Yoshimi, K.; Fujishima, A.; Oyama, G.; Nakazato, T.; Hattori, N.; Kitazawa, S.; Einaga, Y. *Anal. Chem.* 2007, 79, 8608–8615.
(7) Yagi, I.; Ishida, T.; Uosaki, K. *Electrochem. Commun.* 2004, 6, 773–779.
(8) Ivandini, T. A.; Sato, R.; Makide, Y.; Fujishima, A.; Einaga, Y. *Anal. Chem.* 2006, 78, 6291–6298.
(9) Watanabe, T.; Ivandini, T. A.; Makide, Y.; Fujishima, A.; Einaga, Y. *Anal. Chem.* 2006, 78, 7857–7860.
(10) Bauer, C. G.; Eremenko, A. V.; Ehrentreich-Forster, E.; Bier, F. F.; Makower, A.; Halsall, H. B.; Heineman, W. R.; Scheller, F. W. *Anal. Chem.* 1996, 68, 2453–2454.
(11) Honda, H.; Inaba, M.; Katagiri, T.; Shoji, S.; Sato, H.; Homma, T.; Osaka, T.; Saito, M.; Mizuno, J.; Wada, Y. *Biosens. Bioelectron.* 2005, 20, 2306–2309.
(12) Aguilar, J. P.; Vandaveer, W. R.; Fritsch, I. *Anal. Chem.* 2002, 74, 3321–3329.
(13) Zhou, Y. L.; Tian, R. H.; Zhi, J. F. *Biosens. Bioelectron.* 2007, 22, 822–828.
(14) Rubio-Retama, J.; Hernando, J.; Lopez-Ruiz, B.; Hartl, A.; Steinmuller, D.; Stutzmann, M.; Lopez-Cabarcos, E.; Garrido, J. A. *Langmuir* 2006, 22, 5837–5842.
(15) Yang, W.; Auciello, O.; Butler, J. E.; Cai, W.; Carlisle, J. A.; Gerbi, J. E.; Gruen, D. M.; Knickerbocker, T.; Lasseter, T. L.; Russell, J. N.; Smith, L. M.; Hamers, R. J. *Nat. Mater.* 2002, 1, 253–258.
(16) Yang, W. S.; Hamers, R. J. *Appl. Phys. Lett.* 2004, 85, 3626–3628.

* Corresponding authors. E-mail: einaga@chem.keio.ac.jp (Y.E.), corawon@chula.ac.th (O.C.).
† Keio University.
‡ Chulalongkorn University.
§ University of Indonesia.
⊥ Kanagawa Academy of Science and Technology.

serve as binding sites for protein or DNA attachment. Coffinier and co-workers[18,19] used site-specific α-oxo semicarbazone ligation for peptide conjugation. The active surface was prepared from the aminated surface, using NH_3 plasma treatment or from photochemical reaction of aminopropyltriethoxysilane at oxidized BDD surface, followed by the chemical reaction of the terminal amino groups with triphosgene and Fmoc-protected hydrazine. Zhang et al.[20] used direct amination on polycrystalline diamond to produce functionalized surfaces for DNA. The amination was conducted by UV irradiation of diamond in ammonia gas to generate amine groups directly. Ushizawa et al. and Huang and Chang[21,22] reported that the oxidative-acid-treated diamond surface succeeded to covalently bond with protein and DNA, respectively. Zhou and Zhi[23] combined chemical and electrochemical modifications of BDD film with 4-nitrobenzenediazonium tetrafluoroborate to produce aminophenyl-modified BDD, followed by immobilizing tyrosinase covalently at the BDD surface via carbodiimide coupling.

Polymerization at the BDD electrode can provide freely accessible carboxyl groups, which can also be used as the base of a biosensor. Gu's group[24,25] reported the impedimetric sensing of DNA hybridization on a polyaniline/polyacrylate (PANI/PAA)-modified BDD electrode. An ultrathin film of PANI/PAA copolymer was electropolymerized onto the diamond surfaces to provide carboxylic groups for conjugation to DNA sensing probes. However, to the best of our knowledge, only one report existed on the development of the BDD immunosensor, in which impedimetric detection of antigen was investigated.[17]

Immunoglobulin G (IgG) is a 150 kDa monomer that constitutes approximately 75% of the total circulating immunoglobulin. Immunologically, IgG plays a major role in elimination of microbes by facilitating (i) opsonization by phagocytes, (ii) antibody-dependent cell-mediated cytotoxicity by natural killer cells, (iii) complement activation, and (iv) neutralization of viruses and toxins.[26] Therefore, IgG is very well-known to use as the model for immunoassay to compare to other methods.

In this work, we report the investigations of amperometric immunosensors of protein generated at carboxyl groups of modified BDD electrodes. Poly-o-aminobenzoic acid (poly-o-ABA) was electropolymerized by simple cyclic voltammetry to perform carboxyl groups for the base of an immunosensor at BDD surface. Antimouse IgG (GaMIgG) has been used as a model antibody to be immobilized covalently at the poly-o-ABA-modified electrode, whereas mouse IgG (MIgG) was used as antigen target for the

detection. Alkaline phosphatase (ALP, orthophosphoric monoester phosphohydrolase)-conjugated GaMIgG was used as an enzyme label to prepare a sandwich-type immunoassay. ALP assay using electrochemical detection has been reported.[27,28] ALP is a commonly used enzyme label that hydrolyzes orthophosphate from a wide variety of phosphate esters under alkaline conditions with an optimum activity around pH 8−10. ALP has a high turnover number.[29] Various substrates of ALP such as phenyl phosphate, p-hydroxyphenyl phosphate, p-aminophenyl phosphate, p-nitrophenyl phosphate, 1-naphthyl phosphate, 2-phospho-L-ascorbic acid, and 3-indoxyl phosphate were used.[28,30] In this work, 2-phospho-L-ascorbic acid (AAP) was selected for the substrate of ALP as it can produce L-ascorbic acid (AA), which is sensitive to the electrochemical detector, has no occurrence electrode fouling, and has excellent stability.[31,32] Conversion of AAP to AA will give an electrochemical signal related with the quantity of antigen target. Moreover, AAP is commercially available, nontoxic, and inexpensive. The method is successfully reproducible, and a very low detection limit can be achieved. Application of the method for real sample analysis is also demonstrated.

EXPERIMENTAL SECTION

Chemicals and Materials. The immunologic reagents were IgG from mouse (MIgG), antimouse IgG from goat (GaMIgG), and antimouse IgG conjugated alkaline phosphatase (GaMIgG−ALP). All of these reagents were purchased from Sigma (St. Louis, MO). o-Aminobenzoic acid (o-ABA) was purchased from Aldrich. Tween-20, 1-ethyl-3-(3-dimethyl aminopropyl) carbodiimide (EDAC), N-hydroxysulfosuccinimide (NHS), ethanolamine−HCl, and bovine serum albumin (BSA) were purchased from Sigma. L-Ascorbic acid (AA), potassium chloride (KCl), sodium chloride (NaCl), Tris−hydrochloride (Tris), sulfuric acid (H_2SO_4), and hydrogen peroxide (H_2O_2) were obtained from Wako. The 2-phospho-L-ascorbic acid trisodium salt (AAP) was obtained from Fluka. All stock and buffer solutions were prepared using autoclaved double-deionized water (18.2 MΩ cm). The buffer in the immunoassay system prepared the washing buffer solution (Tris buffer pH 7.4, 0.1 M NaCl, 0.005 M KCl, and 0.1% (v/v) Tween-20) and the blocking buffer and the diluted MIgG solution (1% (w/v) BSA in washing buffer solution).

Instruments. Electrochemical measurements were conducted using a potentiostat (Hokuto Denko, HSV-100) at room temperature in a conventional three-electrode electrochemical cell (1.5 mL), which was used for cyclic voltammetric and amperometric experiments. A Ag/AgCl (saturated KCl) reference electrode (BAS, Japan) and a platinum wire counter electrode were used. Boron-doped diamond (BDD, homemade) and glassy carbon (GC, Tokai Carbon Co., Ltd., Tokyo, Japan) electrodes were used as working electrodes. The N_2 gas bubble was used for mixing solution during the amperometric experiment.

(17) Yang, W. S.; Butler, J. E.; Russell, J. N.; Hamers, R. J. *Analyst* **2007**, *132*, 296−306.
(18) Coffinier, Y.; Szunerits, S.; Jama, C.; Desmet, R.; Melnyk, O.; Marcus, B.; Gengembre, L.; Payen, E.; Delabouglise, D.; Boukherroub, R. *Langmuir* **2007**, *23*, 4494−4497.
(19) Coffinier, Y.; Szunerits, S.; Marcus, B.; Desmet, R.; Melnyk, O.; Gengembre, L.; Payen, E.; Delabouglise, D.; Boukherroub, R. *Diamond Relat. Mater.* **2007**, *16*, 892−898.
(20) Zhang, G. J.; Song, K. S.; Nakamura, Y.; Ueno, T.; Funatsu, T.; Ohdomari, I.; Kawarada, H. *Langmuir* **2006**, *22*, 3728−3734.
(21) Ushizawa, K.; Sato, Y.; Mitsumori, T.; Machinami, T.; Ueda, T.; Ando, T. *Chem. Phys. Lett.* **2002**, *351*, 105−108.
(22) Huang, L. C. L.; Chang, H. C. *Langmuir* **2004**, *20*, 5879−5884.
(23) Zhou, Y. L.; Zhi, J. F. *Electrochem. Commun.* **2006**, *8*, 1811−1816.
(24) Gu, H.; Su, X.; Loh, K. P. *J. Phys. Chem. B* **2005**, *109*, 13611−13618.
(25) Gu, H.; Su, X.; Loh, K. P. *Chem. Phys. Lett.* **2004**, *388*, 483−487.
(26) Gorczynski, R.; Stanley, J. *Clinical Immunology*; Gorczynski/Stanley: Georgetown, TX, 1999.

(27) Kwon, S. J.; Kim, E.; Yang, H.; Kwak, J. *Analyst* **2006**, *131*, 402−406.
(28) Fanjul-Bolado, P.; Gonzalez-Garcia, M. B.; Costa-Garcia, A. *Talanta* **2004**, *64*, 452−457.
(29) Cleland, W. W.; Hengge, A. C. *Chem. Rev.* **2006**, *106*, 3252−3278.
(30) Kreuzer, M. P.; O'Sullivan, C. K.; Guilbault, G. G. *Anal. Chim. Acta* **1999**, *393*, 95−102.
(31) Kokado, A.; Arakawa, H.; Maeda, M. *Anal. Chim. Acta* **2000**, *407*, 119−125.
(32) Gyurcsanyi, R. E.; Bereczki, A.; Nagy, G.; Neuman, M. R.; Lindner, E. *Analyst* **2002**, *127*, 235−240.
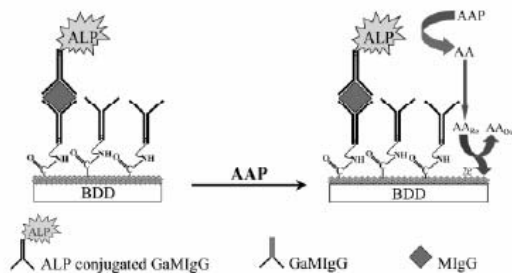
Figure 1. Schematic of the amperometric enzyme immunosensor based on the poly-*o*-ABA-modified electrode.

Figure 2. (A) Cyclic voltammograms of the 1st (dotted line), 2nd (dashed line), and 10th cycle (solid line) of *o*-ABA polymerization at a BDD electrode. The scan rate was 40 mV s⁻¹. (B) SEM image of a BDD electrode before (bright color) and after (dark color) being modified by poly-*o*-ABA.

Substrate Preparation. BDD thin films were deposited on Si(111) wafers in a microwave plasma chemical vapor deposition system (Astex Corp.) using a mixture of acetone and methanol (9:1, v/v) as the carbon source and B_2O_3 as a boron source. The details of the preparation are described elsewhere.[33] The boron doped in diamond film is approximately 10^4 ppm of B/C molar ratio.
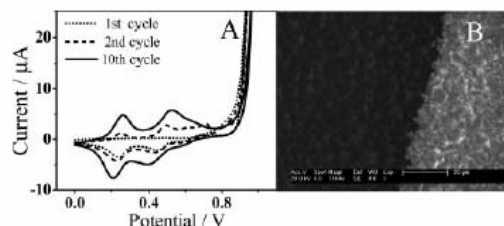
Surface morphology was observed by scanning electron microscopy (SEM) (JSM-5400, JEOL, Japan). An X-ray photoelectron spectrometer (XPS) (JPS-9000MC, JEOL, Japan) equipped with a Mg Kα X-ray source (voltage 10 kV and emission 10 mA) was used for the analysis of the polymer film at BDD surface.

Poly-*o*-ABA-Modified Immunosensors. The GCE was cut into 1×1 cm², polished to a mirror-like surface with 0.5 μm α-alumina on filter paper, and then sonicated prior to use two times with isopropyl alcohol and one time with double-distilled water. The BDD thin film was cut into 1×1 cm², soaked in freshly prepared *piranha solution* (H_2SO_4/H_2O_2 (30% v/v) 3:1) for 30 min (**safety note**: *the piranha solution should be handled with extreme caution*), and rinsed with double-distilled water. The working area was controlled by a silicone rubber gasket of 5 mm diameter.

The schematic of the poly-*o*-ABA-modified immunosensor is shown in Figure 1. The electrode was electropolymerized with 50 mM *o*-ABA in 1 M H_2SO_4 by 10 cycles of cyclic voltammetry with a scan rate of 40 mV s⁻¹ and the potential range of 0−0.97 V. The poly-*o*-ABA-modified electrode was subsequently coated with 50 μL of NHS/EDAC solution (1/1 mg in 100 μL of 100 mM PBS buffer, pH 7.22) for 30 min, and then the supernatant was removed. A drop of 50 μL of 40 ppm GaMIgG was applied to each poly-*o*-ABA-modified electrode. After 120 min of incubation, the solution was removed, and 50 μL of 1 M ethanolamine solution was drop cast onto each poly-*o*-ABA-modified immunosensor and incubated for 30 min. After being taken out of the solution, the poly-*o*-ABA-modified electrodes were washed three times by washing buffer solution.

Sandwich-Type Immunoassay at Poly-*o*-ABA-Modified Immunosensors. The immunosensors were first added with the desired amount of the target MIgG using blocking solution for dilution (for control as absence of the target) at room temperature for 60 min. After washing with washing buffer solution, the immunosensor was finally incubated with GaMIgG−ALP for 60

min and afterward washed three times with washing buffer solution.

Amperometric Detection. Amperometric experiments were performed in 900 μL of a 0.1 M Tris buffer solution (pH 8.5) by applying a potential of +0.4 V at the sandwich IgG poly-*o*-ABA-modified immunosensor at room temperature. A 100 μL aliquot of 30 mM AAP, as a substrate, was added to the stirred solution with N_2 gas once the background current reached a steady state, and the corresponding current versus time curve was recorded.

BDD Poly-*o*-ABA-Modified Immunosensors for Mouse Serum. The BDD poly-*o*-ABA-modified immunosensors were prepared the same as the above method for measurements of MIgG in a mouse serum. The mouse serum was diluted 1:50 000. Two methods, internal and external standard, were used to quantify MIgG in the serum. The internal standard spiked three standard MIgG concentrations in the diluted serum sample, which then were added instead of target MIgG at BDD poly-*o*-ABA-modified immunosensors, and the above method was followed for detection. For external standard, five standard MIgG concentrations were detected, and the calibration curve compared the relationship concentration with current density. The diluted serum sample was measured at the BDD poly-*o*-ABA-modified immunosensor and used the current density to calculate the quantity of MIgG in the serum sample. The mean values of two slopes and MIgG amounts from the two methods were compared using Student's *t* test. Differences were considered to be statistically significant when *p* values were <0.05. Statistical analysis was performed using originPro 7.5.

RESULTS AND DISCUSSION

Characterization of Poly-*o*-ABA-Modified BDD Electrode. Figure 2A shows cyclic voltammograms of 50 mM *o*-ABA with potential scanning from 0 to 0.97 V (vs Ag/AgCl) at a BDD electrode. Previously, similar electropolymerization of *o*-ABA at gold,[34] platinum,[35] and GC[36,37] substrates was reported. In the first cycle, an irreversible oxidation peak at 0.80 V was obtained. It is believed that the peak is related to the oxidation of *o*-ABA to free radicals at the surface of electrode (shown in eq 1). A protonic

(33) Yano, T.; Popa, E.; Tryk, D. A.; Hashimoto, K.; Fujishima, A. *J. Electrochem. Soc.* **1999**, *146*, 1081−1087.

(34) Wang, Y. J.; Knoll, W. *Anal. Chim. Acta* **2006**, *558*, 150−157.
(35) Benyoucef, A.; Huerta, F.; Vazquez, J. L.; Morallon, E. *Eur. Polym. J.* **2005**, *41*, 843−852.
(36) Cheng, W.; Jin, G.; Zhang, Y. *Russ. J. Electrochem.* **2005**, *41*, 940−945.
(37) Zhang, Y. Z.; Jin, G. Y.; Cheng, W. X.; Li, S. P. *Front. Biosci.* **2005**, *10*, 23−29.
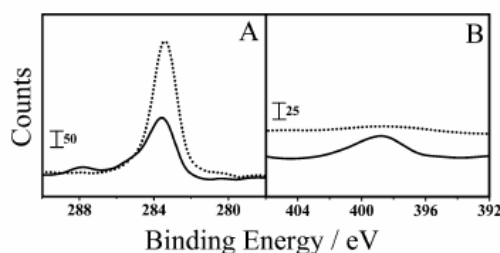
Figure 3. XPS of C1s (A) and N1s (B) spectra of BDD before (dotted lines) and after (solid lines) being modified by poly-o-ABA.

peak at 0.44 V and the dedoping processing at 0.23 V were shown in the cathodic scan.[34]
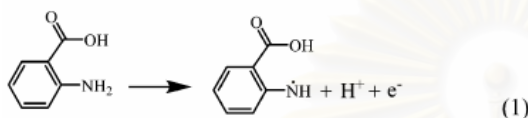
$$\text{(1)}$$

After the first scan, cyclic voltammograms gave two distinct redox processes. The first couple appears at $Ep_{a,1} = 0.26$ V and $Ep_{c,1} = 0.21$ V, which results in a peak separation (ΔEp) close to 50 mV. The second couple is observed at $Ep_{a,2} = 0.51$ V and $Ep_{c,2} = 0.41$ V with ΔEp of 100 mV. The peaks are similar to those reported by Wang and Knoll.[34] Benyoucef's group,[35] they synthesized and characterized with in situ FT-IRS of poly-o-ABA. Assuming that the o-ABA was coupled by a head-to-tail for growing polymeric chains in the main path, the postulated equations were given as follows.[34,35]

$$\text{(2)}$$

$$\text{(3)}$$
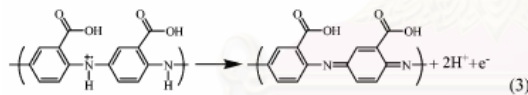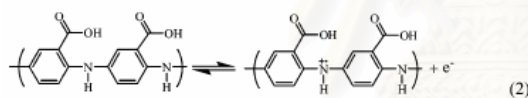
The 2nd through 10th cycles appeared at increasing currents, indicating that the polymer films are grown up. After the 10th cycle, the current increased very slowly. Therefore, the condition of 10 cycles of voltammetry was fixed for the optimum condition of o-ABA electropolymerization. An SEM image of BDD (Figure 2B) shows a haft of bright color of unmodified BDD surface and the other a haft of dark color of poly-o-ABA-modified the BDD surface.

XPS was used to analyze the chemical composition of the BDD surface, C1s and N1s regions, before and after poly-o-ABA electropolymerization. Figure 3A shows the decreasing of the bulk C1s peak at about 283.7 eV after polymer coated the BDD generated. The C1s component at a binding energy of ~288 eV is characteristic of the COOH group of poly-o-ABA modified at BDD surface.[38] This spectrum component is small but appeared

clearly in comparison with the spectrum of the bare BDD. The N1s spectrum in Figure 3B shows the presence of poly-o-ABA. The spectrum is the same N1s spectrum of polyaniline because the o-ABA is one of an aniline derivative. The ratio of the C1s peak of COOH groups to N1s of poly-o-ABA (COOH/N) is about 1:1. This result confirmed the postulation of poly-o-ABA formation that one COOH group and one N come from a monomer of o-ABA.

Immunosensor. Determination of MIgG, the target protein, using a sandwich-type immunoassay by a disposable poly-o-ABA-modified BDD was developed. The scheme is shown in Figure 1. In this approach, comparison was also made between poly-o-ABA-modified BDD and GC immunosensors treated with the same conditions. The sandwich immunoassay involved immobilization of the primary antibody GaMIgG, capture of the target MIgG, association of GaMIgG−ALP, and finally using AAP as substrate. The ALP enzymatically generated AA is an electroactive species that can produce an electrochemical oxidation signal. The electrochemical signal is related to the quantity of MIgG. The enzymatic reaction of ALP and electrochemical oxidation of AA are shown in eqs 4 and 5, respectively.[31]

$$\text{(4)}$$

$$\text{(5)}$$
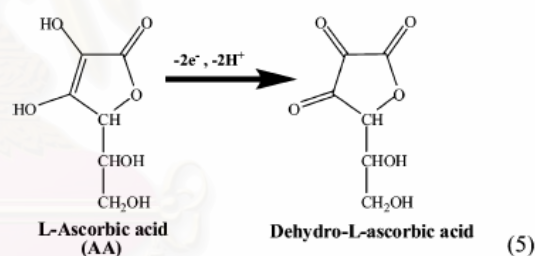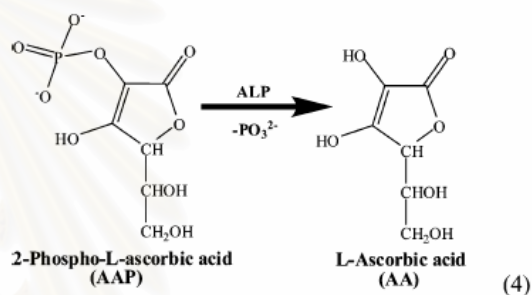
Electrochemical Study. AAP was selected as the ALP substrate because the enzyme can generate AA, which does not produce electrode fouling and is nontoxic to the environment, commercially available, and also inexpensive. A good ALP substrate should not appear to produce any electrochemical signal at the same potential as product signal. The cyclic voltammograms of 100 μM AA and 3 mM AAP in 0.1 M Tris buffer pH 8.5 solution at BDD and GC before and after poly-o-ABA modification are shown in Figures 4 and 5, respectively. The anodic potential peaks of AA before and after poly-o-ABA modification were obtained at 0.28 and 0.44 V for BDD and 0.01 and 0.42 V for GC, respectively. After modification, all of the anodic potential peaks were shifted

(38) Ferro, S.; Dal Colle, M.; De Battisti, A. *Carbon* **2005**, *43*, 1191−1203.
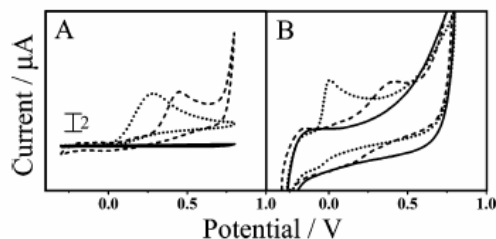
Figure 4. Cyclic voltammograms of electrolyte (0.1 M Tris buffer solution, pH 8.5; solid lines), 100 μM AA at BDD (A) and GC (B) electrodes before (dotted lines) and after (dashed lines) being modified by poly-o-ABA. The scan rate was 50 mV s^{-1}.
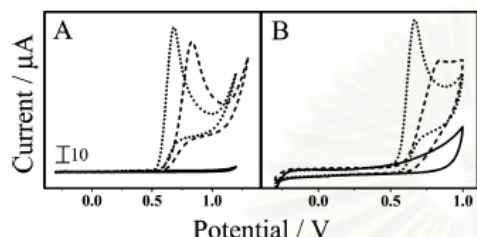
Figure 5. Cyclic voltammograms of electrolyte (0.1 M Tris buffer solution, pH 8.5; solid lines), 3 mM AAP at BDD (A) and GC (B) electrodes before (dotted lines) and after (dashed lines) being modified by poly-o-ABA. The scan rate was 50 mV s^{-1}.

Table 1. Summary of Potentials and Current Responses of Oxidation of AA and AAP at BDD before and after Being Electropolymerized by o-ABA

type of electrode	chemical	bare electrode		poly-o-ABA-modified electrode	
		potential peak (V)	current of peak (μA)	potential peak (V)	current of peak (μA)
BDD	AA	0.28	5.988	0.44	5.813
	AAP	0.68	90.207	0.84	81.436
GC	AA	0.01	7.135	0.42	7.310
	AAP	0.67	94.353	0.84	69.541
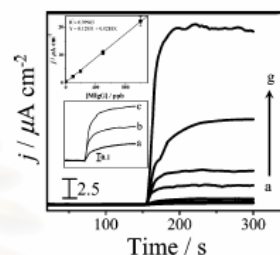
Figure 6. Amperograms of products (AA) after adding substrates (AAP) of ALP in Tris buffer solution (pH 8.5) at a poly-o-ABA-modified BDD immunosensor by various target MIgG concentrations (0, 1, 5, 100, 200, 500, and 1000 ng mL^{-1} (a–g). The potential applied was 0.4 V. The inset in the top is a calibration plot showing the correspondence between the changes in anodic peak current after subtracting the control current (0 ng mL^{-1}; absence of MIgG) and the concentration of MIgG, and that below is a zoom (a) 0, (b) 1, and (c) 5 ng mL^{-1} of MIgG concentration at poly-o-ABA-modified BDD immunosensors.

to more positive potentials as ∼0.16 V for both oxidation of AA and AAP at BDD and 0.41 and 0.17 V for AA and AAP at GC, respectively. A plausible possibility is that after electropolymerization the COOH groups (negative charge species) that covered the electrode surfaces provide electrostatic repulsion to AA and AAP. Therefore, a higher potential is required for the kinetics of electron transfer. Influent of BDD termination on the oxidation of a negative charge molecule has been reported.[39,40] The noticeable point is that the anodic current of AA at both BDD and GC before and after modification with poly-o-ABA showed almost the same current, indicating good electron transfer of poly-o-ABA as a conductive polymer. The poly-o-ABA is a carboxyl-group-functionalized polyaniline. The polymer structure has π-electron backbones for electron transfer.[34–37,41,42] This is a great point to apply for an immunosensor because the surface polymer needs to provide COOH groups for conjugation with protein by covalent bonding and in the same time should also perform good electron transfer for the AA oxidation reaction. A summary of oxidation potentials and current responses of AA and AAP at the BDD and GC before and after poly-o-ABA modification is given in Table 1.

AAP at the concentration of 3 mM was selected for investigation as it is the optimum concentration of substrate that should be added in the immunoassay detection system (data not shown). The difference in potential between 100 μM AA and 3 mM AAP anodic peaks after poly-o-ABA modification was about 400 mV.

The difference is assumed to be enough to avoid the interference with the AA signal generated from the enzymatic reaction.

Amperometry was used for the detection method of the immunosensors. The hydrodynamics of AA at poly-o-ABA-modified BDD and GC electrodes were investigated at the potential from 0.2 to 0.6 V. The highest current peak was observed at 0.4 V for both electrodes (data not shown). Therefore, for further experiments an applied potential of 0.4 V was set up to detect AA in the immunoassay system.

Optimized Immunosensor System. A sandwich immunoassay method was applied for the immunosensor system. The GaMIgG was bound covalently to the COOH groups at the surface of poly-o-ABA-modified electrodes. To link the GaMIgG to the carboxyl surface, NHS/EDAC was added to modify carboxyl groups to *N*-hydrosuccinimide esters, in which immunoassay bonds covalently with amines on antibody at ambient temperature and in a natural pH aqueous solution.[43] The incubation time of GaMIgG, MIgG, and GaMIgG–ALP at the surfaces was optimized.

(39) Ivandini, T. A.; Sarada, B. V.; Rao, T. N.; Fujishima, A. *Analyst* **2003**, *128*, 924–929.
(40) Ivandini, T. A.; Rao, T. N.; Fujishima, A.; Einaga, Y. *Anal. Chem.* **2006**, *78*, 3467–3471.
(41) Ahuja, T.; Mir, I. A.; Kumar, D.; Rajesh. *Biomaterials* **2007**, *28*, 791–805.
(42) Ramanathan, K.; Pandey, S. S.; Kumar, R.; Gulati, A.; Murthy, A. S. N.; Malhotra, B. D. *J. Appl. Polym. Sci.* **2000**, *78*, 662–667.
(43) Johnsson, B.; Lofas, S.; Lindquist, G. *Anal. Biochem.* **1991**, *198*, 268–277.
(44) Wilson, M. S.; Nie, W. *Anal. Chem.* **2006**, *78*, 2507–2513.
(45) Wijayawardhana, C. A.; Halsall, H. B.; Heineman, W. R. *Anal. Chim. Acta* **1999**, *399*, 3–11.
(46) Másson, M.; Rúnarsson, Ö. V.; Jóhannson, F.; Aizawa, M. *Talanta* **2004**, *64*, 174–180.
(47) Yun, Y.; Bange, A.; Heineman, W. R.; Halsall, H. B.; Shanov, V. N.; Dong, Z.; Pixley, S.; Behbehani, M.; Jazieh, A.; Tu, Y.; Wong, D. K. Y.; Bhattacharya, A.; Schulz, M. J. *Sens. Actuators, B* **2007**, *123*, 177–182.

Table 2. Analytical Performance of Poly-*o*-ABA-Modified BDD Immunosensors

type of immunosensor	mean of control ($n = 15$) ($\mu A\ cm^{-2} \pm SD$)	LOD (3 SD) (ng mL^{-1})	linear range (ng mL^{-1})	equation	R^2
BDD	0.2471 ± 0.045	0.30	1–1000	$Y = 0.12851 + 0.0218x$	0.99965
GC	0.7104 ± 0.119	3.50	10–500	$Y = 0.24961 + 0.02298x$	0.99972

Table 3. Comparison of Electroanalytical Data for Determination of MIgG

solid-state-based immunoassay	enzyme label	substrate	method for detection	linear range	LOD (ng mL^{-1})	stability (week)	ref
BDD/poly-*o*-ABA	ALP	AAP	amperometry	1–1000 ng mL^{-1}	0.3	2	a
GC/poly-*o*-ABA	ALP	AAP	amperometry	10–500 ng mL^{-1}	3.5	—[b]	a
glass substrate/ iridium oxide	ALP	HQP[c]	amperometry	0–165 ng mL^{-1}	3	5	44
Dynabeads	ALP	PAPP[d]	GC-RDE[e] amperometry	50–5000 ng mL^{-1}	–	–	45
96-well plate	ALP	ANP[f]	amperometry	0.01–100 μg mL^{-1}	6	–	46
Si substrate/SiO$_2$/Al$_2$O$_3$/ Fe/carbon nanotubes			EIS[g]	range up to 100 μg mL^{-1}	200	–	47

[a] This proposed method. [b] – No report. [c] Hydroquinone diphosphate. [d] 4-Aminophenyl phosphate. [e] Glassy carbon rotating disk electrode. [f] 4-Amino-1-naphthylphosphate. [g] Electrochemical impedance spectroscopy.

The optimum incubation time of 120 min at room temperature was fixed in solutions containing GaMIgG (40 μg mL^{-1}), followed by incubation in ethanolamine solution for 30 min for blocking and quenching active functional group remaining on the surface of poly-*o*-ABA, and in different concentrations of target MIgG for 60 min (including control solution without MIgG), and then the last for 60 min in solutions containing the GaMIgG–ALP.

Amperometric immunosensor was detected by adding electrolyte of 0.1 M Tris solution (pH 8.5) to a cell consisting of immunosensor, Ag/AgCl, and Pt wire as working, reference, and counter electrodes, respectively. N$_2$ bubble was given for mixing the solution during measurement. A potential of 0.4 V was applied to the immunosensor until the baseline of the background was stable before addition of AAP substrate in the solution. The concentration of AAP for the saturated reaction with ALP-conjugated immunosensor was optimized at 3 mM. The current increasing due to the oxidation of AA generated by the enzyme reaction caused an immediate response and reached steady state very fast.

Blocking the surface is one of the most important steps to minimize and to control nonspecific binding. The current density of nonspecific adsorption, in the absence of target MIgG and after being washed in multiple steps, was ∼1.12 μA cm^{-2}. Apparently, the poly-*o*-ABA can decrease the physically nonspecific adsorption by a thin film of polymer-covered surface. The covalent attachment of poly-*o*-ABA reduces the nonspecific binding to 0.33 μA cm^{-2}, which is about 4 times lower than when the polymer is absent. The use of BSA in the concentration range of 0–5% as blocking agent was also investigated. It is found that the use of 1% BSA can decrease the current density of nonspecific adsorption to 0.24 μA cm^{-2}, whereas more than 1% BSA gave almost the same current density as 1% BSA. Therefore, in the next experiments 1% BSA was fixed for blocking nonspecific adsorption.

Reproducibility. Reproducibility of the immunoassay was expressed in terms of relative standard deviation (RSD) of six different immunosensors under the same condition and concentration (intra-assay) and four different days of three replicate immunosensors in each day (interassay). High reproducibility was shown by the obtained current signal for 100 ng mL^{-1} MIgG for replicate analysis in the intra-assay ($n = 6$) and in the interassay ($n = 4$) with RSD values of 2.60 and 5.36 for BDD, respectively. They are acceptable in precision.

Detection Limit and Correlation. Figure 6 shows the amperograms of MIgG calibration using the BDD immunosensor system. The linear calibration curve is shown in the inset. The BDD immunosensor is able to discriminate MIgG concentrations ranging from 1 to 1000 ng mL^{-1}. The analytical performance was compared with the GC immunosensor and is summarized in Table 2. The linear range of the GC immunosensor was 10–500 ng mL^{-1}. The detection limits of BDD and GC were found to be 0.30 ng mL^{-1} (2 pM) and 3.50 ng mL^{-1} (23.3 pM) (3 SD; calculation), respectively. High correlation can be obtained as shown by $r^2 > 0.999$.

Comparison with Other Methods. Table 3 summarizes the MIgG determination at the BDD immunosensor from this study compared to the GCE fabricated by our system and other systems. It can be observed that using the poly-*o*-ABA BDD immunosensor with amperometric detection provides a significantly low detection limit (0.3 ng mL^{-1}). To investigate the stability of immunosensors, the electrode was stored in PBS at 4 °C for an extended period of time. The sensors were evaluated over a period of 14 days (2 weeks) of storage with no detectable loss of activity.

Detection in Real Sample. The poly-*o*-ABA-modified BDD immunosensor was also applied to measure MIgG in a real sample of mouse serum. The internal and external standard curves are shown in Figure 7. The mouse serum was diluted 1:50 000 which is the interval dilution of commercial MIgG ELISA test kits. The external standard was determined using five different MIgG concentrations ($n = 3$) for making a calibration curve. The internal standard was investigated by spiking of three standard different MIgG concentrations ($n = 2$) in the diluted mouse serum. Recoveries of 80–100% were achieved for the poly-*o*-ABA-modified BDD immunosensor. MIgG concentrations in the serum were
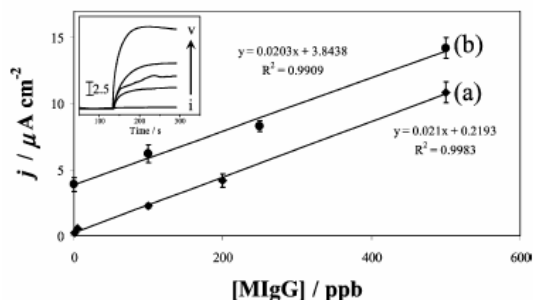
Figure 7. Comparison of two MIgG measurement methods in a mouse serum by (a) external and (b) internal standards. The inset shows (i) control (Tris buffer), (ii) mouse serum diluted 50 000 times, (iii) mouse serum diluted 50 000 times in addition of 100 ppb standard MIgG, (iv) mouse serum diluted 50 000 times in addition of 250 ppb standard MIgG, and (v) mouse serum diluted 50 000 times in addition of 500 ppb standard MIgG.

found to be 189.34 and 174.30 ng mL^{-1} from internal and external standards at the 0.05 level, respectively. The population mean is not significantly different than the test mean (181.82). Moreover, to make sure, a sample t test was used to assess the slopes of two methods, internal and external standard methods. Both slopes were satisfactory at the 0.05 level, and the population mean was not significantly different than the test mean (0.02055). These results indicate that the poly-o-ABA-modified BDD immunosensor has high specificity and sensitivity for real samples of MIgG.

CONCLUSIONS

The alternative immobilization system for a BDD immunosensor was described by a single-step conductive polymer modification method, which is based on a sandwich-type enzyme-amplified electrochemical immunoassay of MIgG. The electrochemically deposited poly-o-ABA thin film provides freely accessible carboxylic groups that have high chemical specificity for covalent immobilization of protein. Stable and selective MIgG sensing was shown by GaMIgG probe-immobilized BDD using poly-o-ABA base. The detection limit and linear range at poly-o-ABA-modified BDD are 0.3 ng mL^{-1} and 1−1000 ng mL^{-1}, and at poly-o-ABA-modified GC they are 3.50 ng mL^{-1} and 10−500 ng mL^{-1}. From these results it can be concluded that the poly-o-ABA-modified BDD provided the lower detection limit and wider linear range when compared to poly-o-ABA-modified GC. The developed method of the BDD immunosensor offers enhanced performance and can be easily extended to other protein detection.

ARTICLE IN PRESS

Contents lists available at ScienceDirect

Talanta

journal homepage: www.elsevier.com/locate/talanta

Investigation of the enzyme hydrolysis products of the substrates of alkaline phosphatase in electrochemical immunosensing

Anchana Preechaworapun[a,b,c], Zong Dai[a,b], Yun Xiang[a,b],
Orawon Chailapakul[c,*], Joseph Wang[a,b,*]

[a] Department of Chemical and Material Engineering, Biodesign Institute, Arizona State University, Tempe, AZ 85287-5801, United States
[b] Department of Chemistry and Biochemistry, Biodesign Institute, Arizona State University, Tempe, AZ 85287-5801, United States
[c] Sensor Research Unit, Department of Chemistry, Faculty of Science, Chulalongkorn University, Patumwan, Bangkok 10330, Thailand

ARTICLE INFO

ABSTRACT

In this paper, we have critically evaluated the electrochemical behavior of the products of seven substrates of the enzyme label, alkaline phosphate, commonly used in electrochemical immunosensors. These products (and the corresponding substrates) include indigo carmine (3-indoyl phosphate), hydroquinone (hydroquinone diphosphate), 4-nitrophenol (4-nitrophenol phosphate), 4-aminophenol (p-aminophenyl phosphate), 1-naphthol (1-naphthyl phosphate), phenol (phenyl phosphate), and L-ascorbic acid (2-phospho-L-ascorbic acid). Cyclic voltammetry and amperometry of these products were carried out at glassy carbon (GC), screen-printed carbon (SPC) and gold (Au) electrodes, respectively. Among the products, L-ascorbic acid showed the most sensitive (24.8 $\mu A\,cm^{-2}$, 12.0 $\mu A\,cm^{-2}$, and 48.0 $\mu A\,cm^{-2}$ of 100 μM ascorbic acid at GC, SPC, and Au electrodes, respectively) and well-defined amperometric response at all electrodes used, making 2-phospho-L-ascorbic acid the best substrate in electrochemical detection involving an alkaline phosphatase (ALP) enzyme label. The 2-phospho-L-ascorbic acid is also commercially available and inexpensive. Therefore, it was the best choice for electrochemical detection using ALP as label. Using mouse IgG as a model, an ALP enzyme-amplified sandwich-type amperometric immunosensor was constructed. The immunosensor was designed by electropolymerization of o-aminobenzoic acid (o-ABA) conductive polymer on the surface of GC, SPC, and Au electrodes. The anti-mouse IgG was subsequently attached on the electrode surface through covalent bonding between IgG antibody and the carboxyl groups from poly(o-ABA). Using 2-phospho-L-ascorbic acid as a substrate, the poly(o-ABA)/Au immunosensor produced the best signal (about 297 times of current density response ratio between 1000 $ng\,mL^{-1}$ and 0 $ng\,mL^{-1}$ of mouse IgG), demonstrating that amperometric immunosensors based on a conducting polymer electrode system were sensitive to concentrations of the mouse IgG down to 1 $ng\,mL^{-1}$, with a linear range of 3–200 $ng\,mL^{-1}$ (S.D. < 2; $n = 3$), and very low non-specific adsorption.

© 2008 Published by Elsevier B.V.

1. Introduction

In recent years, immunoassay has become an important analytical technique. Enzyme immunoassay is an analytical technique that relies on a specific immuno-interaction to quantitatively determine antibody or antigen present in an analyte by measuring the activity of an enzyme label conjugated to either the antibody or antigen. The main advantage of using enzyme labels is the remarkable signal amplification that may be gained by the high turnover of enzyme product molecules for each enzyme label [1]. Alkaline phosphatase (o-phosphoric monoester phosphohydrolase; ALP) [2] is a common

enzyme label used in immunoassays. It has been investigated for more than 70 years and it is easily conjugated to haptens, antibodies, and other proteins. Moreover, ALP has a high turnover number and broad substrate specificity.

Different substrates for ALP have been investigated in different detection systems such as spectrophotometry using fosfestrol [3], fluorescence using 8-quinolyl phosphate [4] and 2-carboxy-1-naphthyl phosphate [5], chemiluminescence using lumiphos [6], bioluminescence using adenosine-3'-phosphate-5'-phosphosulfate [7], and electrochemistry using phenyl phosphate [8].

In electrochemical immunosensors, an ALP enzyme is used to generate organic electroactive products most of which can be detected and quantified. This detector is generally sensitive and rapid for the redox reaction of the product of the enzyme hydrolysis of an ALP substrate. Several substrates for electroanalysis

* Corresponding authors.
E-mail addresses: corawon@chula.ac.th (O. Chailapakul),
Joseph.Wang@asu.edu (J. Wang).

ARTICLE IN PRESS

have been studied in immunoassays involving the substrates of ALP such as catechol monophosphate [9], 3-indoyl phosphate (IP) [10–13], hydroquinone diphosphate (HQDP) [14], 4-nitrophenol phosphate (NPP) [15–17], p-aminophenyl phosphate (APP) [17–23], 1-naphthyl phosphate (NTP) [23–25], phenyl phosphate (PheP) [14,17,20,26], and 2-phospho-L-ascorbic acid (AAP) [19,22,27]. During the enzymatic process, these substrates are converted to the electroactive species catechol, indigo carmine (IC), hydroquinone (HQ), 4-nitrophenol (NP), 4-aminophenol (AP), 1-naphthol (NT), phenol (Phe), and L-ascorbic acid (AA), respectively.

Electrochemical immunosensors, which combine specific immunoreactions with electrochemical transduction, have attracted growing attention in recent years. Different electrode materials have been used for electrochemical immunosensors, including GC [17,22], graphite [19], platinum (Pt) [8,22], SPC [11,15,20,22–25], iridium oxide [14], and Au [21,22,25,28]. The modified electrode surface allows highly dense immobilization of biomolecules, long-term stability of attached biomolecules, low non-specific binding, and proper biomolecular orientation to permit simple and rapid specific interactions. Basically Au material is very good for self-assembled monolayers (SAM) as the basis of the covalent bonding immunosensor, because strong bonding between the Au surface with SAM and the ease to modify the Au surface to cover with a COOH group. Therefore, SAMs of thiol are widely used as a scaffold to immobilize the primary antibody on Au surface. For example, a mixed SAM monolayer of 11-mercaptoundecanoic acid and 6-mercaptoethanol was applied to modify as the base at Au plate for sandwich immunoassay [29]. In our paper also used this mix SAM monolayer modified on Au surface to obtain the carboxyl functional group binding with antibody by covalent bonding. In this work SAM/Au was prepared for comparison with our system. Alternately, conducting polymers [30] based on electrodes have gained increasing applications in the development of immunosensors, such as poly(pyrrole) [31,32], polyaniline [33], poly(3-hexylthiophene) [34], poly 5,2':5'2"-terthiophene-3'-carboxylic acid [35], polyanionic perfluorosulfonated Nafion polymer [36].

Previous works, the electropolymerized o-ABA synthesis at Au [37], Pt [38], and GC [39,40] were reported. Wang and Knoll [37] fabricated the self-doped conducting polyaniline by electrochemical polymerization of aniline and o-ABA, and investigated the carboxyl groups by in situ electrochemistry and surface plasmon resonance spectroscopy (SPR). Benyoucef et al. [38] synthesized the homo-polymer of o-ABA on Pt electrode by electrochemical cyclic scanning of the potential and characterized this polymer with in situ FTIR. The FTIR result showed carboxyl groups on the electrode surface. This functional group is connected to the antibody by covalent bond. Therefore, poly(o-ABA) as a derivative polyaniline was used as the base of covalent bonding for orientation of the immobilized primary antibody by electropolymerization at electrode surface. The five main factors involved in the design of a sensitive immunoassay are optimized orientation of the immobilized primary antibody, the format of the assay, the type of label used, the method of detection, and the minimization of non-specific binding.

The goal of this paper is to critically compare different substrates and products of the ALP enzymatic reaction towards the development of a sensitive electrochemical immunosensor. The seven products of substrates (Scheme 1) for the ALP reaction have been investigated by cyclic voltammetry and amperometry with three electrode materials as GC, SPC, and Au in the same condition. The highest amperometric response was obtained from AA, which is the product of AAP substrate of ALP enzyme. Therefore, this substrate was applied to amperometric immunosensors based on an electropolymerized poly(o-ABA) as their electrode materials. Electrode modified with poly(o-ABA) can be used to attach to the abundant carboxyl groups on the polymer surfaces, leading to fast and reli-
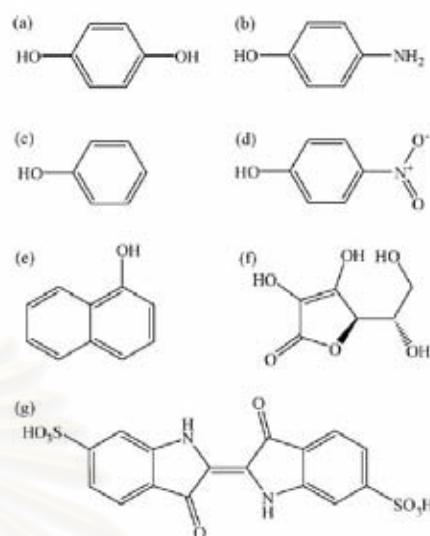
Scheme 1. Structures of the seven substances: (a) hydroquinone; (b) 4-aminophenol; (c) phenol; (d) 4-nitrophenol; (e) 1-naphthol; (f) L-ascorbic acid and (g) indigo carmine.

able amperometric responses. In our studies, mouse IgG is selected as a model analyte and its detection is conducted using the sandwich mode with anti-mouse IgG and anti-mouse IgG conjugated to ALP as the primary and second antibodies, respectively. Also, a mix SAM of 11-mercaptoundecanoic acid and 6-mercaptoethanol modified Au electrode surface was compared with poly(o-ABA)-modified Au electrode surface using the same sandwich immunoassay system. The performance of the immunosensor with respect to detection sensitivity and reliability is presented and discussed in detail.

2. Experimental

2.1. Reagents

NT, AA, Phe, IC, Tris–hydrochloride (Tris), sodium chloride (NaCl), Tween 20, 1-ethyl-3-(3-dimethyl aminopropyl) carbodiimide (EDAC), N-hydroxysulfosuccinimide (NHS), ethanolamine–HCl, o-ABA, sulfuric acid, bovine serum albumin fraction V (BSA), anti-mouse IgG antibody (produced in goat), mouse IgG (from serum), and ALP conjugated anti-mouse IgG antibody (from goat) were purchased from Sigma. HQ, NP, acetic acid, sodium acetate, and 11-mercaptoundecanoic acid were purchased from Aldrich. AP, AAP, and 6-mercapto-1-hexanol were obtained from Fluka. All stock and buffer solutions were prepared using autoclaved double-deionized water (18.2 MΩ cm).

2.2. Apparatus

Electrochemical measurements were conducted using a μAutolab III analysis system with GPES 4.9 software (Eco Chemie) at room temperature in a conventional three-electrode electrochemical cell (1.5 mL), which was used for cyclic voltammetric and amperometric experiments. An Ag/AgCl reference electrode (CH Instruments), and a platinum wire counter electrode were used. A Au disk electrode (2-mm diameter, CH Instruments), a GC disk electrode (3-mm diameter, CH Instruments) and a SPC electrode

ARTICLE IN PRESS

were used as working electrodes, respectively. Magnetic stirring was employed during the amperometric experiment.

The SPCEs were manufactured using a semi-automatic screen printer (Model SPM/B, MPM, Franklin, MA), using a carbon ink (Ercon, G-449(I), Wareham, MA) and alumina ceramic plates. The electrodes were cured for 1 h at 200 °C. A layer of insulator (Ercon, E6165-116 Blue Insulayer, Wareham, MA) was then printed on a portion of the conducting lines, exposing a rectangular (1.5 mm × 6.0 mm) working electrode area.

2.3. Electrochemical measurement products of substrates of ALP

The Au and the GC electrodes were polished to a mirror-like surface with 0.05 μm alumina slurries and then rinsed with deionized water prior to use.

Electrochemical measurements were performed at room temperature. A 0.5 M Tris buffer solution (pH 8.5) was used as a supporting electrolyte for IC, HQ, AP, Phe, NT and AA, and a 0.1 M acetate buffer solution (pH 4.6) for NP. The responses of different products on different electrode materials were detected by cyclic voltammetry with a scan rate of 100 mV s^{-1} and the corresponding voltammograms were recorded.

Hydrodynamic amperometric measurements were performed under stirring in 1.0 mL of the same electrolyte as used in cyclic voltammetric measurements. The anodic potentials (+0.50 V, +0.30 V, +1.10 V, +0.15 V, +0.35 V, +0.70 V and +0.50 V for IC, HQ, NP, AP, NT, Phe and AA, respectively) and cathodic potentials (−0.40 V, −0.20 V and −0.70 V for IC, HQ and NP, respectively) were applied to the SPC working electrode. The Au and GC working electrodes were applied anodic potentials at +0.50 V, +0.10 V, +1.10 V, +0.20 V, +0.35 V, +0.65 V and +0.40 V for IC, HQ, NP, AP, NT, Phe and AA, respectively, and cathodic potentials of −0.40 V, −0.10 V and −0.70 V for IC, HQ and NP, respectively. After the background current reached steady state, the aliquots of each ALP substrate were added, and the corresponding current responses were recorded as a function of time.

2.4. Mouse IgG detected at poly(o-ABA)-modified electrode immunosensors

2.4.1. The poly(o-ABA)-modified electrode immobilization
The GCEs were polished with alumina (0.05 μm) prior to use. The SPCEs were pretreated with 0.1 M H$_2$SO$_4$ applying an anodic current of 25 μA for 300 s. Then, the electrodes were washed using a 0.1 M Tris buffer solution (pH 7.4). The Au electrodes were first polished with alumina (0.05 μm) prior to use. The electrodes were soaked in freshly prepared piranha solution (H$_2$SO$_4$:H$_2$O$_2$ (30%, v/v) 3:1) for an hour (safety note: the piranha solution should be handled with extreme caution) and rinsed with double-distilled water. The cleaned Au electrodes were scanned with a cyclic potential between 0.0 V and 1.6 V in 0.2 M H$_2$SO$_4$ continuously until the characteristic Au peak was observed [41].

All electrodes were electropolymerized in the potential range 0–1.0 V in the presence of 50 mM o-ABA in 1 M H$_2$SO$_4$ by cyclic voltammetry at a scan rate of 40 mV s^{-1}. Poly(o-ABA)-modified electrodes were then immersed in 40 μL of NHS/EDAC solution (1/1 mg in 100 μL of 100 mM MES buffer, pH 6.0) for 30 min, and then the solution was removed. A drop of 40 μL of 40 ppm antimouse IgG (in 20 mM PBS buffer pH 8.6) was applied to every poly(o-ABA)-modified electrode. After 120 min of incubation, the solution was removed, and 40 μL of 1 M ethanolamine solution was applied on every poly(o-ABA)-modified electrode and incubated for 30 min. After removal from the solution, the poly(o-ABA)-modified electrodes were washed three times using 40 μL of a washing solution of 0.1% (w/v) Tween 20 in 50 mM Tris buffer solution (containing 0.1 M NaCl, pH 7.4).

Fig. 1. (A) Cyclic voltammograms (dotted lines: background; solid lines: 100 μM substances) and (B) amperograms (solid lines: anodic current; dashed lines: cathodic current) of different substances at GCE. (a) IC; (b) HQ; (c) NP; (d) AP; (e) NT; (f) Phe and (g) AA. The electrolyte for (a), (b), and (d)–(g) were 0.5 M Tris buffer solution (pH 8.5); and for (c) was 0.1 M acetate buffer solution (pH 4.6). The scan rate for cyclic voltammetry was 100 mV/s. The potentials applied for anodic amperometry (solid lines) were (a) +0.50 V; (b) +0.10 V; (c) +1.10 V; (d) +0.20 V; (e) +0.35 V; (f) +0.65 V and (g) +0.40 V; and for cathodic amperometry (dashed lines) were (a) −0.40 V; (b) −0.10 V and (c) −0.70 V.

ARTICLE IN PRESS

4   *A. Preechaworapun et al. / Talanta xxx (2008) xxx–xxx*

Fig. 2. (A) Cyclic voltammograms (dotted lines: background; solid lines: 100 μM substances) and (B) amperograms (solid lines: anodic current; dashed lines: cathodic current) of different substances at SPCE. (a) IC; (b) HQ; (c) NP; (d) AP; (e) NT; (f) Phe and (g) AA. The potentials applied for anodic amperometry (solid lines) were (a) +0.50 V; (b) +0.30 V; (c) +1.10 V; (d) +0.15 V; (e) +0.35 V; (f) +0.70 V and (g) +0.50 V; and for cathodic amperometry (dashed lines) were (a) −0.40 V; (b) −0.20 V and (c) −0.70 V. The other conditions were the same as Fig. 1.
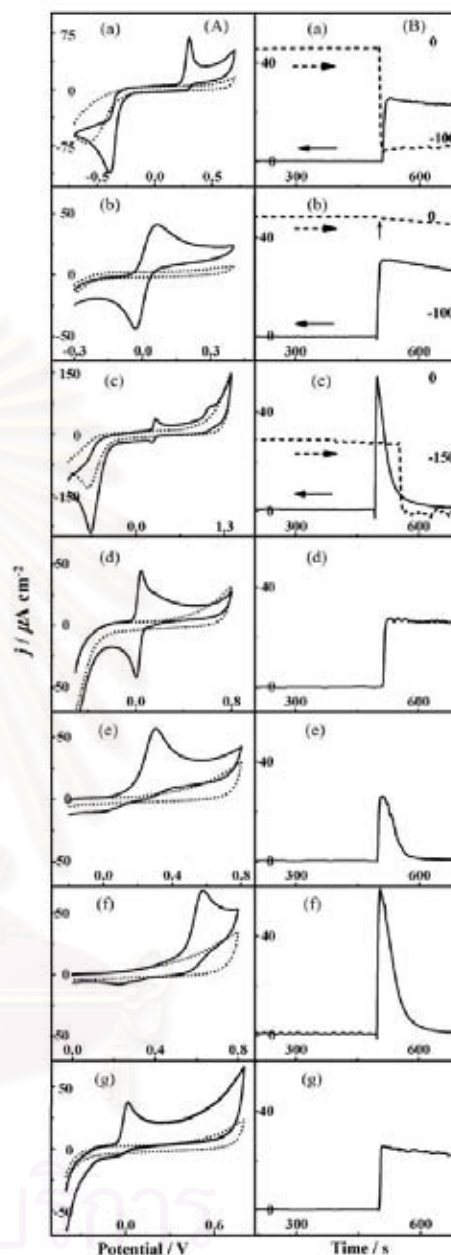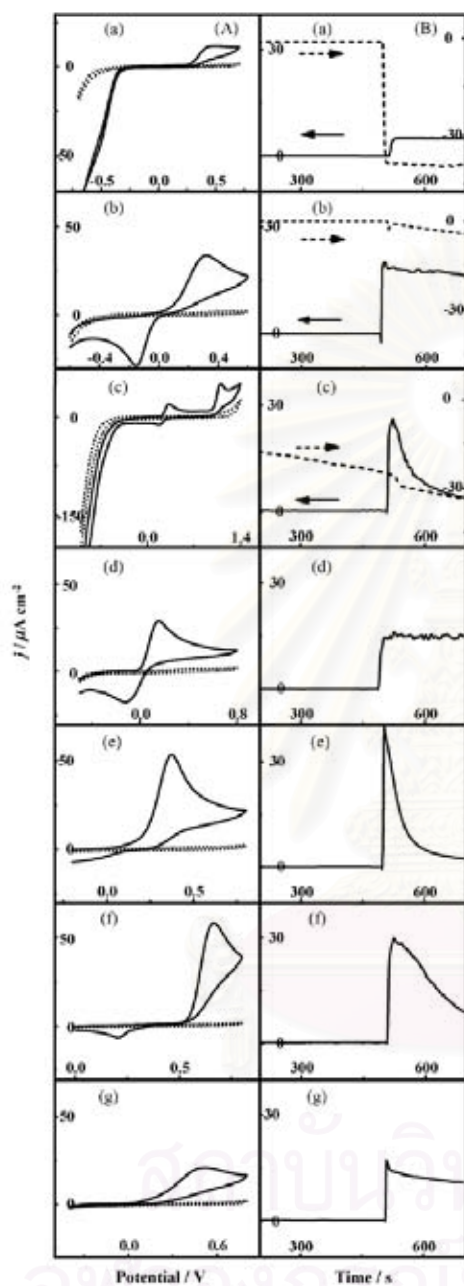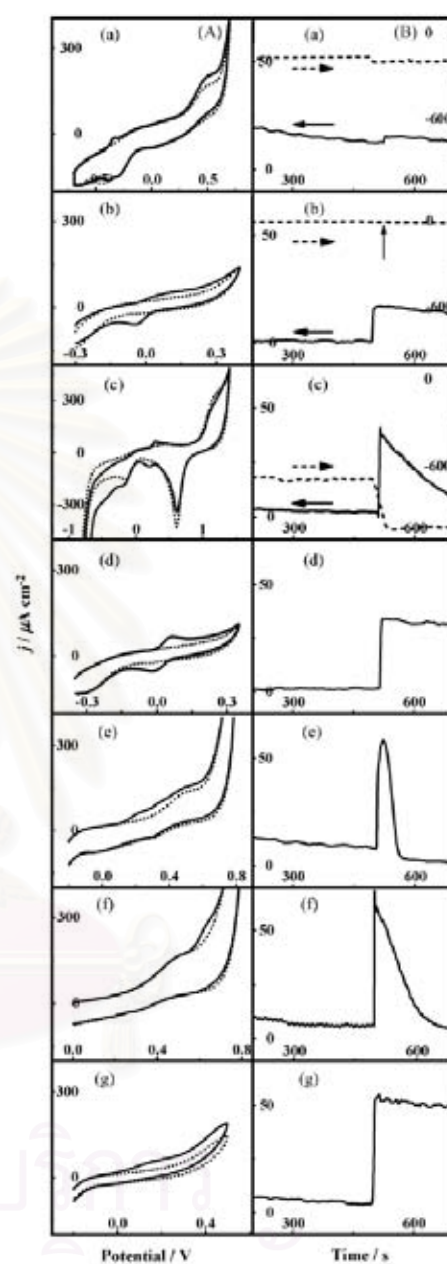
Fig. 3. (A) Cyclic voltammograms (dotted lines: background; solid lines: 100 μM substances) and (B) amperograms (solid lines: anodic current; dashed lines: cathodic current) of different substances at Au electrode. (a) IC; (b) HQ; (c) NP; (d) AP; (e) NT; (f) Phe and (g) AA. The other conditions were the same as Fig. 1.

2.4.2. Sandwich assay using poly(o-ABA)-modified electrode immunosensors

The immunosensors were first coated with the desired amount of the target mouse IgG (in 0.1 M Tris buffer solution containing 1% (w/v) BSA and 0.1% (w/v) Tween 20, pH 7.4) at room temperature for 60 min. After washing with the washing solution, the immunosensor was finally incubated with ALP-conjugated anti-mouse IgG for 60 min and afterwards washed three times as described above.

2.4.3. The poly(o-ABA)-based immunosensor detection

Amperometric measurements were performed in 1.2 mL of a 0.5 M Tris buffer solution (pH 8.5) by applying a potential of +0.4 V (for GC and Au) and +0.5 V (for SPC) on the poly(o-ABA)-modified electrode immunosensors at room temperature. A 100 μL aliquot of 50 mM substrate (AAP) was added to the stirred solution once the background current reached a steady state, and the corresponding current vs. time curve was recorded.

### 2.5. Mouse IgG detected at SAM/Au immunosensor

The Au electrodes were cleaned by the above method. After cleaning, a mixture of 11-mercaptoundecanoic acid and 6-mercapto-1-hexanol (1 mM each in ethanol, respectively) with volume ratio of 1:9 was applied on the clean, dried Au surface and kept overnight for the co-assembly process. After washing twice with ethanol, the Au electrodes were subsequently coated with 40 μL of NHS/EDAC solution (1/1 mg in 100 μL of 100 mM MES buffer, pH 6.0) for 30 min, and then processed in the same manner as the poly(o-ABA)-modified electrode for immobilization, sandwich assay and detection.

3. Results and discussion

3.1. Electroanalysis of products of substrates of ALP

Under alkaline conditions, ALP hydrolyses the phosphate ester (RHPO$_4^-$) functional group of its substrates (IP, HQDP, NPP, APP, NTP, PheP, and AAP) to the respective alcoholic (ROH) products (IC, HQ, NP, AP, NT, Phe, and AA), as shown in reaction (1). These products can then be electrochemically detection via reaction (2).

Enzyme reaction:

$$RHPO_4^- + H_2O \xrightarrow{ALP} RHO + H_2PO_4^- \qquad (1)$$

Electrochemical reaction:

$$ROH \rightarrow R=O + ne^- + nH^+ \qquad (2)$$
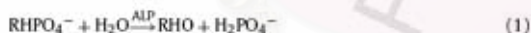
A substrate of ALP should not produce any electrochemical signal at the same potential as its of dephosphorylated form (product; ROH). The electrochemical behaviors of seven most commonly used products named, IC, HQ, NP, AP, NT, Phe, and AA (the structures shown in Scheme 1), were examined by cyclic voltammetry and amperometry at unmodified GC, SPC and Au electrodes. Figs. 1–3 display the corresponding cyclic voltammograms (Figs. 1–3A) and amperograms (Figs. 1–3B) that indicated the different products have different electrochemical behaviors on the same electrode material, and the same products also show different behaviors on different electrode materials. Figs. 1–3A show the voltammograms at GC and SPC and Au electrodes. It can be observed that the background CV signals at GC and SPC background CV signals are lower than at Au electrode. This can be explained that GC and SPC are less conductive than Au electrode, resulting in less electrical double layer at GC and SPC electrodes. Therefore, the large background current is obtained at Au electrode. The cyclic voltammogram in Figs. 1–3A, Phe was obtained the highest anodic current density of 58.10 μA cm^{-2} and 66.00 μA cm^{-2} at anodic potential peak at 0.66 V, and 0.64 V at SPC, and Au electrodes, respectively. Using GC electrode, the highest anodic current density of IC 62.5 μA cm^{-2} was obtained at 0.30 V. The lowest anodic potentials of AA were obtained at 0.01 V for GC, and AP at 0.15 V and 0.07 V for SPC and Au electrodes, respectively.

Basically, the IC (Figs. 1–3a), HQ (Figs. 1–3b), NP (Figs. 1–3c), and AP (Figs. 1–3d) show both oxidation and reduction peaks in their cyclic voltammograms. The reduction peaks of IC (Figs. 1–3A(a)) and NP (Figs. 1–3A(c)) at the potential −0.39 V and −0.68 V (for GC), −0.50 V and −0.70 V (for SPC), and −0.38 V and −0.60 V (for Au) provided very high current in solid lines. The electrolyte also gave a hydrogen evolution at about −0.7 V. HQ provided quasi-reversible shapes of cyclic voltammogram at all of three electrodes. Using AP at SPC and Au electrodes, quasi-reversible behavior was obtained. Only, at GC, AP exhibited reversible behavior (the ratio of i_{pc}/i_{pa} is 0.95 and peak separation is 0.6/nV).

Normally in an ALP reaction, IP substrate can generate indigo blue (IB) by the enzymatic hydrolysis as shown in reaction (3). IB is less soluble in aqueous solution. Therefore, fuming sulphuric acid was added in the solution to form soluble IC. IC is redox couples, which can be investigated by electrochemical detection [17]. It is complicated, therefore; IP is not good choice as a substrate:


3-Indoxyl phosphate (IP) → Indigo blue (IB) → Indigo carmine (IC)
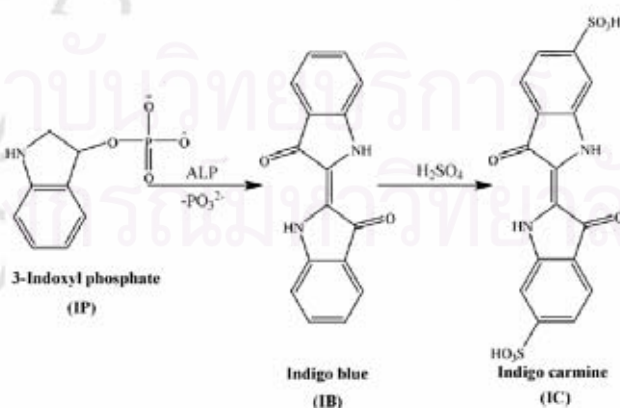
$$ \qquad (3)$$
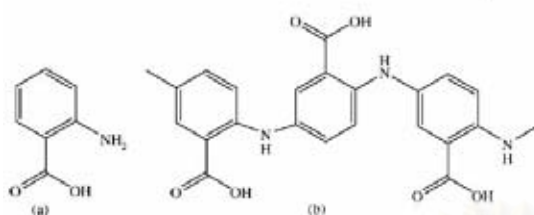
Scheme 2. Structures of (a) o-aminobenzoic acid (o-ABA) and (b) poly(o-aminobenzoic acid) (poly(o-ABA)).

In contrast, NT (Figs. 1–3e), Phe (Figs. 1–3f) and AA (Figs. 1–3g) display only an oxidation peak due to their irreversible chemical reaction corresponding to the previous works in the literatures [15,17,19,20,22,23,25]. Phe, NP, and NT cyclic voltammograms display a poor redox reversibility in all oxidation studies [15,17,25]. The NP, and NT electrochemical reactions were similar to Phe reaction. Their amperometric responses quickly decayed to zero (or base line current density) as electrode fouling occurred as shown in solid lines of Figs. 1–3B(c), (e), and (f) for NP, NT, and Phe, respectively. The NP, NT, and Phe electrooxidation reactions caused the accumulation of electroinactive species at the electrode surface, polymer formation on the electrode leads to passivation of the electrode. Electrode passivation or fouling can pose problems for the development and application of electrochemical immunosensors. For AA in Figs. 1–3A(g), cyclic voltammograms showed the oxidation peaks at 20 mV, 500 mV, and 200 mV for GC, SPC, and Au, respectively. These irreversible reactions were consistent with the previous studies [19,22]. Figs. 1–3B(g) demonstrated the amperometric response of AA, after added AA in electrolyte solution. The current was nearly constant indicating that less passivation occurring at all of electrodes.

Most electrochemical immunoassay methods are based on the application of a constant potential to an electrode transducer and measurement of the current generated by oxidation of enzyme hydrolysis products. Thus amperometric detection was performed to evaluate the behavior of these products. When NP, NT and Phe solutions were added, the responds rapidly decayed due to electrode fouling. These results were similar to the results reported in the literatures [19,22]. Then contrast, HQ, AP, and AA amperograms in Figs. 1–3B(b), (d), and (g) displayed nearly constant anodic current signals after standard of HQ, AP, and AA solution were added in electrolyte. The electrode was reused to repeat experiments for three times. The sensitivity (±S.D.) of the detection of HQ, AP, and AA were $0.29 \pm 0.02\,\mu A\,cm^{-2}\,\mu M^{-1}$, $0.17 \pm 0.01\,\mu A\,cm^{-2}\,\mu M^{-1}$, and $0.15 \pm 0.01\,\mu A\,cm^{-2}\,\mu M^{-1}$ for HQ; $0.25 \pm 0.00\,\mu A\,cm^{-2}\,\mu M^{-1}$, $0.14 \pm 0.02\,\mu A\,cm^{-2}\,\mu M^{-1}$, and $0.32 \pm 0.01\,\mu A\,cm^{-2}\,\mu M^{-1}$ for AP; and $0.24 \pm 0.02\,\mu A\,cm^{-2}\,\mu M^{-1}$, $0.12 \pm 0.02\,\mu A\,cm^{-2}\,\mu M^{-1}$, and $0.47 \pm 0.01\,\mu A\,cm^{-2}\,\mu M^{-1}$ for AA at GC, SPC, and Au electrodes, respectively. For ALP enzyme reaction HQ, AP, and AA are generated from HQP, APP, and AAP substrates, respectively. The AAP substrate was commercially available, less expensive, non-fouling, not-toxic nature of AA product, good chemical stability, and very sensitive response at electrodes [19,22,27]. It was compared with the no-commercially available HQDP, and to the high price of APP. Thus, AAP was chosen as the enzyme substrate for the immunoassay experiments.

3.2. The o-ABA electropolymerization

Poly(o-ABA), conducting polymer [30], has π electron backbone in the structure as shown in Scheme 2. In previous works [37,38], this polymer was characterized by in situ FTIR. The FTIR results displayed that there was the carboxyl group on the surface after
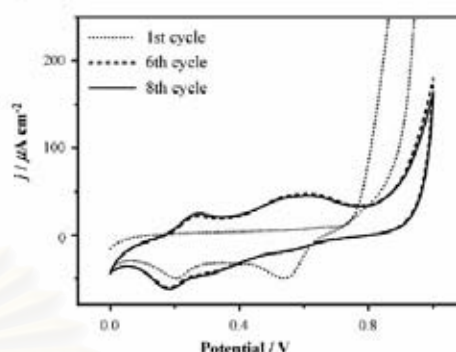

Fig. 4. Cyclic voltammogram of o-ABA electropolymerization at Au electrode: 1st cycle (dotted line); 6th cycle (dashed line); and 8th cycle (solid line). Scan rate is 40 mV s⁻¹.

electropolymerization. The o-ABA solution was electropolymerized in the potential range of 0–1 V at GC, SPC, and Au electrodes with 40 mV s⁻¹ by cyclic voltammetry. The cyclic voltammograms of poly(o-ABA) at Au electrode was shown in Fig. 4. The polymerization of o-ABA at SPC and GC were also analogous to Au electrode. Fig. 4 showed 1st, 6th, and 8th cycle of o-ABA cyclic voltammetric electropolymerization indicating that voltammogram grew very fast in the first six cycles. Thus we selected eight cycles for electropolymerization of these sandwich immunoassay system.

3.3. Mouse IgG poly(o-ABA)-modified electrode immunosensors

In this paper, an enzyme-amplified electrochemical immunosensor based on poly(o-ABA) conducting polymer for sensing antibody–antigen interaction was developed. The immunosensing system is illustrated in Scheme 3, where a poly(o-ABA)-modified electrode serves as the scaffold of the sandwich immunoassay for mouse IgG, and uses ALP as the enzyme label and AAP as the enzyme substrate. Once the poly(o-ABA) is deposited on electrodes, the carboxyl group on the surface can react, via the reactions involving EDAC/NHS, to form a covalent bonding with the amine group of an anti-mouse IgG. In this way, the capture mouse IgG can be immo-
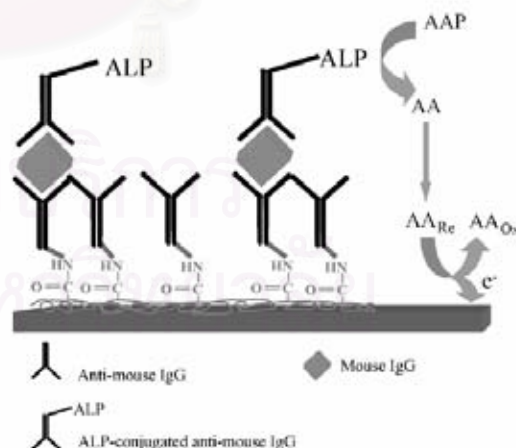
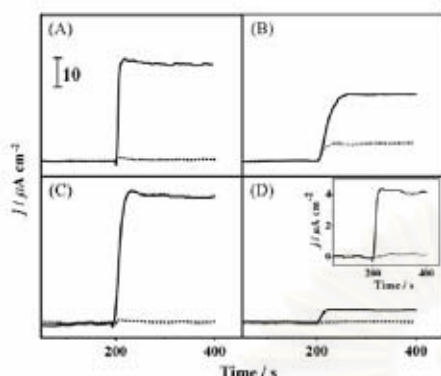Scheme 3. Schematic illustration of an enzyme-amplified immunosensor using poly(o-ABA)-based electrode.

ARTICLE IN PRESS

Fig. 5. Amperometric responses of 1000 ng mL^{-1} (solid lines) and 0 ng mL^{-1} mouse IgG (dotted lines) at poly(o-ABA)/GC (A), poly(o-ABA)/SPC (B), poly(o-ABA)/Au (C), and SAM/Au (D) immunosensors in 0.5 M Tris buffer solution (pH 8.5) at +0.40 V (A, C, and D) and +0.50 V (B) vs. Ag/AgCl. Inset of (D) shows the amperogram responses zooming from SAM/Au immunosensors.

electrodes (immunosensor showed in Scheme 3) at the potentials of 0.40 V, 0.50 V, and 0.40 V, respectively. The suitable potentials of their electrode immunosensors were obtained from hydro-dynamic voltammetric measurement at each immunosensors. The current density of target, solid lines (1000 ng mL^{-1} mouse IgG) at the poly(o-ABA)/GC (Fig. 5A), poly(o-ABA)/SPC (Fig. 5B), and poly(o-ABA)/Au (Fig. 5C) immunosensors was 33.10 μA cm^{-2}, 22.49 μA cm^{-2}, and 43.50 μA cm^{-2}. The current density of control, dotted lines (zero concentration of mouse IgG) was 0.33 μA cm^{-2}, 5.88 μA cm^{-2}, and 0.15 μA cm^{-2}, respectively. We found that mouse IgG immunosensor on poly(o-ABA)/Au gave the highest current density response ratio between target and control of approximately 297, which implied that the poly(o-ABA) on the Au surface would produce a surface with the least non-specific adsorption. Thus, we used this immunosensor for mouse IgG sensor in the subsequent experiments. For the behavior of larger molecule of substrate may exhibit slower turnover in the enzymatic reaction and may also exhibit slower diffusion though the biolayer towards the electrode surface. In this case, using small molecules of AAP, after the AAP substrate is added in the Tris buffer solution, it can be generated to AA very fast, becoming a stable current within 30 s at all of three immunosensors.

3.4. Comparison of SAM/Au and poly(o-ABA)/Au immunosensors

The preparation of mouse IgG SAM/Au immunosensors was optimized by changing the 11-mercaptoundecanoic acid to 6-mercapto-1-hexanol at ratios of 1:9, 1:4,1:3, 1:1 and 4:1. The

bilised on the electrode surface. Anti-mouse IgG-conjugated ALP was bound to mouse IgG to catalyze the conversion of AAP to AA, as shown in reaction (4). The AA product can be detected electro-chemically, giving an anodic current response proportional to the mouse IgG quantity:

$$(4)$$
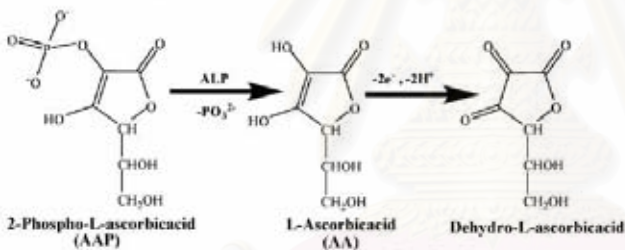
The incubation times were varied by soaking of anti-mouse IgG, mouse IgG, and anti-mouse IgG conjugated with ALP solutions for 60 min, 120 min, and 180 min. The current signal of target and con-trol of mouse IgG were measured. The ratio of target signal and control signal were calculated to obtain the optimum incubation time. It was found that the incubation times of anti-mouse IgG, mouse IgG, and anti-mouse IgG conjugated with ALP as 120 min, 60 min, and 60 min, respectively.

The preparation of mouse IgG immunosensor on poly(o-ABA)/SPC electrode was optimized by non pre-treatment and pre-treatment with an applied current of 25 μA for 300 s, and curing temperatures of 200 °C, 250 °C, and 300 °C for SPC elec-trode preparation before poly(o-ABA) electropolymerization. The best curing temperatures were selected from the highest current response of 1 mM K$_4$Fe(CN)$_6$. The maximum response was found on SPC electrodes with a curing temperature of 200 °C after pre-treatment with an anodic current of 25 μA for 300 s. The optimum pre-treatment of SPC electrode was measured by immunoassay process at the highest ratio of target as 1000 ng mL^{-1} mouse IgG to control as 0 ng mL^{-1} mouse IgG. After pre-treatment, the SPC electrode surface has hydrophilic property, so it can be electropoly-merized better than a non pre-treated SPC electrode.

Fig. 5A–C shows the amperometric responses of AA gener-ated from AAP by ALP enzyme on mouse IgG immunosensors based on poly(o-ABA)/GC, poly(o-ABA)/SPC, and poly(o-ABA)/Au

highest ratio for target (1000 ng mL^{-1} mouse IgG) to control was obtained when using 1:9 as mixed-monolayer. This could be because the high ratio of 6-mercapto-1-hexanol could efficiently minimize non-specific adsorption, and the 11-mercaptoundecanoic acid could also provide enough binding for anti-mouse IgG at the same time. This is shown in Fig. 5D.

The current densities of 1000 ng mL^{-1} of target and 0 ng mL^{-1} of control were 4.19 μA cm^{-2} and 0.13 μA cm^{-2}, respectively. SAM/Au (Fig. 5D) and poly(o-ABA)/Au (Fig. 5C) were compared at the same condition of sandwich immobilization, detection, and target concentration (1000 ng mL^{-1} mouse IgG). The results showed tar-get/control ratios between SAM/Au and poly(o-ABA)/Au as 33 and 297, respectively.

Therefore, using poly(o-ABA) conductive polymer has more sensitivity than using SAM for base Au immunosensor, because electron transfer on conductive polymer is very good. In compari-son, layers of SAM and biomolecules make electron transfer difficult and lead to blocking of the direct electron transfer between elec-troactive species and an electrode.

3.5. Calibration curve of immunosensor

The poly(o-ABA)/Au immunosensing system display the most sensitive response to the mouse IgG detection. Fig. 6 represents amperograms of various mouse IgG concentrations on the relation-
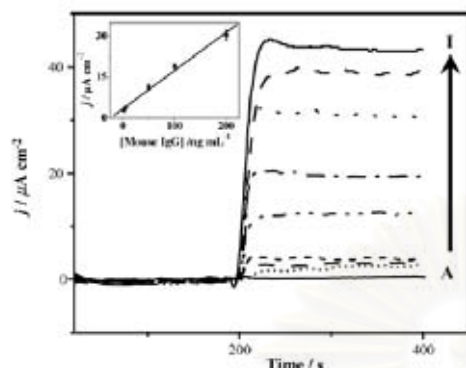
8   A. Preechaworapun et al. / Talanta xxx (2008) xxx–xxx

Fig. 6. Amperograms of 0 ng mL^{-1}, 1 ng mL^{-1}, 3 ng mL^{-1}, 5 ng mL^{-1}, 50 ng mL^{-1}, 100 ng mL^{-1}, 200 ng mL^{-1}, 500 ng mL^{-1}, and 1000 ng mL^{-1} mouse IgG (A to I) at poly(o-ABA)/Au immunosensor in 0.5 M Tris buffer solution (pH8.5) at +0.40V vs. Ag/AgCl. Inset shows the linear range 3–200 ng mL^{-1} of mouse IgG (R^2 = 0.9905 and y= 0.1401x + 3.3893).

ship between current density response and time. Measurements were performed in triplicate using three different immunosensors. The inset shows the dynamic range of the relationship between the average of current density responses ($n = 3$) and mouse IgG concentration. It can be seen that the dynamic range is from 3 ng mL^{-1} to 200 ng mL^{-1} (R^2 = 0.9905), the sensitivity is 0.1401 μA cm^{-2} (ng mL^{-1})$^{-1}$, S.D. < 2 ($n = 3$), and the detection limit is 1 ng mL^{-1}. Poly-o-ABA-modified Au electrode is comparable to electrochemical immunosensor studied by Wilson [43,44]. That found our immunosensor is wider dynamic range and lower detection limit than Wilson's electrochemical immunosensor system using HQDP as substrate of ALP. For our sensitivity is higher than the microelectrochemical immunoassay using SAM modified Au and APP as substrate of ALP report [45].

4. Conclusions

Alkaline phosphatase can be used as an effective label for sensitive immunoelectrochemical assays, which has many substrates for use. Seven products of ALPs substrates were examined and compared by cyclic voltammetry and amperometry. The AA product of the AAP substrate gave a large and stable signal, along with an inexpensive substrate. It was selected for immunosensors at GC, SPC, and Au electrodes, using mouse IgG as a model analyte. Immunosensors using the conductive polymer of o-ABA were based on all electrodes and coupled with sandwich-type immunoassay technique. We found that not only did poly(o-ABA)/Au immunosensor gave the most favorable response (linear range 3–200 ng mL^{-1}), with good sensitivity, reproducibility (S.D. < 2; $n = 3$) for mouse IgG sensor, but also had very low non-specific adsorption.

Uncited reference

[42].

References

[1] A. Brajter-Toth, J.Q. Chambers, Electroanalytical Methods for Biological Materials, Marcel Dekker, Inc., New York, 2002.
[2] W.W. Cleland, A.C. Hengge, Chem. Rev. 106 (2006) 3252.
[3] P.D. Tzanavaras, D.G. Themelis, B. Karlberg, Anal. Chim. Acta 462 (2002) 119.
[4] X.J. Zhu, C.Q. Jiang, Clin. Chim. Acta 377 (2007) 150.
[5] X.J. Zhu, Q.K. Liu, C.Q. Jiang, Anal. Chim. Acta 570 (2006) 29.
[6] B.A. Tannous, M. Verhaegen, T.K. Christopoulos, A. Kourakli, Anal. Biochem. 320 (2003) 266.
[7] H. Arakawa, M. Shiokawa, O. Imamura, M. Maeda, Anal. Biochem. 314 (2003) 206.
[8] M.P. Kreuzer, C.K. O'Sullivan, G.G. Guilbault, Anal. Chim. Acta 393 (1999) 95.
[9] D. Szydlowska, M. Campas, J.L. Marty, M. Trojanowicz, Sens. Actuators B 113 (2006) 787.
[10] M. Diaz-Gonzalez, C. Fernandez-Sanchez, A. Costa-Garcia, Anal. Sci. 18 (2002) 1209.
[11] M. Diaz-Gonzalez, M.B. Gonzalez-Garcia, A. Costa-Garcia, Biosens. Bioelectron. 20 (2005) 2035.
[12] P. Fanjul-Bolado, M.B. Gonzalez-Garcia, A. Costa-Garcia, Talanta 64 (2004) 452.
[13] S. Martinez-Montequin, C. Fernandez-Sanchez, A. Costa-Garcia, Anal. Chim. Acta 417 (2000) 57.
[14] M.S. Wilson, R.D. Rauh, Biosens. Bioelectron. 20 (2004) 276.
[15] P. Fanjul-Bolado, M.B. Gonzalez-Garcia, A. Costa-Garcia, Anal. Bioanal. Chem. 385 (2006) 1202.
[16] H.J. Kim, J. Kwak, J. Electroanal. Chem. 577 (2005) 243.
[17] I. Rosen, J. Rishpon, J. Electroanal. Chem. 258 (1989) 27.
[18] H. Dong, C.M. Li, W. Chen, Q. Zhou, Z.X. Zeng, J.H.T. Luong, Anal. Chem. 78 (2006) 7424.
[19] R.E. Gyurcsanyi, A. Bereczki, G. Nagy, M.R. Neuman, E. Lindner, Analyst 127 (2002) 235.
[20] J.P. Hart, R.M. Pemberton, R. Luxton, R. Wedge, Biosens. Bioelectron. 12 (1997) 1113.
[21] S.J. Kwon, E. Kim, H. Yang, J. Kwak, Analyst 131 (2006) 402.
[22] E.J. Moore, M. Pravda, M.P. Kreuzer, G.G. Guilbault, Anal. Lett. 36 (2003) 303.
[23] R.M. Pemberton, J.P. Hart, P. Stoddard, J.A. Foulkes, Biosens. Bioelectron. 14 (1999) 495.
[24] M. Chikae, K. Kerman, N. Nagatani, Y. Takamura, E. Tamiya, Anal. Chim. Acta 581 (2007) 364.
[25] V.K. Rao, M.K. Sharma, P. Pandey, K. Sekhar, World J. Microbiol. Biotechnol. 22 (2006) 1135.
[26] X.M. Sun, N. Gao, W.R. Jin, Anal. Chim. Acta 571 (2006) 30.
[27] A. Kokado, H. Arakawa, M. Maeda, Anal. Chim. Acta 407 (2000) 119.
[28] Z.H. Wang, A.S. Viana, G. Jin, L.M. Abrantes, Bioelectrochemistry 69 (2006) 180.
[29] Z. Dai, A.-N. Kawde, Y. Xiang, J.T.L. Belle, J. Gerlach, V.P. Bhavanandan, L. Joshi, J. Wang, J. Am. Chem. Soc. 128 (2006) 10018.
[30] M. Gerard, A. Chaubey, B.D. Malhotra, Biosens. Bioelectron 17 (2002) 345.
[31] G. Lillie, P. Payne, P. Vadgama, Sens. Actuators B 78 (2001) 249.
[32] M.A. Rahman, M.J.A. Shiddiky, J.-S. Park, Y.-B. Shim, Biosens. Bioelectron. 22 (2007) 2464.
[33] J.-H. Kim, J.-H. Cho, G.S. Cha, C.-W. Lee, H.-B. Kim, S.-H. Paek, Biosens. Bioelectron. 14 (2000) 907.
[34] T.L. Fare, M.D. Cabelli, S.M. Dallas, D.P. Herzog, Biosens. Bioelectron. 13 (1998) 459.
[35] F. Darain, S.-U. Park, Y.-B. Shim, Biosens. Bioelectron. 18 (2003) 773.
[36] Y.-M. Zhou, Z.-Y. Wu, G.-L. Shen, R.-Q. Yu, Sens. Actuators B 89 (2003) 292.
[37] Y.J. Wang, W. Knoll, Anal. Chim. Acta 558 (2006) 150.
[38] A. Benyoucef, F. Huerta, J.L. Vazquez, E. Morallon, Eur. Polym. J. 41 (2005) 843.
[39] W. Cheng, G. Jin, Y. Zhang, Russian J. Electrochem. 41 (2005) 940.
[40] Y.Z. Zhang, G.Y. Jin, W.X. Cheng, S.P. Li, Front. Biosci. 10 (2005) 23.
[41] C. Berggren, P. Stalhandske, J. Brundell, G. Johansson, Electroanalysis 11 (1999) 156.
[42] H.R. Gu, X. di Su, K.P. Loh, J. Phys. Chem. B 109 (2005) 13611.
[43] M.S. Wilson, Anal. Chem. 77 (2005) 1496.
[44] M.S. Wilson, W. Nie, Anal. Chem. 78 (2006) 2507.
[45] Z.P. Aguilar, W.R. Vandaveer IV, I. Fritsch, Anal. Chem. 74 (2002) 3321.

VITA

Name   :   Miss Anchana Preechaworapun

Date of Birth :   March 20, 1977

Place of Birth: Phitsanuloke, Thailand

Gender   :   Female

Education   :   1995-1999   Bachelor Degree of Science (Chemistry),
                                                     Naresual University

                                   1999-2003   Master Degree of Science (Chemistry),
                                                     King Mongkut's Institute of Technology
                                                     Ladkrabang

                                   2004-2007   Post graduate study leading to a Doctoral of
                                                     Philsophy (Analytical Chemistry),
                                                     Chulalongkorn University

Research Grants: Staff Development Program, Commission on Higher Education
                                   through the Department of Chemistry, Faculty of Science,
                                   Pibulsongkram Rajabhat University, Phisanuloke, Thailand, 2005-
                                   2006.

Home Address   :   777/130, Moo 9, Tambol Arunyik, Amphur Mouang,
                                   Phitsanuloke 65000, Thailand

Publications   :

1. **Preechaworapun, A.**; Ivandini, T. A.; Suzuki, A.; Fujishima, A.; Chailapakul, o.; and Einaga, Y. The development of amperometric immunosensor using boron-doped diamond with poly (o-aminobenzoic acid). Analytical Chemistry 80 (2008): 2077-2083.

2. **Preechaworapun, A.**; Dai, Z.; Xiang, Y.; Chailapakul, O.; and Wang, J. Investigation of the enzyme hydrolysis products of the substrates of alkaline phosphatase in electrochemical immunosensing. Talanta In press.